A unified diagrammatic approach to topological fixed point models

A. Bauer[1*], J. Eisert[1], C. Wille[2]

1 Freie Universität Berlin, Arnimallee 14, 14195 Berlin, Germany
2 University of Cologne, Zülpicher Straße 77, 50937 Cologne, Germany
* andibauer@zedat.fu-berlin.de

Abstract

We introduce a systematic mathematical language for describing fixed point models and apply it to the study to topological phases of matter. The framework established is reminiscent to that of state-sum models and lattice topological quantum field theories, but is formalized and unified in terms of tensor networks. In contrast to existing tensor network ansatzes for the study of ground states of topologically ordered phases, the tensor networks in our formalism directly represent discrete path integrals in Euclidean space-time. This language is more immediately related to the Hamiltonian defining the model than other approaches, via a Trotterization of the respective imaginary time evolution. We illustrate our formalism at hand of simple examples, and demonstrate its full power by expressing known families of models in 2+1 dimensions in their most general form, namely string-net models and Kitaev quantum doubles based on weak Hopf algebras. To elucidate the versatility of our formalism, we also show how fermionic phases of matter can be described and provide a framework for topological fixed point models in 3+1 dimensions.

Contents

1 Introduction

The *phase* of a physical model is central to understanding the its qualitative properties. Studying quantum phases of matter has been a major task in physics ever since quantum many-body theory was first formulated. This work addresses the question of classifying phases, that is, predicting which phases exist and providing models for each phase. Intuitively speaking, a phase of matter corresponds to a parameter range in which key physical properties of a material are essentially uniform. Over the last more than a quarter of a century, condensed matter physicists have discovered a wealth of new exotic phases of matter: Some of them are of emergent nature, reflecting collective states of interacting quantum systems that share little resemblance with the solids, liquids and gases of our commonplace experience. The study of quantum phases of matter – and the quest for classifying and even enumerating them in the first place – has, moreover, gained considerable momentum since the discovery of phases other than symmetry-breaking phases, known as *topologically ordered phases* [1].

More concretely, two translationally invariant quantum lattice models can be seen as being in the same *phase* if they are equivalent up to locally restructuring their degrees of freedom. The fact that many properties are uniform within a given phase is not only of conceptual importance. This uniformity also reflects their usability for, say, the storage and processing of quantum information, the simulatability by a classical computer, or its behaviour concerning thermalization. That is to say, the quest for a solid understanding of phases of matter draws also inspiration and motivation from practical and technological considerations.

Efforts aimed at studying phases of matter can be roughly divided into three areas of research: The first area is concerned with the study of microscopic (commuting-projector) fixed-point models, which has been most successful for non-chiral phases [2]. Such fixed-point models are paradigmatic models characteristic for a quantum phase as fixed points of renormalization group transformations. The second field is aimed at the study of abstract invariant data describing phases, known as (non-fully extended axiomatic) TQFT, including anyon data for topological phases in $2 + 1$ dimensions, or cobordism data for invertible phases. Those approaches have been specifically successful in targeting also chiral phases. However, they have the problem that it is hard to know whether given invariant data extends uniquely to a phase of microscopic models. The third field concerns the detailed study of specific microscopic models that are solvable by other means, such as quadratic fermionic Hamiltonians, or models solvable by means of perturbation analysis. This also includes the study of models and their phases diagrams via extensive numerical analysis.

The present work aims at introducing a new picture of fixed-point models of quantum phases of matter from a fresh perspective, deviating from the perspective put forth in Ref. [2]. In doing so, it makes progress concerning the first two approaches. Those approaches usually use very complex mathematical tools (namely higher order category theory), which are hardly accessible to a broader physics community. The goal of this work is to introduce a comprehensive systematic, unified, easily accessible, and generalized language for understanding and exploring fixed-point

models for quantum phases of matter. Subsequently, we list a number of new features of our approach, and also stress what it does and what it does not deliver.

To start with, we formalize different kinds of physical models in terms of tensor networks [3–6]. In this sense, the approach introduced here shares some resemblance with the approach put forth in Refs. [7–11], in which tensor networks – specifically *projected entangled pair states (PEPS)* [3] – for instances of *Levin-Wen models* [2] have been devised. In one spatial dimension, the classification of phases with *matrix product states (MPS)* [12–14] can be considered largely complete [15–17]. The key difference, however, is that here, we do not construct a tensor network representation of the ground state of a quantum model, living in the physical space of the model. Instead, the connection to the Hamiltonian formulation of quantum mechanics is made by means of a suitable Trotter approximation of *imaginary time evolution*, yielding a *tensor network in Euclidean space-time*. Note that, unlike the common usage of tensor networks for approximating ground states (via MPS or PEPS), those tensor networks do not distinguish between "virtual" and "physical" indices, and only have open indices at their space-time boundaries.

No known approach can in practice genuinely "classify" phases straight from their definition. In our approach, we will rely on an *extendibility hypothesis*. That is, we will assume that the models we want to classify can be extended to "fixed point models" with a strong notion of deformability. For example consider the toric code on a square lattice. As such it is just particular instance of a microscopical model and defies a phase-classification. However, it can naturally be extended to a class of models defined on arbitrary lattices. This kind of deformability carries over to the discretized imaginary time evolution and is the central property in our formalism. While the deformability related to topological order is clearly the proto-typical example one should have in mind here, we emphasize, that the extendibility hypthosis and our formalism that builds upon it can be applied to various types of deformability. Each one corresponds to a different *class of phase*. For example apart from "topological order in $2 + 1$ dimensions", other deformabilities/classes of phases would be "invertible topological order on spin manifolds", "topological boundary of topological order", "anyons in topological order", or "conformal order".

A specific notion of deformability (i.e., class of phases) will be formalized by a so-called *liquid* (or better, a *liquid class*), as we explain. A liquid can be seen as a prescription to construct combinatorial representations of space-times, called *networks*, together with a combinatorial representation of the space-time deformations, called *moves*. For large parts of this paper, the networks can be geometrically interpreted in terms of triangulations or more general cellulations, and the moves correspond to local topology-preserving changes of the triangulations.

A network can be denoted using the same notation as it is commonly used for tensor networks and a move is formalized by a cut-and-paste operation, where a specific network is cut out from a larger network structure and replaced by another network. Invariance under such a deformation for any surrounding network structure implies that a move can also be interpreted as an equation between the cut and pasted tensor network. A solution to those equations will be called a *model* of the liquid. Note that a model in this sense is not a Hamiltonian, but a list of tensors that constitute a tensor network formalizing a discrete (Euclidean) path integral in space-time. However, for the liquids in the scope of this paper (but not always), we can obtain commuting-projector Hamiltonian models from the liquid models via standard constructions. The resulting models are known as fixed point models. If we want the models to have a standard quantum mechanical interpretation, we need to impose an additional *Hermiticity constraint*, which can also be interpreted as a move.

There are different types of matter formalized as "spin systems", "systems with fermions", "free fermionic systems", "spin systems with time-reversal symmetry", and different physical theories such as classical versus quantum physics. The type of matter and the interpretation as classical or quantum mechanical system is also part of the class of the phase. In our formalism, it is incorporated by using different a so-called *tensor types*. Different tensor types are different interpretations of the graphical calculus of tensor networks. A tensor type consists of a "data type"

describing the tensors and two operations on this data, tensor contraction and tensor product. The standard interpretation of tensor networks, via Kronecker products and Einstein summations over indices of arrays, is one particular tensor type. It is the tensor type used to describe spin systems. In this introduction, we mostly focus on this tensor type, but we also encounter tensors with symmetries, fermionic tensors, and projective tensors. The idea of tensor types is reminiscent of concepts in category theory: There, string diagrams can be interpreted in terms of an arbitrary monoidal category. In fact, tensor types are similar to compact closed categories.

We do *not* show how to find concrete models of a liquid, or how to "classify" (e.g., efficiently enumerate) them. This is a difficult mathematical problem that also is not addressed in other approaches either: Let us not forget that there is no "classification of fusion categories" known to date. However, we would like to stress that most likely only the simplest phases will be realizable in physical systems and therefore practically relevant. For those it might be possible to find and explore them via exhaustive numerical search. In the simple case of conventional tensors, one might use a gradient descent, or a Gauss-Newton method to find solutions to the corresponding polynomial equations.

If the moves and the resulting equations are restrictive enough, the liquid models fall into discrete families (of models related by basis changes), and can be classified practically. Often we will find that that the different families are in different phases, though this is not always the case. We give a natural definition for when two models are in the same phase. It is a theoretically hard (and maybe even undecidable) problem to find out whether two models are in the same phase. However, in the world of fixed point models, it is often possible to "confirm by looking" that this is the case, and otherwise prove that it is not the case by computing invariants. The following relational diagram summarizes the approach that we take here. In the course of this work, the precise meaning of the terms used will become clear.

$$
\text{(1)}
$$
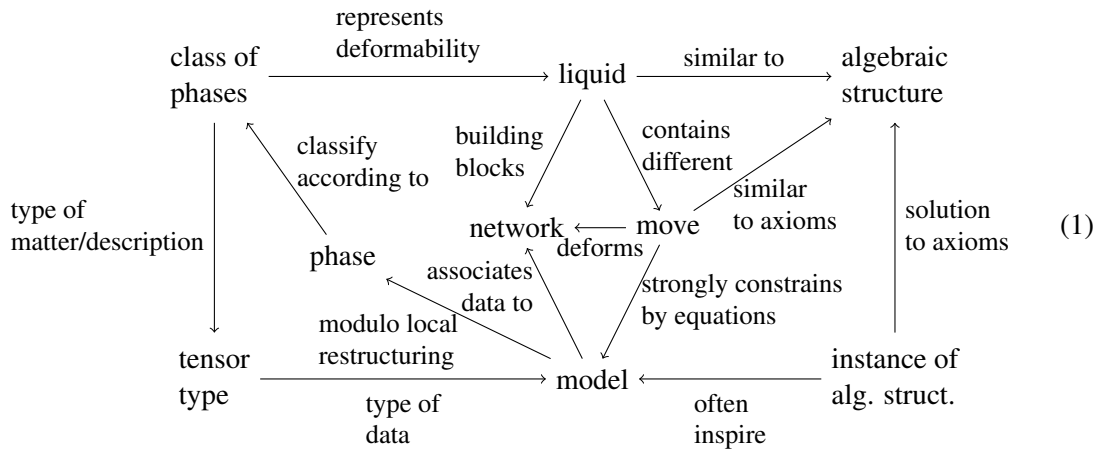
2 Physical systems as tensor networks

At the heart of our approach are tensor networks. A *tensor* (in the conventional sense) is simply a multi-dimensional array $A_{i,j,l,\dots}$. Each of the indices $i, j, l, \dots$ can take a finite number of values, e.g., $i \in \{0, \dots, n_i - 1\}$, where n_i is called the *dimension* of the index. The values can be real or complex numbers. There are two operations we apply to tensors: On the one hand, the *tensor product* is the entry-wise product of two arrays, yielding an array with indices from both arrays, acting as

$$
(A \otimes B)_{i,j,\dots,k,l,\dots} = A_{i,j,\dots} \cdot B_{k,l,\dots} . \tag{2}
$$

On the other hand, the *contraction* is the Einstein summation over two indices with the same bond dimension, yielding a tensor with those two indices removed, acting as

$$A_{i,j,l,\dots} \quad \mapsto \quad ([A]_{i,l})_{j,\dots} = \sum_x A_{x,j,x,\dots} \,. \tag{3}$$

Following the familiar Penrose notation, a tensor can be graphically represented by a box with one line sticking out for each index, e.g.,

$$k - \boxed{A} - i \quad . \tag{4}$$

A computation using tensor products and contractions can be represented by a network-like diagram: For every (copy of a) tensor, we draw (a copy of) the corresponding shape at an arbitrary location (possibly rotated or reflected). For every contraction between two indices, we connect the corresponding lines. E.g., the computation

$$\sum_{x,y,z,w} A_{x,y,i,z} A_{j,y,x,w} B_{w,z,k} \tag{5}$$

could be represented by

$$i - \boxed{A} \quad \boxed{A} - j \atop B \atop k \quad . \tag{6}$$

In general, we might also use shapes without labels for tensors. For a more detailed introduction into tensor networks and the corresponding notation, see, e.g., Section 2.1 in Ref. [18].

The language of tensor networks can be used to formalize local physical models. Readers familiar with tensor networks might think of MPS or PEPS approximating the ground states of gapped local quantum Hamiltonians. It is neither proven in full generality nor completely clear that ground states can be approximated by MPS or PEPS. Also, being gapped is a strong constraint. Thus, this is not the way in which tensor networks are used to describe quantum systems in the approach taken here. Instead we use a simpler and more direct translation by writing the (imaginary) time evolution of a system as a tensor network in space time.

In order to get a tensor network from a continuous (imaginary) time evolution of a quantum many-body system with a local translation-invariant Hamiltonian we have to discretize it using a procedure known as *Trotterization*. As a simplest non-trivial example, let us consider a 1-dimensional quantum spin chain with a translation-invariant nearest-neighbour Hamiltonian

$$H = \sum_i h_{i,i+1}, \tag{7}$$

where $h_{i,i+1}$ is the 2-spin Hamiltonian acting on the spins $i, i+1$. Global properties such as e.g. the boundary conditions are not relevant for the following considerations, which are applied to some small patch in the bulk of the translation-invariant model.

We can divide the Hamiltonian terms into the ones acting on even-odd site pairs and those acting on odd-even site pairs as

$$H = \sum_i h_{2i,2i+1} + \sum_i h_{2i+1,2i+2} = H_1 + H_2. \tag{8}$$

All terms within H_1 act non-trivially only on non-overlapping sets of spins and therefore commute. The same holds for H_2. H_1 and H_2 however do not commute, and therefore

$$e^{it(H_1+H_2)} \neq e^{itH_1} e^{itH_2}. \tag{9}$$

We can still use the following *Suzuki-Trotter expansion*

$$e^{it(H_1+H_2+\dots)} = \lim_{n\to\infty} \left(e^{i\frac{t}{n}H_1} e^{i\frac{t}{n}H_2} \dots \right)^n \tag{10}$$

to obtain

$$e^{itH} = \lim_{n\to\infty} \left(\prod_i e^{i\frac{t}{n}h_{2i,2i+1}} \prod_i e^{i\frac{t}{n}h_{2i+1,2i+2}} \dots \right)^n. \tag{11}$$

Consider the expression on the right-hand side for a fixed n. It is a product of operators acting on different degrees of freedom. $e^{ith/n}$ is a linear operator acting on two spins, so it is a tensor with 4 indices, two for both input and output of the operator

$$e^{i\frac{t}{n}h} \quad \to \quad \text{\Large$\times\!\!\!\otimes$} . \tag{12}$$

With this interpretation, the product of operators becomes a tensor network. E.g., for $n = 3$, we get the network

The tensor network we are looking for should have the same notion of locality structure as the continuum time evolution. That is, every tensor should correspond to a finite space-time volume $\Delta x \times \Delta t$. So it does not make sense to directly take the above tensor network, as the time interval corresponding to a tensor scales like $1/n$. In addition, this tensor network has a trivial limit for $n \to \infty$

$$\text{\Large$\times\!\!\!\otimes$} = e^{i\frac{t}{n}h} \quad \xrightarrow{n\to\infty} \quad \mathbb{1} = \Big|\ \Big|. \tag{14}$$

Instead, we have to pick a fixed Δt, Trotterize $e^{i\Delta tH}$ for some fixed n and divide the resulting tensor networks into spatial unit cells. Evaluating the whole tensor-network patch inside the unit cell yields the tensor P_n of the tensor network we are looking for. E.g., for $n = 3$ and Δx consisting of 4 sites, we can choose

This blocked tensor does not have a sensible large n-limit as well. If we let $n \to \infty$, the number of indices to block on the right and left, and therefore the bond dimension of those indices, grows with n. More precisely, the number of blocked indices grows linearly, and thus the bond dimension increases exponentially with n. It turns out, though, that the tensor can be well approximated by a tensor with much lower bond dimension. We conjecture the following. There

is a sequence of tensors P^x of (horizontal) bond dimension x, numbers numbers α_x, and integers N_x. Additionally, for every x, there is a sequence of left-invertible matrices I_n^x (i.e., there is a matrix $(I_n^x)^{-1}$ such that $(I_n^x)^{-1} I_n^x = \mathbb{1}$), such that for all x, we have

$$
\left\| \; a\!-\!\!\boxed{}_{P_n}^{v'}\!\!-\!a' \; - \; a\!-\!\!\boxed{}_{\;}^{I_n^x}\!\boxed{}_{P^x}^{v'}\!\boxed{}^{(I_n^x)^{-1}}\!\!-\!a' \; \right\| < \alpha_x, \quad \forall n > N_x,
$$

$$
\left\| \; a\!-\!\!\boxed{}_{P^x}^{v'}\!\!-\!a' \; - \; a\!-\!\!\boxed{}_{P^{x+1}}^{v'}\!\!-\!a' \; \right\| < \alpha_x,
$$

$$
\alpha_x \sim e^{-x}.
$$

(16)

To be concrete, we fix the norm above to be the 2-norm of the tensors (when reshaped into vectors), though we do not provide a particularly good reason for this choice, and we would expect other reasonable norms to work as well. This conjecture is based on observations in MPS algorithms like iTEBD, where we apply the Trotterized time-evolution to an MPS. In general, the bond dimension of the MPS might grow exponentially with time. However, the rate of growth does not depend on the Trotterization step we choose. After time evolution for a fixed time interval we see an eigenvalue spectrum in the MPS transfer operator that decays exponentially.

After picking a tensor P for a bond dimension which we consider a sufficient approximation, the (imaginary) time evolution is given by a square lattice tensor network

(17)

It is at this point important to note that we do *not* apply the Trotterized time evolution to a product state to obtain a ground state MPS/PEPS representation, as it is done in algorithms such as the so-called iTEBD method. Instead, we work with the (Trotterized, blocked, truncated) time-evolution tensors themselves. Those tensors correspond to a block in Euclidean space-time with finite, constant imaginary-time length, whereas the ground state MPS/PEPS tensors correspond to a whole "column" with infinite imaginary-time length. The claim that we can truncate the finite block to a small bond dimension is much weaker than the same claim for the infinite column. While the latter is famously conjectured for *gapped* Hamiltonians, a formulation has only been proven in $1 + 1$D. In higher dimensions, such proofs remain elusive, and there are even doubts concerning chiral phases in 2+1D. In contrast, we believe that our conjecture (or some slight variation) about truncating a finite-size block in (Euclidean) space-time holds without any conditions on the Hamiltonian.

It is easy to see how to generalize the Trotterization procedure to other geometric setups, such as higher dimensions, higher spatial support of the Hamiltonian terms, or presence of boundaries or defects of any kind. First we divide the terms into a constant (system-size independent) number of subsets, such that the terms in one subset all commute with each other. Then we proceed using the Suzuki-Trotter expansion applied to the division into subsets, resulting in a tensor network, which we block and truncate into finite unit cells.

Also local classical/quantum thermal models can be written as tensor networks. In the classical case, the partition function is represented by a tensor network made of Boltzmann weights and

delta tensors, without any approximation. In the quantum thermal case, we Trotterize the imaginary time evolution, with imaginary time compactified into a loop of circumference β, where β is the inverse temperature. In both cases, we get a tensor network living in space instead of space time.

Quantum phases of matter are phases of ground states. Thus, the relevant tensor network to consider for the study of quantum phases is the one arising from the *imaginary*, not the real, time evolution: The operator $e^{-\beta H}$ converges to the ground state projector for a gapped system, if we scale both the inverse temperature/imaginary time β and the system size simultaneously.

The evaluation of a tensor network can be seen as a "computation" in the following way. The input data to the computation are the tensors. The "network" itself describes the combinatorial nature of the computation, i.e., in which order and to which components the individual operations (such as copying tensors, evaluating Kronecker products, or Einstein summations) are applied. The graphical notation makes sense, because the steps of the computation obey certain "axioms", e.g., different contractions commute with each other, or, the Kronecker product is associative.

There are types of data other than arrays, and types of operations other than Kronecker products and Einstein summations, which obey the same axioms. In other words, there are other structures which yield different interpretations for the same graphical network notation. We will call such other structures *tensor types* [19]. We will later see that, e.g., models with fermions can be formalized by using a different tensor type in Section 8. In fact, we have already encountered two different tensor types, namely complex tensors and real tensors.

3   Phases of matter and the extendibility hypothesis

Conventionally, quantum phases of matter are equivalence classes of local translation-invariant gapped Hamiltonians $H \in \mathcal{H}$. By *gapped*, we mean that there is an integer $g \geq 0$ called *ground state degeneracy* and a real number $\epsilon > 0$ called the *gap*, such that for every system size n (greater than some n_0), the g lowest eigenvalues of H are separated from the rest of the spectrum by ϵ, and among each other by β_n such that $\beta_n \to 0$ for $n \to \infty$. Two gapped Hamiltonians $H_1, H_2 \in \mathcal{H}$ are considered equivalent if there is a continuous path of gapped Hamiltonians connecting H_1 and H_2 [1]:

$$\widetilde{H} : [0, 1] \to \mathcal{H} \ ,$$
$$\widetilde{H}(0) = H_1, \quad \widetilde{H}(1) = H_2 \ . \tag{18}$$

Recall that $\mathcal{H}$ contains only gapped Hamiltonians, so all $\widetilde{H}(s)$ for $s \in [0, 1]$ must be gapped, otherwise one speaks of a "gap closing" inducing a "phase transition". If we aim at comparing two Hamiltonians with different local Hilbert spaces, we can arbitrarily embed both into the same local Hilbert space and use the same definition.

This definition is mathematically clear and formal but has two disadvantages: First, it is not very constructive: Checking all possible paths between two Hamiltonians is practically infeasible, and the fact that a path is something continuous does not make it easier. Moreover, there is evidence that it might not even be decidable in general, whether a family of Hamiltonians is uniformly gapped for different system sizes [20]. Second, it does not make very clear why phases are such a fundamental concept. It is not directly evident just from the fact that two Hamiltonians are connected by a gapped path that they share a lot of common features.

Those two disadvantages are resolved by an alternative definition: Two states are in the same phase if they are related via a finite-depth local (generalized) unitary circuit [21]. This definition immediately makes the physical meaning of phases very clear: Two states in the same phase are the same up to locally restructuring their degrees of freedom. Also, instead of having to search for a continuous path, we now need to find a discrete circuit, which seems to make the definition

a bit more constructive. However, this definition is not mathematically formal, and we have to put some work in to achieve this. First, it is unclear what a "state" even means in the context of a thermodynamic limit. The generic way to define a physically reasonable family of states of different system sizes is by specifying them as ground states of local gapped Hamiltonians, which brings us back to the original definition. Second, the definitions are only equivalent if we allow the local unitary equivalence to be approxmiate, with an approximation error decreasing with the depth or the locality of the circuit. Alternatively, we can directly use a "fuzzy circuit", corresponding to the time evolution under a local time-dependent Hamiltonian. In this case, the equivalence has been shown using the notion of quasi-adiabatic evolution [22].

In the subsequent, we propose a third definition of phases, which is suitable for our formalization of models not in terms of Hamiltonians or states, but tensor-network path integrals. Essentially, two such path integrals are in the same phase, if they are equivalent up to locally reshaping the tensor network. This definition is in spirit more similar to the local unitary definition, however, it does not suffer from the problem of having to define what a "state" is in the thermodynamic limit. It still has the problem that such an equivalence can only hold approximately, and we haven't yet found the most natural way of defining those approximations.

Quantum phases, once again, describe the ground state properties of Hamiltonians. Such ground states can be obtained directly from the Hamiltonian by applying the imaginary time evolution to some initial state vector $|x\rangle$ as

$$\lim_{t\to\infty} e^{-tH}|x\rangle.\tag{19}$$

However, for any finite system size, the lowest eigenvalue will not generically have a g-fold degeneracy, but the "ground states" will have slightly different energies. So, at a particular system size, e^{-tH} will not converge to a ground state projector with g-dimensional support, but to the projector on the lowest eigenstate only. We see that in order to talk about ground states, we do not only have to scale the imaginary time t, but also simultaneously the system size n. Thus, it is natural to represent the model as something living in euclidean space-time. We consequently choose to represent models by their *imaginary-time evolution tensor network* instead of their Hamiltonians.

A very simple case of two models being in the same phase is if they are related by an on-site unitary. If we conjugate Hamiltonian terms by a unitary operator, the tensors in the imaginary-time evolution get conjugated in the same way. So, if we apply an on-site unitary $U^{\otimes N}$ to a $1+1$-dimensional model as in Section 2, the tensor P in Eq. (17) gets conjugated by U,

$$\tag{20}$$

The unitarity of U can be denoted in network notation by

$$\tag{21}$$

Imagine starting from the conjugated square lattice tensor network. Now, replace every occurrence of the conjugated tensor $\widetilde{P}$ by its definition in terms of Eq. (20). This will create a pair of U and $U^\dagger$, that is, an occurrence of the left hand side of Eq. (21), at every bond of the original network. We can remove those pairs by replacing each occurrence with the right hand side of Eq. (21),

yielding the non-conjugated network

$$
\cdots \begin{array}{c} \widetilde{P} \quad \widetilde{P} \\ \widetilde{P} \quad \widetilde{P} \end{array} \cdots \quad \rightarrow \quad \cdots \begin{array}{c} U \quad U \\ U^\dagger \quad U^\dagger \\ U \quad U \\ U^\dagger \quad U^\dagger \end{array} \cdots \quad \rightarrow \quad \cdots \begin{array}{c} P \quad P \\ P \quad P \end{array} \cdots \tag{22}
$$

in Eq. (17). As we have seen, applying an on-site unitary in our tensor-network picture corresponds to "rewriting" the tensor network by replacing subnetworks with other subnetworks which evaluate to the same tensor. We will call such a replacement operation a *circuit move*, and define two tensor networks to be in the same phase if they are related by a circuit move.

The above reasoning also works if U is not an on-site operator, but is only a product of operators acting on constant-size non-overlapping patches. Furthermore, it suffices if U is an isometry rather than a unitary, such that it can also change the local Hilbert space dimension. Last, we can conjugate by more than one layer of unitaries. So for any two Hamiltonians related by a finite-depth generalized local unitary circuit, the corresponding tensor networks are related by a circuit move. But circuit moves also go beyond conjugation by unitaries. Consider the following example for a different circuit move acting on square lattices. First, we split each tensor into a network consisting of 4 tensors:

$$
\begin{array}{c} \square \\ \widetilde{P} \end{array} = \diamondsuit \ . \tag{23}
$$

The dimension of the bonds between the new tensors can be different, which we reflect by using a different line style. At every bond of the original network, we will get two of the new 3-index tensors. We replace those two by two other tensors, connected by a bond perpendicular to the old bond

$$
\rangle\!-\!\langle = \begin{array}{c} \otimes \\ \otimes \end{array} \ . \tag{24}
$$

Now, at every vertex of the square lattice there are 4 tensors on the adjacent edges. We can block those into a single tensor again according to

$$
\diamondsuit = \begin{array}{c} \square \\ P \end{array} \ . \tag{25}
$$

Applying this circuit move, we obtain a network whose tensors are now located at the positions where the vertices of the old square lattice have been previously,

$$
\begin{array}{c} \widetilde{P} \quad \widetilde{P} \\ \widetilde{P} \quad \widetilde{P} \end{array} \rightarrow \cdots \rightarrow \cdots \rightarrow \begin{array}{c} P \quad P \\ P \quad P \end{array} \ . \tag{26}
$$

Note that also the definition via circuit moves has the difficulty of having to deal with approximations, and we have not found the most natural way to do this yet.

11

No known approach can classify general phases starting from a fundamental definition. In our approach, we will instead rely on an observation which we call the *extendibility hypothesis*: Models coming from condensed matter physics are typically defined on regular spatial grids, times a linear time. That is, they are defined in a flat Euclidean space time. Sometimes one can extend the definition of such a model from only flat space times to arbitrary curved space time. Moreover, there is a very powerful set of deformations under which the extended model is invariant. The extendibility hypothesis is the (admittedly vague) assumption that, the more "generic" a model is, the more "powerful" are the deformations that it is invariant under after extension.

The most relevant example for extendibility are models with topological or symmetry-breaking order: Such models can be extended from flat space to arbitrary topological manifolds, such that the extended model is invariant under arbitrary homeomorphisms, i.e. deformations leaving the topology invariant. Irreducible topological phases are known to be *robust under perturbations* [23] and generic in that sense. The "second most generic" type of models are those at transitions between two topological or symmetry-breaking phases. Such critical models are known to be described by CFTs. That is, they can be extended to manifolds with a conformal metric, and the extension is invariant under arbitrary transformations that leave this conformal structure invariant. On the other hand, there are also models with a more powerful extendibility than topological phases: E.g., models with invertible topological order can be extended to topological manifolds, and the extension is not only invariant under homeomorphisms but additionally under arbitrary surgery moves. Equivalently, those manifolds are not defined up to homoemorphism, but only up to cobordisms.

Extendibility helps classifying phases of matter in the following way: The invariance of the extended models under deformations is very restrictive. This makes it possible to "classify" such extended models by identifying them with instances of some algebraic structure. Those instances often fall into discrete families, which makes the problem of classifying phases practically feasible. The extended models have special properties, such as some notion of being "exactly solvable". Models of that kind are often called "fixed-point models".

4 Extendibility and liquids: Toy examples

We can use the language of tensor networks to formalize the extendibility hypothesis. By this, we do not try to answer the question of which models are extendible in which way, or what it means for a model to be "generic" in full generality. Instead, the latter will remain the central guess that we rely on, but that we find to be true in all considered cases. We will at this point merely formulate what it means for a specific model to be extendible in a specific way and provide 3 simple examples for how models extend in a topological way in the following sections.

4.1 Topological extendibility in $1 + 1$ dimensions

As a first example we consider models with topological extendibility in $1 + 1$ dimensions, that is, in one spatial dimension. Despite the fact that non-trivial intrinsic topological order in the conventional sense only exists in $2 + 1$ dimensions, this example is well suited to illustrate the concept. Moreover, we would like to mention that, even though they are not robust to perturbations, symmetry-breaking phases have a topological deformability as well. Also, if we impose on-site or time-reversal symmetries, there are non-trivial *symmetry protected topological (SPT)* phases. For pedagogical reasons, we neglect the following two important technical details in this section. In Section 5 we will see that we need to distinguish the indices of a tensor for a better representation of topological space-time, and in Section 6 we will see that we need to add an orientation and Hermiticity move in order to give the models a standard quantum mechanical interpretation.

4.1.1 Square lattice model and extended model

We start with a 4-index tensor from which we can build tensor networks on arbitrary square lattices. Such a tensor can be obtained from a quantum Hamiltonian by Trotterization or directly from a classical model, as explained in Section 2, as

$$\tag{27}$$

One of the main points of this work is to keep the *combinatorial structure* (the "network") of a tensor network separate from the *data* (the "content of the tensors"). On the combinatorial side, the places to which we assign the tensors will be referred to as *atoms*, and the places where the contractions happen will be called *bonds*. The "graph" formed by atoms and bonds will be referred to as *network*. In contrast to an actual graph, a network can have bonds with "loose ends" which will be referred to as *open indices*. The different types of atoms (referred to as *elements*) form the so-called *substrate*. In this case the substrate is given by only one single type of atom representing a 4-index tensor. On the data side, the 4-index tensor itself will be called a *model* of the substrate.

The "extended model" is a prescription that assigns tensor networks to arbitrary triangulations of 2-manifolds. One of the simplest ways to arrive at such a prescription is to take a 3-index tensor, and to associate one copy of this tensor to each triangle, with contractions between tensors at adjacent triangles as
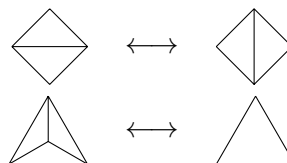
$$\tag{28}$$

So the extended model is a model with a different substrate, as it is given by a 3-index tensor. There is a canonical prescription to turn models of the extended substrate into models of the square-lattice substrate: We can restrict the extended model to regular triangulations of flat space. Specifically, we can divide each square into two triangles, and use as square tensor the tensor obtained by contracting two triangle tensors according to

$$\tag{29}$$
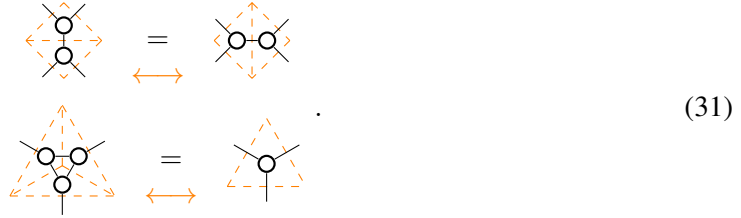
The pure combinatorics of an equation like this will be referred to as a *substrate mapping*. In the above case, the substrate mapping goes from the square lattice substrate to the extended substrate, which means that, conversely, it will map models of the extended substrate to models of the square lattice substrate.

In order to define the "invariance under homoemorphisms", we need a combinatorial analogue of the latter in terms of triangulations. This is given by the so-called *Pachner moves* [24] which act as

$$\tag{30}$$

It is known that any two (combinatorial) triangulations of the same manifold are related by Pachner moves. Conversely, it is easy to see that Pachner moves preserve the topology of a triangulation.

We can associate tensor networks to the patches on the left- and the right hand side of the Pachner moves. Topological invariance of the model means that the evaluations of the two corresponding tensor networks are equal as

$$\tag{31}$$

We will refer to the pure combinatorics of an equation like this as a *move*. The collection of moves will be referred to as a *liquid*. A model of a substrate fulfilling all the equations corresponding to the moves will be called a *model* of the liquid. A square lattice model X is *extendible* if there exists a model of a liquid (in our case the liquid Eq. (31)), such that the square lattice model obtained by applying the corresponding mapping (in our case Eq. (29)) is in the same phase as X.

4.1.2 Relation to algebraic structures
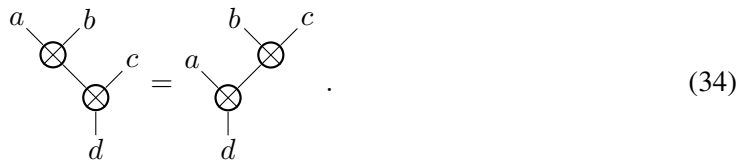
In this section, we relate the above moves to algebraic structures. An *algebra* is a linear map $\cdot : V \otimes V \to V$, where V is a vector space. A finite-dimensional algebra is represented by its structure coefficients, which form a 3-index tensor,

$$\tag{32}$$

Here, we think of $\cdot$ as a linear map from the top two indices to the bottom index. So, an algebra is nothing but a model of the substrate depicted above. An algebra is *associative*, if

$$(a \cdot b) \cdot c = a \cdot (b \cdot c) . \tag{33}$$
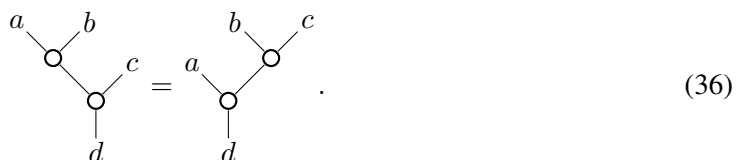
This can be formulated as an equation between two tensor networks, namely

$$\tag{34}$$

So, associativity defines a move, and associative algebras are models of the liquid defined by that move. There are many other examples of algebraic structures which are models of liquids, such as Frobenius algebras, unital algebras, commutative algebras, Hopf algebras, representations of algebras, etc. Every model of the topological liquid can be turned into an algebra by a substrate mapping from the algebra liquid to the topological liquid

$$\tag{35}$$

Let us substitute this definition into the associativity axiom above. We obtain

$$\tag{36}$$

This is nothing but the 2-2 Pachner move of the extended liquid. Thus, every model of the extended liquid yields an algebra which is automatically associative. On the level of combinatorics, we have a mapping between two substrates which are also liquids. Each move of the algebra liquid yields a move for the topological liquid by substituting the mapping. We found that each of these *mapped moves* is also a move of the topological liquid. We call such a substrate mapping which is compatible with the moves of two liquids a *liquid mapping*.

We often observe that topological liquids have liquid mappings from well-known algebraic structures. However, usually there is no inverse liquid mapping from the topological liquid to the algebraic liquid. This means that models of topological liquids define some algebraic structure, but the algebraic structure misses some additional axioms which are needed for a topological fixed point model. This is mostly due to the fact that the networks in the moves of algebraic structures always allow for a global "flow of time" (in case of the associativity above from the top to the bottom), whereas the topological liquid includes moves with "closed time-like loops".

4.1.3 Models

As we have seen in the paragraph above, models of the extended liquid correspond to associative algebras, for which a few additional axioms hold [1]. Such algebras fall into discrete families, up to basis changes. One family of algebras which also yield topological models is given by the algebra of complex functions over an x-element set under point-wise multiplication, for arbitrary x. This corresponds to the choice

$$
\underset{c}{\overset{a \quad b}{\circ}} = \underset{c}{\overset{a \quad b}{\bullet}} = \begin{cases} 1 & \text{if } a = b = c \\ 0 & \text{otherwise} \end{cases} , \tag{37}
$$

for $0 \leq a, b, c < x$, which will also be referred to as the *delta tensor*, and denoted by a small dot. Delta tensors can be defind for an arbitrary number of indices, with entry 1 if all the index values are equal and 0 otherwise.

If we evaluate such a model on a network representing a triangulation of a sphere, we get the number x. So we see that every family yields a different topological invariant and thus all families correspond to different phases. Physically speaking, these phases are *symmetry-breaking phases*. E.g., for $x = 2$, the liquid is equivalent to the ordered-phase fixed point of the $1 + 1$-dimensional *Ising model*. This is a chain of qubits with a nearest-neighbour Hamiltonian

$$
H = \sum_i h_i = - \sum_i Z_i Z_{i+1} . \tag{38}
$$

If we apply the Trotterization procedure in Section 2 to any Hamiltonian, we never obtain a topological tensor liquid. This is because the first excited state always has a finite energy, corresponding to a finite "correlation length in time direction". In contrast, a topological tensor liquid has zero correlation length in any direction due to its topological deformability. Luckily, the Hamiltonian above has the special property that its terms are commuting, so we do not need to divide time into small Trotter steps. In this case, we can directly take the limit $\beta \to \infty$ for the individual terms, which corresponds to taking the local ground state projector
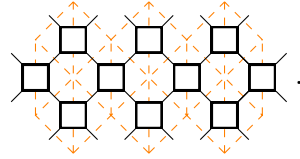
$$
\lim_{\beta \to \infty} e^{-\beta h} \sim P = \frac{1}{2}(\mathbb{1} - Z_0 Z_1) . \tag{39}
$$

The imaginary time evolution is represented by a product of these operators P at different places. If we write P as a tensor

$$
P \to \underset{c \quad d}{\overset{a \quad b}{\square}} = \begin{cases} 1 & \text{if} \quad a = b = c = d \\ 0 & \text{otherwise} \end{cases} , \tag{40}
$$

---
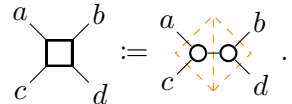
[1] We are not yet fully precise here, but in the end the models will be equivalent to something like *commutative special Frobenius algebras*.

the imaginary time evolution is represented by a network of the form

$$\tag{41}$$

In order to compare the above model (given by a 4-index tensor) with our topological model (given by a 3-index tensor), we have to choose an according substrate mapping which transforms the network above into the network representing a triangulation of the plane. One such mapping is, e.g., given by

$$\tag{42}$$
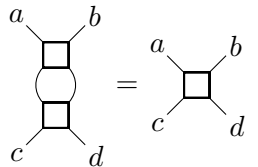
If we evaluate the right hand side, we get indeed the tensor P from Eq. (40).

4.1.4 Commuting-projector Hamiltonians and stacking

We have already introduced the notion of a liquid mapping to formalize the relation between the "original" and the "extended" model, and between the algebraic liquid and the topological liquid. Here, we will give two more examples for operations which can be neatly formalized by a liquid mapping, namely the construction of a commuting-projector Hamiltonian from the section before, and the operation of embedding two copies of a model into the same space-time. Both will lead to generalizations of the notion of liquid mapping we introduced so far.
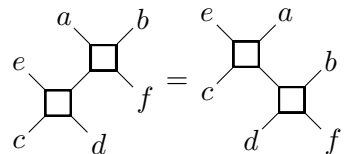
H is a commuting-projector Hamiltonian, meaning that P is a projector, and operators P acting on different pairs of sites commute. I.e., the following two equations are fulfilled.

- The projector property is

$$\tag{43}$$

- the commutativity is
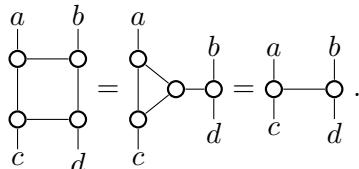
$$\tag{44}$$

So "commuting-projector Hamiltonians" themselves are models of the above liquid. Now, if we plug the mapping Eq. (42) into the move Eq. (43), we get

$$\tag{45}$$

This is not a move of the topological liquid. However, it is equivalent to a sequence of moves

$$\tag{46}$$

In the first step we applied the 2-2 Pachner move, and in the second step the 1-3 Pachner move. We will refer to moves equivalent to sequences of moves of a liquid as *derived moves*, and the corresponding sequences as *derivations*. We will generalize our notion of a liquid mapping by allowing the mapped moves to be derived moves of the target liquid.

For the second example, consider "stacking two copies" of a model, i.e., embedding both models in the same space(-time) in a non-interacting way. If a model has topological deformability, then so will the stacked model. Stacking is nothing but a mapping from a liquid (here the $1 + 1$ dimensions topological liquid) to itself

$$\tag{47}$$

This example shows a slight generalization of the concept of a liquid mapping introduced so far, as every open index on the left hand side corresponds to two open indices on the right hand side. If we apply this mapping to any network, we will obtain two copies of that network. E.g., the mapped 2-2 Pachner move gets mapped to a move relating two disconnected networks consisting of two atoms each on each if its sides. Obviously, this mapped move can be derived by applying the original move to both copies independently.

4.1.5 Phases

In this section, we will illustrate how the definition of a phase in terms of circuit moves of tensor networks from Section 3 applies to models of liquids. The algebra of functions over a 2-element set yields a model as we have seen above. Another model of the liquid is given by the $\mathbb{Z}_2$ group algebra

$$\mathbb{Z}_2 \quad = \quad \begin{cases} \frac{1}{\sqrt{2}} & \text{if } a + b + c = 0 \mod 2 \\ 0 & \text{otherwise} \end{cases} . \tag{48}$$

The two algebras are isomorphic via a basis change known as the *Hadamard transformation*

$$a - \boxed{} - b = \frac{1}{\sqrt{2}} \begin{pmatrix} 1 & 1 \\ 1 & -1 \end{pmatrix} . \tag{49}$$

Basis changes are a very specific example of circuit moves, and thus the two liquid models are in the same phase. Concretely, we have

$$\tag{50}$$

H happens to be its own inverse

$$a - \boxed{} \boxed{} - b = a - b . \tag{51}$$

The circuit move starts with a network of the δ liquid, e.g.,

$$\delta \quad - \quad \delta \quad . \tag{52}$$

We identify all different occurrences of the network on the right hand side of Eq. (50), and replace them by the network on the left hand side. We obtain

$$\tag{53}$$

Now we identify all different occurrences of the network on the left hand side of Eq. (51) and replace them by the right hand side. For this to be a well-defined procedure, the different occurrences must not overlap. This is ensured by how we obtained the network in the previous step. We obtain

$$
\begin{array}{c}
\text{H} \quad \text{H} \\
\mathbb{Z}_2 \!\!—\!\! \mathbb{Z}_2 \\
\text{H} \quad \text{H}
\end{array}
\tag{54}
$$

As we have seen, using Eqs. (50), (51), we can transform any closed δ-tensor network into the according $\mathbb{Z}_2$-tensor network. If the network has open indices, we will end up with some residual Hadamard transformations near this open boundary. We found that the $\mathbb{Z}_2$-model and the δ-model are related by an exact circuit move, and thus in the same phase. Note that generic square lattice tensor networks are generically only connected by circuit moves up to exponential tails. However, for liquid models as highly restricted by moves as the present one, we tend to find that there are exact, and even rather simple circuit moves connecting them.

As another example, consider the model

$$
\begin{array}{c}
a \quad b \\
x \quad \\
c
\end{array}
= 2^{(-3/2)} \quad (\forall a,b,c) .
\tag{55}
$$

We will show that this model is in the same phase as the trivial model where each tensor is the number 1. We notice that the tensor above is the tensor product of three times the same vector

$$
\begin{array}{c}
a \quad b \\
x \quad \\
c
\end{array}
=
\begin{array}{c}
a \quad b \\
\quad \\
c
\end{array},
\tag{56}
$$

where

$$
\bullet\!\!—a = \frac{1}{\sqrt{2}} \quad (\forall a) .
\tag{57}
$$

Furthermore, this vector is normalized, i.e. (note that the empty network evaluates to the scalar 1),

$$
\bullet\!\!—\!\!\bullet = \qquad .
\tag{58}
$$

From the above two moves, we can again construct a circuit move. We start with a tensor network of the x-model

$$
x \!\!\diamond\!\!—\!\!\diamond\!\! x \quad ,
\tag{59}
$$

and then apply Eq. (56) by replacing every occurrence of the left hand side by the right hand side

$$
\begin{array}{c}
\bullet \;\bullet\!\!—\!\!\bullet\; \bullet \\
\bullet \qquad \bullet
\end{array}.
\tag{60}
$$

Finally, we apply Eq. (58), which yields the empty network everywhere except for at a potential boundary

$$
\begin{array}{c}
\bullet \qquad \bullet \\
\bullet \qquad \bullet
\end{array}.
\tag{61}
$$

So we see that this model is in the same phase as the trivial model, again via an exact and very simple circuit move.

Surely, in more general examples of liquid models being in the same phase, the circuit moves will not always be quite as simple as basis changes. However, we continue to observe that they are exact and consist of a small number of steps.

4.2 Topological extendibility in $2 + 1$ dimensions

In the next example, we explore extendibility in $2 + 1$ dimensions. Again, we start from a tensor network on a cubic lattice obtained by Trotterization of a Hamiltonian or by other means. The extended model is a tensor network that can be defined on arbitrary triangulations of 3-dimensional manifolds. The most straight-forward construction would be to consider cellulations into simplices and to associate one tensor to every simplex. For this liquid the topological invariance would then be formulated analogous to the $1 + 1$-dimensional case, i.e., as invariance under 3-dimensional Pachner moves. In this section we will instead sketch a less standard formulation of topological invariance, which will be presented in more detail in Section 7.2. The equivalence between the two formulations will be shown in Section 7.3.

4.2.1 The face-edge liquid

For the liquid we introduce here we allow arbitrary cellulations of a 3-manifold, but we demand that every face is either a triangle or a 2-gon and that every edge is 3-valent or 2-valent (i.e., it is adjacent to three or two faces). A moment of thought reveals that every cell complex can be brought into this form, e.g., a 4-gon can be split into two triangles with a 2-valent edge in between as

$$\text{} \tag{62}$$

Dually, a 4-valent edge can be split into two 3-valent edges with a 2-gon face in between,

$$\text{} \tag{63}$$

There is one 3-index tensor (or, combinatorially, a 3-index atom) associated to every triangle and another 3-index tensor to every 3-valent edge. At every pair of adjacent triangle and 3-valent edge, the corresponding tensors share a contracted index pair, i.e., the corresponding atoms are connected by a bond. The edge tensors are different from the face tensors, thus we use two different shapes to represent them

$$\text{} \tag{64}$$

The combinatorial data of such tensor networks are networks with two kinds of atoms. Different kinds of atoms will be referred to as *elements* of the corresponding substrate. Thus, this substrate has two 3-index elements, whereas the topological substrate from the section above had only one 3-index element. Accordingly, a model of the face-edge substrate consists of two 3-index tensors.

The 2-gons and 2-valent edges are not explicitly represented by atoms. Instead, the two edges adjacent to a 2-gon, and likewise the two faces adjacent to a 2-valent edge are directly connected by a bond. E.g., two 3-valent edges separated by a 2-gon are represented as

$$\text{} \tag{65}$$
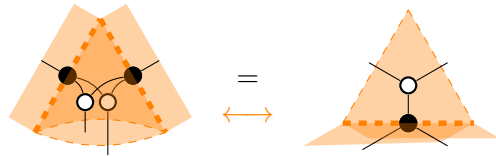
As in $1 + 1$ dimensions, two combinatorial triangulations correspond to the same manifold exactly if they are related by 3-dimensional Pachner moves. For the particular combinatorial network structure chosen here there is an equivalent set of moves, which can be divided into 3 groups.

- Moves involving only triangles separated by 2-valent edges, which equal the 2-dimensional Pachner moves for the face atoms only, namely

$$
\text{(66)}
$$

and the same for the 1-3 Pachner move.

- Moves involving only 3-valent edges separated by 2-gon faces. In terms of cell complexes, those moves are Poincaré dual to the moves above. In network notation they look the same apart from that we have to use filled circles instead of empty circles.

- The most powerful move is the following move relating face and edge elements. It merges two triangles with two shared 3-valent edges into a single triangle with one adjacent 3-valent edge, i.e.,

$$
\text{(67)}
$$

4.2.2 Bi-algebras

As in the $1+$-dimensional case, the present liquid has a great similarity to a well known algebraic structure. To see this, we first note that there is an obvious liquid mapping from the $1 + 1$-dimensional liquid to the present liquid, in which the triangle (as part of the 2-dimensional cell complex) is mapped to the triangle (as part of the 2-dimensional cell complex). Dually to that, there is a liquid mapping in which the triangle is mapped to the 3-valent edge. Thus, by the means of these two mappings every model of the present liquid contains two associative algebras.

Two associative algebras (more precisely, an algebra and a *co-algebra*) are called a *bi-algebra*, if they fulfil certain additional axioms. The main axiom (which states that the co-algebra is an algebra homomorphism) is precisely the move Eq. (67). Thus, the present liquid is basically the bi-algebra liquid, together with a few additional moves which make it "more topological". This observation could be formalized as a liquid mapping from bi-algebras to the present liquid.

4.2.3 Models

Specifying the tensor type to array tensors, we look for models of the liquid, i.e., solutions to the move equations. The similarity to bi-algebras greatly helps assessing the situation: First, we know that bi-algebras fall into a discrete set of families related by basis changes, and so do the models of the present liquid. Second, there are many known examples for bi-algebras, many of which also yield models of the present liquid. Thus, in practice, we can look at the simplest examples of bi-algebras, see whether they can be turned into models of the present liquid, and check whether some of the models are in the same phase. Moreover, we will see that it is "rather unusual" for different models to be in the same phase, and that one can usually show their distinctness by evaluating closed networks.

As a particular example we recall that every group defines a bi-algebra, which can be turned into a model of the present liquid. Those models are equivalent to the *Kitaev quantum double models* [25], which are models for *intrinsic topological order* in $2 + 1$ dimensions. E.g., if we pick the group $\mathbb{Z}_2$, the index configurations are the group elements $\{0, 1\}$, and the edge and face tensors

are

$$
\begin{aligned}
{}_{a}\!\!\diagdown\!\!\!\!\!\underset{c}{\circ}\!\!\!\!\!\diagup\!\!{}^{b} &= \begin{cases} 1 & \text{if } a + b + c = 0 \mod 2 \\ 0 & \text{otherwise} \end{cases}, \\
{}_{a}\!\!\diagdown\!\!\!\!\!\underset{c}{\bullet}\!\!\!\!\!\diagup\!\!{}^{b} &= \begin{cases} 1 & \text{if } a = b = c \\ 0 & \text{otherwise} \end{cases}.
\end{aligned}
\tag{68}
$$

It is easy to see that each tensor satisfies the 2-2 and 1-3 Pachner move, and both tensors together fulfil the move in Eq. (67). Actually, for the sake of simplicity, we are ignoring a global factor of $1/2$ missing in the 1-3 Pachner move for face atoms. This will be fixed in Section 7.2.

This model corresponds to a commuting-projector Hamiltonian model known as the *toric code* [25] defined for qubits on the edges of a square lattice and Hamiltonian given by

$$
H = \sum_i A_i + \sum_j B_j .
\tag{69}
$$

Here, i runs over all plaquettes of the lattice and each A_i is defined as (suppressing the site index)

$$
A = -Z_0 Z_1 Z_2 Z_3 ,
\tag{70}
$$

where $0, 1, 2, 3$ label the 4 edges adjacent to the corresponding plaquette. Dually, j runs over all vertices and

$$
B = -X_0 X_1 X_2 X_3 ,
\tag{71}
$$

where $0, 1, 2, 3$ label the 4 edges adjacent to the corresponding vertex. The commuting projectors themselves can be written as 8-index tensors

$$
P_A = \frac{1}{2}(\mathbb{1} - Z_0 Z_1 Z_2 Z_3) \quad \rightarrow \quad \boxed{\begin{array}{c} a'\ b'\ c'\ d' \\ \hline P_A \\ \hline a\ \ b\ \ c\ \ d \end{array}} ,
$$

$$
P_B = \frac{1}{2}(\mathbb{1} - X_0 X_1 X_2 X_3) \quad \rightarrow \quad \boxed{\begin{array}{c} a'\ b'\ c'\ d' \\ \hline P_B \\ \hline a\ \ b\ \ c\ \ d \end{array}} .
\tag{72}
$$

They are commuting because adjacent plaquettes and vertices always share two adjacent edges, and $Z_0 Z_1$ commutes with $X_0 X_1$. A tensor network representing the imaginary time evolution of the model is given by stacking layers of those commuting projectors.

To compare our topological model with the given commuting-projector model, we need a liquid mapping from the commuting-projector liquid to the topological liquid. A little bit of geometric imagination shows that the replacement

$$
\tag{73}
$$

will turn a stack of commuting projectors into a cellulation of the same space-time. Indeed, we find that via this mapping, the topological model Eq. (68) is mapped to the commuting-projector model Eq. (72).

4.3 Topological models with boundary in $1 + 1$ dimensions

4.3.1 Regular-lattice and extended model

As a third example, let us look at models in $1 + 1$ dimensions with physical boundary, where both the bulk and the boundary have a topological deformability. After Trotterization we obtain a tensor network like the following

$$\tag{74}$$

on a regular square lattice with boundary. So, formally, we have a model of a substrate with two elements, the 4-index circle-shaped element associated to the bulk plaquettes, and the 3-index square-shaped element associated to the boundary edges. The degrees of freedom at the boundary (as well as the Trotterization procedure) can be different from the bulk. Thus, the dimension of the indices contracted between boundary tensors can be different from those of the indices contracted between the bulk tensors, which we denoted by using thicker lines. Combinatorially, there are two different kinds of bonds, which we will refer to as *bindings*. We are generalizing our notion of substrate by associating to each index of each element a binding, and allowing only bonds between indices with the same binding.

The extended model is a model of a substrate representing arbitrary triangulations of $1 + 1$ dimensions-manifolds with boundary. Again, there is one tensor associated to each boundary edge and one tensor associated to each bulk triangle, given by

$$\tag{75}$$

The mapping from the square-lattice substrate to the topological substrate is obvious.

The substrate is turned into a liquid by adding the following moves: First, we have the 2-2 and 1-3 Pachner moves for the triangle element, which makes the liquid from Section 4.1 a sub-liquid of the current liquid. Second, we add the following additional move

$$\tag{76}$$

The geometric interpretation of this move is to attach/remove a triangle to/from the boundary, which allows us to arbitrarily deform the boundary without changing the topology.

4.3.2 Representations and models

As the liquids above, our boundary liquid is again very similar to a very well-known algebraic structure, namely *representations*. A *representation* of an algebra A is a linear map

$$R : V \otimes A \to V \ , \tag{77}$$

satisfying

$$R(R(x, a), b) = R(x, a \cdot b) \ . \tag{78}$$

This equation can written in tensor-network notation, and looks exactly like Eq. (76).

In order to find models of the present liquid, we start with models of the $1 + 1$-dimensional liquid in Section 4.1, and extend them by a choice of boundary tensor. Let's start with the model given in Eq. (37) related to the algebra of functions over some finite set B. For every $x \in B$, there is the corresponding *irreducible representation*, which defines a choice of boundary tensor:

$$
\begin{array}{c} a \\ \bigtriangledown \\ \square \end{array} = \begin{cases} 1 & \text{if} \quad a = x \\ 0 & \text{otherwise} \end{cases} . \tag{79}
$$

The boundary indices without labels are trivial, that is, they have dimension 1. For a 2-element set B, this corresponds to a boundary condition of the Ising model, where any spin near the boundary is fixed to the value x.

4.3.3 Bulk-to-boundary mapping

A 2-manifold with boundary might also be interpreted as a manifold with one puncture for every boundary circle. Imagine filling each such a puncture with a disk. On the combinatorial level, we can do this by adding one additional vertex corresponding to the centre of the disk, and one additional triangle for every boundary edge, spanned by this boundary edge and the central vertex. Consider the boundary-less network for the filled, and the network-with-boundary for the non-filled triangulation. They can be mapped onto each other by reinterpreting the triangle atoms for the additional triangles as the boundary edge atoms for the boundary edges. Such a reinterpretation can be formalized as the liquid mapping

$$
\begin{array}{c} \square \end{array} := \begin{array}{c} \circ \end{array} , \qquad \begin{array}{c} \circ \end{array} := \begin{array}{c} \circ \end{array} . \tag{80}
$$

If we apply this mapping to the move Eq. (76) of the boundary liquid, it turns directly into the 2-2 move in Eq. (31) of the bulk liquid. This example shows two new features of liquid mappings. 1) For a mapping from a substrate (or liquid) with different elements, we have to give one network for each element. 2) If the substrate (or liquid) has different bindings, then each binding of the source liquid is mapped to a binding of the target liquid. In the present example, both the bulk and boundary binding are mapped to the bulk binding,

$$
| := | , \qquad | := | . \tag{81}
$$

In general, each binding of the source substrate can be associated with a collection of bindings of the target substrate, which can contain the same binding multiple times.

5 Topology and non-commutativity

In this section we will revisit the example of topological order in $1+1$ dimensions from Section 4.1 and discuss an important issue that we have not addressed so far. If we want the liquid to represent topological manifolds, we need to add more structure to the network. In particular we will motivate that it is necessary to distinguish the different indices of an element and show how this can be implemented concretely. The additional structure makes the liquid more complicated than the liquid from the previous example. To handle this complexity in the most efficient way, we seek a way to simplify the liquid without losing its ability to describe topological phases. In doing so, we invoke the concept of liquid mappings and introduce the notion of equivalent tensor liquids. We present what we believe to be the simplest representative of a topological liquid in $1+1$ dimensions and classify its phases.

5.1 Distinguishing indices

In Section 4.1, we have represented the triangulation of a manifold by a graph that we referred to as network, with vertices referred to as atoms and edges referred to as bonds. The graph is dual to the triangulation, that is, for every triangle there is one atom, and between every pair of adjacent triangles there is a bond

$$\triangle \quad \rightarrow \quad \curlyvee \quad . \tag{82}$$

We would like the combinatorics of networks and moves to reflect continuum manifolds and homeomorphisms in a faithful way. However, the network combinatorics introduced so far does not uniquely encode the full combinatorial information of the triangulation. Imagine rebuilding the triangulation from the network's graph by replacing each vertex with a triangle and gluing the triangles associated to connected vertices along common edges. We encounter two problems: 1) The combinatorial structure of the graph does not distinguish between the three adjacent bonds, so we cannot tell which edges of the triangles we have to glue together. 2) Two edges can be glued in two opposite ways. E.g., consider the following graph that corresponds to two triangles with all edges glued together pairwise as

$$\bigcirc\!\!-\!\!\bigcirc \quad . \tag{83}$$

This graph does not determine the topology of the resulting manifold. If we glue one of the three edge pairs, we obtain a 4-gon. Depending on how we glue the remaining edges of the 4-gon, we can obtain a sphere, a real projective plane, a torus, or a Klein bottle.

The second problem can be solved by giving each edge an orientation and demanding that those orientations match when we glue two edges of two triangles. The first problem is solved by realizing that any manifold can be triangulated using only triangles with non-cyclic edge orientations [2]. This is also known as a triangulation with a *branching structure*. For a fixed triangle, the non-cyclic edge orientations induce an ordering of its vertices,

$$\begin{array}{c} 1 \\ {}_{01}\!\!\diagup\!\!\diagdown{}_{12} \\ 0 \underset{02}{\bullet\!\!-\!\!\bullet} 2 \end{array} \quad . \tag{84}$$

This allows us to distinguish the three edges and refer to them by their source and target vertex. In our network notation, we allow rotating/reflecting the shapes of individual atoms, which makes it impossible to distinguish the three indices if the shape is a small circle. The shape for the element representing a branching-structure triangle should have less symmetry, which we implement by next-to-shape markers as

$$\begin{array}{c} {}_{01}\!\!\diagdown \quad \diagup{}_{12} \\ \bigcirc \\ {}_{02} \end{array} \quad . \tag{85}$$

The clockwise or counter-clockwise flags allow to uniquely identify the 3 indices of the element with the edges 01, 02 or 12 of the branching structure triangle, as indicated by the red labels. Note that here and in the subsequent, such red labels are not part of the formal graphical notation, but serve as a help to identify the network notation with its geometric interpretation in terms of cell complexes. Networks using the new shape representing a branching structure triangle uniquely specify the triangulation and thus the topology. E.g., the network

$$\bigcirc\!\!=\!\!\bigcirc \tag{86}$$

---

[2]This can be seen by refining a non-oriented triangulation via a construction known as *barycentric subdivision*, which can be equipped with a canonical non-cyclic edge orientation.

represents a sphere unambiguously.

In our new (and final) notion of networks, the indices of an element are always distinct. However, we can still interpret the old notion, where (some of) the indices have not been distinguished. Indistinguishability of indices means that we are allowed to permute them, which is nothing but a move. Now, whenever we choose a shape for an element which has rotation/reflection symmetries due to which we cannot distinguish some of the indices, we implicitly assume that all the corresponding index permutation moves (or better, a set of moves generating all the permutation moves) are part of the liquid. Explicitly, we will denote such permutation moves using cycle notation, e.g.,

$$\overset{a}{\underset{c}{\diagdown}}\overset{b}{\diagup} \;\overset{\text{sym}}{=}\; (ab)\,, \qquad \overset{a}{\underset{c}{\diagup}}\overset{b}{\diagdown} \;\overset{\text{sym}}{=}\; (bc)\,. \tag{87}$$

If we use a shape without any symmetries, such as the one in Eq. (85), the index permutations can be denoted as ordinary moves

$$\overset{a}{\underset{c}{\diagdown}}\overset{b}{\diagup} = \overset{b}{\underset{c}{\diagdown}}\overset{a}{\diagup}\,, \qquad \overset{a}{\underset{c}{\diagdown}}\overset{b}{\diagup} = \overset{a}{\underset{b}{\diagdown}}\overset{c}{\diagup}\,. \tag{88}$$

If we interpret those moves in terms of triangulations, they correspond to cutting out a triangle and gluing it in a different way. Such an operation generally changes the topology of the triangulation. So the liquid we introduced in Section 4.1 has moves which are sufficient to have topological deformability, but also additional moves which go beyond topological deformability. We therefore expect that models of this liquid are too restricted and do not contain the most general fixed point models for topological order.

5.2 Non-simplified liquid

The branching structure/flags also need to be incorporated into the moves of the liquid. There are different ways a branching structure can be added to the Pachner moves. For the 2-2 Pachner moves (keeping in mind moves are not actually different if they are just rotated/reflected or we exchanged the left and right side), we count 3 different versions. One of them is

$$\begin{array}{c}\text{(diagram)}\end{array} \quad \leftrightarrow \quad \begin{array}{c}\text{(diagram)}\end{array}\,. \tag{89}$$

Another one can obtained by, e.g., inverting the orientation of the $2-3$ edge. Note that if we glue the two patches above at their boundary, we obtain the surface of a branching-structure tetrahedron. In general, every Pachner move corresponds to a decomposition of that tetrahedron into two parts, and the 3 versions of the 2-2 Pachner move correspond to the 3 different decompositions of the tetrahedron into two faces on each side.

In the new network notation, the move becomes

$$\begin{array}{c}\text{(diagram)}\end{array} = \begin{array}{c}\text{(diagram)}\end{array}\,. \tag{90}$$

The red labels identify the atoms in the network with the triangles in the geometric interpretation. E.g., 023 refers to the triangle in Eq. (89) whose 0-vertex is the vertex 0, 1-vertex is 2, and 2-vertex

is 3. Note again that the red labels are only hints for the reader and not part of the actual notation. Also, the open index labels were chosen in accordance with the names of the corresponding edges.

Analogously, there are now 4 different versions of the 1-3 Pachner move, corresponding to the 4 decompositions of the branching structure tetrahedron into two patches with 1 and 3 triangles each. One of them is

$$\leftrightarrow \qquad . \tag{91}$$

As some sort of convention, we might also want to introduce the following *triangle cancellation move*

$$\leftrightarrow \quad , \tag{92}$$

implying that a non-cyclic 2-gon can be shrunk to a single edge, which is represented by a free bond in network notation as

$$_{02l} \quad = \quad _{02l} \text{———} _{02r} \quad . \tag{93}$$

If we glue one edge of the left hand side of Eq. (92) to one boundary edge of any patch of a triangulation (including itself), this can be undone with Pachner moves. So the Pachner moves imply that the corresponding tensor is a projector, and contracting any index of any other tensor of the model with this projector yields the same tensor again. However, they do clearly not imply the triangle-cancellation move, and formally, the liquids with and without that move are inequivalent (in a sense that we will make precise soon).

However, when considering ordinary models of the liquid (with real or complex tensors), Eq. (93) can be viewed as a convention that does not hurt to impose. The projector in Eq. (93) has a n-dimensional support, and there exists an isometry which identifies this n-dimensional support with an n-dimensional vector space. Applying this isometry to every index of every tensor yields a model which is equivalent, as the tensors are invariant under applying the corresponding projector. In doing so, the tensor corresponding to the projector itself becomes the identity matrix.

In total, we end up with a liquid with 8 moves that we refer to as the "non-simplified liquid". As the moves correspond to equations between tensor networks that we need to solve in order to find models, it is important that the moves of a liquid are as simple as possible. In the following, we will find a "simplified liquid" which is equivalent to the non-simplified liquid, but has less and simpler moves.

5.3 Simplified liquid

The simplified liquid has one additional element whose geometric interpretation is a 2-gon cell with cyclic edge orientations,

$$\rightarrow \quad _{01} \text{———} _{10} \quad . \tag{94}$$

The new element will be denoted by a circle as well, however, it can be distinguished from the triangle element due to the different number of indices. Of course, a 2-gon cannot be embedded non-degenerately into Euclidean space without bending its edges. But this is no cause of a problem as we are talking about combinatorial/topological cell complexes and not geometric ones. The 2-gon is rotation symmetric which corresponds to a move

$$a \text{———} b \overset{\text{sym}}{=} (ab) \tag{95}$$

justifying the choice of shape. This move can be derived from the moves below, however.

The moves of the simplified liquid only contain one single Pachner move, namely the 2-2 Pachner move in Eq. (90). All other 2-2 Pachner moves can be derived via additional moves of the simplified liquid related to symmetries of the triangle. In contrast to the liquid in Section 4.1, rotating or reflecting the triangle would change the branching structure. However, the changes of the edge orientations can be undone by gluing the cyclic 2-gon to the involved edges. This yields, e.g., the *(12)-triangle symmetry move*

$$\text{(96)}$$

where the nomenclature refers to effectively interchanging the role of the vertices 1 and 2. In network notation, this is

$$\text{(97)}$$

In order to generate the full symmetry group S_3 of the triangle, one only needs one further move, the *(01) triangle symmetry move*

$$\text{(98)}$$

Again, in network notation, this amounts to

$$\text{(99)}$$

The 1-3 Pachner moves can be derived from the 2-2 Pachner moves via the triangle cancellation move in Eq. (93), which is also part of the simplified liquid. Analogously, there is the *2-gon cancellation move*

$$\text{(100)}$$

In network notation, we have

$$a \rightarrow\!\!\bigcirc\!\!\rightarrow\ \rightarrow\!\!\bigcirc\!\!\rightarrow b = a \!-\!\!- b \ . \tag{101}$$

5.4 Equivalence of the simplified and non-simplified liquid

In this section, we will motivate why the simplified and non-simplified liquids are "equivalent". For this, we should be able to rewrite networks of the simplified liquid as networks of the non-simplified liquid, and vice versa. This can be formalized by two liquid mappings $\mathcal{M}_1$ and $\mathcal{M}_2$, going from the non-simplified liquid to the simplified liquid, and back.

Note that the elements of the non-simplified liquid are identified with a subset of the elements of the simplified liquid. So there is a "trivial" candidate for the mapping $\mathcal{M}_1$, mapping the triangle of the non-simplified liquid to the triangle of the simplified liquid. In order to show that this defines indeed a liquid mapping, we need to show that the mapped non-simplified moves are derived from the simplified moves. As the mapping is "trivial", the mapped non-simplified moves just look like the non-simplified moves.

- One of the branching-structure 1-3 Pachner moves is derived from the 2-2 Pachner move in Eq. (90) and the triangle cancellation move in Eq. (93):

$$\text{(102)}$$

- All other versions of branching structure 2-2 Pachner moves are derived from the 2-2 Pachner move in Eq. (90), together with the two triangle symmetry moves. E.g., the following 2-2 Pachner move

$$\leftrightarrow \qquad \text{(103)}$$

is derived by

$$\text{(104)}$$

The bar over the referenced equation denotes that the move is applied from right to left.

- Similarly, all other 1-3 Pachner moves are derived from the move above in Eq. (102), together with the 2-gon cancellation move and the triangle symmetry moves.

The mapping $\mathcal{M}_2$ is only slightly more complicated.

- The triangle part of both liquids and accordingly mapped onto the itself (as part of the non-simplified liquid).

- A 2-gon cell can be triangulated using two triangles

$$\rightarrow \qquad \text{(105)}$$

Accordingly, the mapping for the 2-gon is given by

$$a \,\text{—}\bigcirc\text{—}\, b := a \,\text{—}\bigcirc\bigcirc\text{—}\, b \ . \qquad \text{(106)}$$

Again, we have to find derivations for the mapped simplified moves from the non-simplified moves. E.g., if we plug the mapping Eq. (106) into the 2-gon cancellation move Eq. (101), we obtain

$$a \,\text{—}\bigcirc\bigcirc\text{—}\bigcirc\bigcirc\text{—}\, b = a \,\text{—}\, b \ . \qquad \text{(107)}$$

This can be derived by 1) a 2-2 Pachner move, 2) a 1-3 Pachner move, and 3) the triangle cancellation move. We will not explicitly give derivations for each mapped move here. Instead, we would

like to remark that the mapped moves (except for the 2-gon and triangle cancellation moves) correspond to re-triangulations of a disk. It is known that any two triangulations of the same (piece-wise linear) manifold are related by a sequence of Pachner moves [24]. So, if we rely on this statement about the geometric interpretation, we know that derivations for all mapped moves must exist.

So, we have found two liquid mappings going from the non-simplified liquid to the simplified liquid and back. However, this alone does not really mean anything, e.g., between any two liquids there's the *trivial mapping* which maps every binding to the empty collection of bindings, and every element to the empty network. What we additionally need is that that if we go from the non-simplified liquid to the simplified liquid and back, we end up with the same network. In other words, $\mathcal{M}_2 \circ \mathcal{M}_1$ should be the identity, and the same should hold for $\mathcal{M}_1 \circ \mathcal{M}_2$.

We find indeed that $\mathcal{M}_2 \circ \mathcal{M}_1$ is the identity on the triangle, and also $\mathcal{M}_1 \circ \mathcal{M}_2$ is the identity on the triangle. However, if we apply $\mathcal{M}_1 \circ \mathcal{M}_2$ to the cyclic 2-gon

$$a \rightarrow\!\!\bigcirc\!\!\rightarrow b \overset{\mathcal{M}_2}{:=} a \rightarrow\!\!\bigcirc\!\!\bigcirc\!\!\bigcirc\!\!\rightarrow b \overset{\mathcal{M}_1}{:=} a \rightarrow\!\!\bigcirc\!\!\bigcirc\!\!\bigcirc\!\!\rightarrow b \ , \tag{108}$$

we find that it does not map the 2-gon to itself. This is again fine, as the equation between the very left and the very right is a derived move of the simplified liquid,

$$a \rightarrow\!\!\bigcirc\!\!\rightarrow b \overset{\overline{(93)}}{=} a \rightarrow\!\!\bigcirc\!\!\bigcirc\!\!\bigcirc\!\!\rightarrow b$$

$$\overset{\overline{(101)}}{=} a \rightarrow\!\!\bigcirc\!\!\overset{\bigcirc}{\underset{}{\bigcirc}}\!\!\bigcirc\!\!\bigcirc\!\!\rightarrow b \tag{109}$$

$$\overset{(97)^2}{=} a \rightarrow\!\!\bigcirc\!\!\bigcirc\!\!\bigcirc\!\!\bigcirc\!\!\rightarrow b \overset{(99)}{=} a \rightarrow\!\!\bigcirc\!\!\bigcirc\!\!\bigcirc\!\!\rightarrow b \ .$$

If we apply $\mathcal{M}_1 \circ \mathcal{M}_2$ to any model of the simplified liquid, we will get the same model again. So the models of the simplified liquid are in one-to-one correspondence with the models of the non-simplified liquid, which motivates the use of the word "equivalent". We will call two mappings such that both $\mathcal{M}_2 \circ \mathcal{M}_1$ and $\mathcal{M}_1 \circ \mathcal{M}_2$ are the identity up to moves *weak inverses* of another. Two liquids are considered *equivalent* if there are mappings between them which are weak inverses, and equivalence classes of liquids will be referred to as *liquid classes*.

One might think that reducing the number of moves from 8 to 5 is not a significant improvement. Let us justify why it actually is. The key task is finding models for our liquid, which means solving the tensor-network equations given by the moves. As a measure of "complexity" of a liquid it thus makes sense to consider the computational cost of evaluating the two networks of each move, and in particular its scaling with the index dimension d. This scaling is always polynomial, but the exponents depend on the move. Very roughly, the exponent will increase proportionally to the "linear size" of a network. Thus, we have a strong preference for moves with small networks. For evaluating a 2-2 Pachner move we need of the order of d^5 $+$ and $\cdot$ operations. The same holds for a 1-3 Pachner move. All other moves in this section have smaller exponents and thus have a vanishing contribution to the overall complexity when scaling d. So from that perspective we have reduced the complexity from 7 moves to 1 move rather than from 8 to 5 moves.

5.5 Models

We might look for models of the liquid with complex tensors as tensor type. However, we will see in Section 6, that such models are unphysical, as they are not Hermitian. In contrast, models with real tensors as tensor type have a physical interpretation, namely as fixed-point models for topological order in spin systems protected/enriched by a *time-reversal symmetry*: For a spin system, a time-reversal symmetry is an anti-unitary which squares to the identity. We can always change the basis, such that this anti-unitary is given by complex conjugation in that basis. Then, obeying the symmetry means that all tensors of the model are only allowed to have real entries.

5.5.1   Matrix algebra models

The point of this section was to get rid off all index permutation symmetries. For the related algebra liquid, this corresponds to removing the commutativity axiom. Thus, also non-commutative algebras yield models of the new liquid, such as the algebra of $n \times n$ matrices (for any n):

$$
\begin{array}{c}
a_0 b_0 \quad a_1 b_1 \\
M \\
a_2 b_2
\end{array}
= (n^{-1/2})
\begin{array}{c}
a_0 \quad b_1 \\
b_0 \quad a_1 \\
\\
b_2 a_2
\end{array}
\quad . \tag{110}
$$

However, we observe that this model is not in an interesting phase. If we consider the network representing some triangulation and use the tensors from Eq. (110), we see that it decomposes into disconnected loops around vertices and scalars $n^{-1/2}$ at every triangle. Each loop evaluates to the scalar n. Physically, a tensor network consisting only of scalars corresponds to a trivial model without any degrees of freedom.

Another way to motivate that this model is trivial is to see that due to the quantum mechanical interpretation of the model we can generally neglect scalar pre-factors. This is because the predictions of a quantum model are tensors whose entries are probabilities of measurement outcomes, which have to sum to 1. Alternatively, we can be fine with any tensor and fix the latter constraint by hand by normalizing with a prefactor. Then, tensors which differ by a prefactor correspond to the same physical predictions. The measurement-outcome tensors can be obtained by simply contracting space-time tensor networks containing the time-evolution tensors of the model as well as state-preparation and measurement tensors [18]. Instead of neglecting prefactors after contraction, we can already do this at the level of the single tensors constituting the model. As neglecting pre-factors is compatible with Kronecker products and Einstein summations, "arrays modulo prefactors" defines another tensor type, which we will refer to as *projective tensors*. If we interpret the model in terms of projective tensors, it is actually formally in a trivial phase.

Mathematically, the evaluation of such a model can be computed as a sum of local numbers after taking the logarithm of each scalar, which is known as a *classical invariant* of a manifold. Simple combinatorics shows that the evaluation is given by n^χ, where χ is a classical invariant known as the *Euler characteristic* of the manifold.

5.5.2   Quaternion models

Another model is given by the quaternion algebra, whose indices take values in the set $\{\mathbf{1}, \mathbf{i}, \mathbf{j}, \mathbf{k}\}$,

$$
\begin{array}{c}
a \quad\quad b \\
\mathbb{H} \\
c
\end{array}
=
\begin{cases}
1/2 & \text{if} \quad b = \mathbf{1} \text{ and } a = c \\
1/2 & \text{if} \quad a = \mathbf{1} \text{ and } b = c \\
1/2 & \text{if} \quad (a, b, c) \text{ is even permutation of } (\mathbf{i}, \mathbf{j}, \mathbf{k}) \\
-1/2 & \text{if} \quad (a, b, c) \text{ is even permutation of } (\mathbf{i}, \mathbf{k}, \mathbf{j}) \\
-1/2 & \text{if} \quad c = \mathbf{1} \text{ and } a = b \\
0 & \text{otherwise}.
\end{cases}
\tag{111}
$$

If we interpret this algebra as a complex algebra, it is isomorphic to the algebra of 2×2 matrices, which would correspond to a physically trivial model again. However, as a real algebra it is distinct from any matrix algebra or δ-algebra, and corresponds to a non-trivial phase. This can again be seen by evaluating the model for a closed network representing a non-orientable manifold, e.g., on the real projective plane, where we get -2. The fact that the model becomes trivial when we drop the reality constraints indicates that we have a model for a time-reversal *SPT phase*, i.e., a phase which becomes trivial after we allow breaking the symmetry, in contrast to a *symmetry breaking phase* or a *symmetry enriched topological (SET)* phase.

5.5.3 Cluster Hamiltonian

The quaternion algebra model is equivalent to a commuting-projector model known as *cluster Hamiltonian* [26, 27], which is known to represent the only non-trivial SPT phase protected by time-reversal symmetry in $1 + 1$ dimensions [28]. The Hamiltonian is given by

$$H = \sum_i -X_{i-1} Z_i X_{i+1} \ . \tag{112}$$

Its time reversal symmetry is given by the anti-unitary operator

$$T = K \bigotimes_i Z \ , \tag{113}$$

where K denotes complex conjugation. After a change of basis, the time-reversal symmetry operator is given by complex conjugation in that basis alone:

$$H = \sum_i -Y_{i-1} Z_i Y_{i+1} = \sum_i (XZ)_{i-1} Z_i (XZ)_{i+1} \ ,$$
$$T = K \ . \tag{114}$$

The local ground state projector acting on three neighbouring qubits is given by

$$P = (1 - XZ \otimes Z \otimes XZ)/2 \ . \tag{115}$$

In order to compare the cluster Hamiltonian with our liquid model, we actually have to break translation invariance, and block pairs of neighbouring qubits. The new local ground state projector acting on two qubit pairs is given by the product of two old ground state projectors, i.e.,

$$P_{\text{blocked}} = (1 - XZ \otimes Z \otimes XZ \otimes \mathbb{1})$$
$$(1 - \mathbb{1} \otimes XZ \otimes Z \otimes XZ)/4$$
$$= (1 - XZ \otimes Z \otimes XZ \otimes \mathbb{1} - \mathbb{1} \otimes XZ \otimes Z \otimes XZ$$
$$- XZ \otimes X \otimes X \otimes XZ)/4 \ . \tag{116}$$
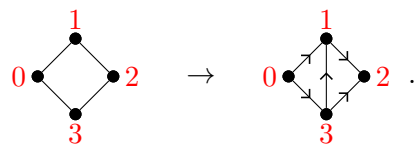
As in Section 4.1, this projector is interpreted as a 4-index tensor

$$\tag{117}$$

which defines a model of a liquid for rhombus-like cellulations of space-time.

Again, the comparison between the topological liquid model and the commuting-projector model is done by a liquid mapping. As before, the geometric interpretation is given by refining the "rhombic cellulation" of spacetime into a triangulation

$$\tag{118}$$

The only difference is that now the triangulation has a branching structure. In network notation, we get

$$\tag{119}$$

To show that the mapping above is in fact an equality for the chosen models, we identify the basis elements of the quaternion algebra $\{\mathbf{1}, \mathbf{i}, \mathbf{j}, \mathbf{k}\}$ with the two-qubit configurations $\{|0,0\rangle, |0,1\rangle, |1,0\rangle, |1,1\rangle\}$ and write the tensors appearing in Eq. (119) as a collection of two-qubit operators from the vector space associated to index a to the vector space associated to the index b, indexed by the index c

$$
\begin{aligned}
&\raisebox{-1.5em}{$\overset{b}{\underset{a}{\bigcirc}}$}\!\!-c = \left(\mathbb{1} \otimes \mathbb{1}, \mathbb{1} \otimes XZ, XZ \otimes Z, XZ \otimes X\right)/2\,, \\[1em]
&c-\!\!\raisebox{-1.5em}{$\overset{b}{\underset{a}{\bigcirc}}$} = \left(\mathbb{1} \otimes \mathbb{1}, -Z \otimes XZ, -XZ \otimes \mathbb{1}, X \otimes XZ\right)/2\,.
\end{aligned}
\tag{120}
$$

Summing over the index c yields the right hand side of Eq. (116), which shows that our liquid model is equivalent to the cluster Hamiltonian model under the chosen mapping.

6 Orientation and unitarity

In this section we will provide a liquid whose models have a standard quantum mechanical interpretation, by adding an orientation and a Hermiticity move to the liquid from the previous section. The corresponding models are basically equal to 2-dimensional *lattice TQFTs* as formulated in Ref. [29].

6.1 Hermiticity and orientation-reversal

Objects like Hamiltonians, state vectors or time evolution operators, which occur in the usual pure-state formulation of quantum mechanics, are complex tensors. A "physical" Hamiltonian is Hermitian, which means that interchanging input and output indices of the corresponding complex tensor is equal to complex conjugation, e.g.,

$$
\raisebox{-1.5em}{$\overset{a\quad b}{\underset{a'\ b'}{\boxed{H}}}$} = \raisebox{-1.5em}{$\overset{a'\ b'}{\underset{a\ \ b}{\boxed{H^*}}}$} := \raisebox{-1.5em}{$\overset{a'\ b'}{\underset{a\ \ b}{\boxed{H}}}$}_K .
\tag{121}
$$

As complex conjugation is not part of network notation, we introduce the following extension to network notation. Every part of a network encircled by a line of the following style

$$
\overset{K}{\wwwwwwwwwwww}
\tag{122}
$$

will be complex conjugated. We will sometimes omit the label K. Complex conjugation commutes with tensor products and contractions, which gives us diagrammatic equivalences such as

$$
\raisebox{-1.5em}{$b-\boxed{}\,\triangleright$}^{a\qquad d}_{c\qquad e} = \raisebox{-1.5em}{$b-\boxed{}\,\triangleright$}^{a\qquad d}_{c\qquad e} = \raisebox{-1.5em}{$b-\boxed{}\,\triangleright$}^{a\qquad d}_{c\qquad e} = \raisebox{-1.5em}{$b-\boxed{}\,\triangleright$}^{a\qquad d}_{c\qquad e} .
\tag{123}
$$

The Hermiticity of the Hamiltonian carries over to the tensors of the tensor network in the Trotterized imaginary time evolution, and implies that inverting the time direction is equivalent to complex conjugation. In a topological manifold there is no "time direction", but inverting any direction is still an orientation-reversing map. Thus, a "physical" model of a topological liquid

in complex tensors should have the property that orientation reversal equals complex conjugation. The networks of the liquids we introduced so far represent manifolds without an orientation, so it's impossible to formulate the Hermiticity condition for their models.

On the other hand, we could say that for liquids without orientation, orientation reversal is a trivial operation. Thus, for models of such liquids the Hermiticity condition implies that they are invariant under complex conjugation alone, i.e., purely real. As we have seen Section 5, such models are indeed physical and correspond to phases with a time-reversal symmetry.

There is the possibility of real models of unoriented liquids to emulate general physical models (even ones without time-reversal symmetry) by increasing the bond dimension, called *realification* (cf. Ref. [18, 30]). Realification is an operation that maps every Hermitian complex model of an oriented liquid to a real model of the corresponding unoriented liquid, such that the former can be identified with a subset of the latter. However, it is more straight-forward to add an orientation to the liquid and consider models with complex tensors.

6.2 Non-simplified liquid

An orientation can be added to a triangulation by specifying for each triangle whether it is oriented "clockwise", or "counter-clockwise". Clockwise and counter-clockwise triangles are represented by two different elements in a network. The clockwise triangle is defined by the fact that its 01 edge (with respect to the branching structure) is oriented clockwise,

$$\tag{124}$$

The opposite is true for the counter-clockwise triangle

$$\tag{125}$$

In network notation, the two elements are distinguishable, as we add an inward arrow marker to every index corresponding to a clockwise oriented edge. The clockwise triangle has two clockwise edges, whereas the counter-clockwise triangle only has one. As we allow reflecting the shapes of individual atoms in a network, it would be impossible to distinguish the two input indices of the clockwise triangle. To fix this problem, we add a little "spiral" to the circle, which defines what the counter-clockwise direction is.

In an oriented triangulation every edge is a clockwise edge of one triangle, and a counter-clockwise edge of another triangle. Thus, the networks obey the constraint that every bond is between an index with an arrow and an index without an arrow. Alternatively, the diagrams can be interpreted as instances of a slightly refined graphical calculus, where indices are divided into *output* and *input* indices, and bonds must always connect one input and one output index. The refined graphical calculus can be fulfilled by more general data structures, namely tensor types where each basis has a *dual*. For all the tensor types in this work (i.e., arrays and fermionic tensors) the dual will be trivial. Thus, we will not explicitly distinguish input and output indices.

Each Pachner move exists with two different orientations as well. So naively we would end up with a liquid with 14 Pachner moves plus the triangle cancellation move (which is reflection symmetric), which we will call the "non-simplified liquid". Alternatively, we could take the simplified unoriented liquid with two copies of every element and every move (unless they are reflection symmetric). However, there is a simpler equivalent liquid, as the next section shows.

6.3 Simplified liquid

The simplified liquid contains the clockwise triangle in Eq. (124) as an element, but not the counter-clockwise triangle. The latter can be constructed from the former by gluing with a cyclic 2-gon, as shown in Eq. (135). For the cyclic 2-gon, we take both the clockwise and counter-clockwise version,

$$
\tag{126}
$$

The moves only contain a single 2-2 Pachner move, namely the one consisting of only clockwise triangles

$$
\tag{127}
$$

In the oriented case, the triangle only has a $\mathbb{Z}_3$ rotation symmetry, generated by the *(120) triangle symmetry move*

$$
\tag{128}
$$

In network notation we have

$$
\tag{129}
$$

Furthermore, there are two cancellation moves. The triangle cancellation move depicted in Eq. (92) has one clockwise and one counter-clockwise triangle. The latter is not part of our elements, so the *oriented triangle cancellation move* has the cyclic 2-gon instead a free bond on the other side:

$$
\tag{130}
$$

In network notation, we find

$$
\tag{131}
$$

Second, the *oriented 2-gon cancellation move* is

$$
a \rightarrow\hspace{-0.3em}\bigcirc\hspace{-0.3em}\leftarrow \bigcirc\hspace{-0.3em}— b = a — b \ . \tag{132}
$$

The clockwise 2-gon is rotation symmetric, so we would expect the following symmetry move

$$
a \rightarrow\hspace{-0.3em}\bigcirc\hspace{-0.3em}\leftarrow b \overset{\text{sym}}{=} (ab) \ , \tag{133}
$$

which is also implied by the choice of shape. Indeed, this move is directly derived from the oriented triangle cancellation move in Eq. (131). The analogous symmetry move for the counter-clockwise 2-gon

$$
a — \bigcirc\hspace{-0.3em}— b \overset{\text{sym}}{=} (ab) \tag{134}
$$

can be derived from the oriented 2-gon cancellation move. The proof that the non-simplified and simplified liquids are equivalent is analogous to the non-oriented case.

6.4 Hermiticity move

As we mentioned above, physical models should obey the Hermiticity condition that orientation reversal equals complex conjugation. Using the extended network notation introduced in Eq. (122), this condition can be written down as a move as well. This move equates the complex conjugated clockwise triangle and the counter-clockwise triangle. The latter can be constructed from the former by gluing a cyclic 2-gon according to

$$
\tag{135}
$$

One would expect that we also need to add the analogous move which relates the clockwise 2-gon and the counter-clockwise 2-gon via complex conjugation. However, this move can be derived from the moves defined so far. For the sake of demonstrating how to operate with networks containing (complex conjugation) mappings, we will explicitly give the derivation

$$
\tag{136}
$$

6.5 Models

As in the unoriented case, the oriented liquid is equal to associative algebras with some extra axioms, and thus, its models can be classified. Complex models of the oriented Hermitian liquid are not actually more general than real models of the unoriented liquid: By a change of basis, each complex model can be brought into a form where it is purely real. Contrary, there are even less models, in the sense that models which are in different phases as real models can be in the same phase as complex models.

An example for this is the model coming from the quaternion algebra. As a complex model, it is equal to the model coming from the 2×2 matrix algebra, after the following basis change:

$$
G := 2^{-1/2} \left(\mathbb{1}, iX, iZ, iY \right) \,,
\tag{137}
$$

where X, Z and Y are the corresponding Pauli matrices, and the four entries correspond to $\mathbf{1}, \mathbf{i}, \mathbf{j}$, and $\mathbf{k}$. If we choose an ordering of the four entries of 2×2 matrices, we can write G properly as a 4×4 unitary matrix.

6.6 Invertibility

In this section, we look at invertible models, and see how invertibility can be phrased as a set of moves going beyond the topological moves introduced so far. A model or phase is said to be *invertible* if "stacking two orientation-reversed copies yields a trivial phase". Thus, there must be a circuit move which transforms this double-layered tensor network into the empty tensor network. One way of ensuring this is to demand invariance not only under homeomorphisms, but also under the following *surgery operations*:

- A 0-surgery (or, equivalently, a backwards 3-surgery) consists in removing a 2-sphere

$$
\leftrightarrow \qquad .
\tag{138}
$$

- A 1-surgery (or backwards 2-surgery) consists in cutting out an annulus and pasting two disks

$$\leftrightarrow \qquad . \tag{139}$$

Two manifolds are related by surgery operations iff they are cobordant, i.e., their disjoint union can be identified with the boundary of a manifold of one dimension higher. Two layers of 2-manifold can be removed by a circuit move using surgery operations as

$$\rightarrow \qquad \rightarrow \qquad \rightarrow \qquad . \tag{140}$$

We start by applying 2-surgeries with one disk in each of the two layers, as indicated by the blue circles. This yields a "double-layer with holes". For each pair of neighbouring holes there is a non-contractible loop winding through both of them. Next, we apply a 1-surgery to the annulus-like neighbourhood of every such non-contractable loop, (whose boundaries were indicated by blue lines). This yields a collection of disconnected 2-spheres, which can be removed by 0-surgeries.

Combinatorially, surgery operations can be implemented by the following moves.

- The 0-*surgery move*

$$\leftrightarrow \qquad , \tag{141}$$

where the left hand side depicts a cellulation of a sphere by a clockwise (front) and a counter-clockwise (back) 2-gon, and the right hand side is the empty manifold. In network notation, this looks like

$$= \qquad . \tag{142}$$

- The 1-*surgery move*

$$\leftrightarrow \qquad , \tag{143}$$

where the left hand side depicts a triangulation of an annulus, and on the right we have a triangulation of two disks. In network notation, we find

$$00 \xrightarrow{001} \xleftarrow{011} 11 \;=\; 00 \xrightarrow{002} \qquad \xleftarrow{113} 11 \;. \tag{144}$$

Note that both moves are non-topological, as at least one of their networks (in fact both) does not represent a disk. In particular, the right hand side of the 1-surgery move consists of two disconnected components.

Models of the invertible liquid are models of the topological liquid which fulfil the additional equations Eq. (142) and Eq. (144). As such only the trivial model (every tensor being equal to the number 1) fulfils these equations. However, physically it is fine if the equations only hold up to

pre-factors, such that we can ignore Eq. (142) as it is only equates scalars. In this case, also the model based on the matrix algebra in Eq. (110) is invertible, as plugging it into Eq. (144) yields

$$
\begin{array}{c} a \\ a' \end{array} \!\!\!\!\!\! \text{(diagram)} \!\!\!\!\!\! \begin{array}{c} c \\ c' \end{array} = \begin{array}{c} a \\ a' \end{array} \!\!\!\!\!\! \text{(diagram)} \!\!\!\!\!\! \begin{array}{c} c \\ c' \end{array} . \tag{145}
$$

As we have seen in Section 5.5, this model is still in a trivial phase, as the defining tensor is a tensor product of three identity matrices and thus the resulting network can be reshaped into a product of independent loops. However, it can become non-trivial if we add symmetries. That is, we equip each index with a representation of a group (or some form of Hopf algebra, see Ref. [19]). Tensors with symmetries (of a fixed group) constitute a different tensor type, as symmetries are consistent with contraction and tensor product.

The tensor in Eq. (110) can be equipped with many different symmetries. In particular having a representation act twice on each of the two (row and column) index components independently leaves the tensor invariant, because each of the three identity matrices is invariant under that symmetry separately. For that exact same reason though, the model with such symmetries is still in a trivial phase. So we need a representation that does not split into a product of two representations on the two index components. One possibility for that is to take a projective representation on each of the two components, such that both projective representations together form a proper representation on the composite index. The simplest group which has a non-trivial projective representations is the Klein 4-group $\mathbb{Z}_2 \times \mathbb{Z}_2$. The projective representation R is given by the Pauli matrices:

$$
\begin{aligned}
R((0,0)) &= \mathbb{1}, & R((0,1)) &= X, \\
R((1,0)) &= Z, & R((1,1)) &= iY .
\end{aligned} \tag{146}
$$

In Section 5.5, we have seen models for SET (or SPT) phases protected by a time-reversal symmetry. The present model is an example for an SPT phase protected by an ordinary symmetry, which is also invertible. Note that projective representations are classified by the second $U(1)$-valued cohomology group of the symmetry group, and our liquid models are equivalent to the isometric MPS in Ref. [31] and to the models in terms of "dimer cristals" in Ref. [28].

6.7 Vertex weights

As a last point, let us briefly discuss the following variant of the above liquid, which is slightly more general. The main reason for introducing this variant is that it shows up as sub-liquid of a $2 + 1$-dimensional liquid in Section 7.2.

- The variant has one more element, called the *vertex weight*

$$
\text{—}\square\!\!\leftarrow . \tag{147}
$$

- The *weighted oriented triangle cancellation move* replaces the oriented triangle cancellation move

$$
a \rightarrow \!\!\bigcirc\!\!\frown\!\!\bigcirc\!\!\leftarrow b = a \rightarrow\!\!\bigcirc\!\!\leftarrow b . \tag{148}
$$

- There is the additional *weight commutation move*

$$
a \rightarrow\!\square\!\rightarrow\!\!\bigcirc\!\!— b \atop c = a \rightarrow\!\!\bigcirc\!\!\rightarrow\!\square\!— b \atop c . \tag{149}
$$

Every vertex of the triangulation corresponds to a loop of bonds in the network. Each vertex weight is bound to one such loop, that is, it can be moved around that loop using the weight

commutation and other moves. Topological manifolds are represented by networks, where each loop has exactly one vertex weight bound to it. Vertices/loops with more or less vertex weights can never be removed, as the weighted cyclic triangle cancellation move involves exactly one vertex weight. Thus, they should be thought of as some kind of singularity. The position of the vertex weight corresponds to an edge in the triangulation, which can be interpreted as the "favourite edge" of the corresponding vertex. The weight commutation move makes the evaluation of networks independent of those favourite edge decorations.

The variation is "more general" than the original liquid, in that there is a liquid mapping

$$a—\square\!\!\!\!\leftarrow b := a——b \tag{150}$$

from the variant to the original liquid, but no obvious inverse mapping. Indeed, the models of the variant (in real array tensors) are slightly more general. E.g., for each $\alpha \in \mathbb{R}$ [3], there is the following model where all tensors are scalars: The triangle is the scalar $\alpha^{-1/2}$, the 2-gons are the scalar 1, and the vertex weight is the scalar α. One can easily see that the evaluation of this model on a space-time manifold M is $\alpha^{\chi(M)}$, where χ is the euler characteristic. Note, however, that as a physical model using projective tensors (as explained in Section 5.5), this model is immediately trivial. In fact, using this tensor type, we do not get any new phases compared to the liquid without vertex weights.

7 Non-chiral topological order in $2+1$ dimensions

In this section, we discuss *non-chiral intrinsic* topological order for spin systems, i.e., systems without fermionic degrees of freedom. Whereas global symmetries and fermions (see Section 8) can be easily incorporated into our framework, it is an open question whether there exist models for topological liquids which represent chiral phases. For all liquids presented in this paper there are mappings from a commuting-projector liquid, and there exist no-go theorems about commuting-projector models describing chiral phases [32]. In our framework we can circumvent those no-go theorems as there exist more general liquids which do not yield commuting-projector models (cf. Ref. [33]), however, concrete examples of models representing chiral phases remain elusive as of to date. On the contrary non-chiral topological order is well captured within our formalism and we illustrate this fact by providing two different, yet equivalent topological liquids that cover the most general known models of non-chiral topological order.

7.1 Volume liquid

In this section we describe a liquid whose models are similar to fixed point models originally introduced as a state-sum invariant by Turaev and Viro [34, 35]. Later this construction has been rephrased as a Hamiltonian model for topological order by Levin and Wen [36] referred to as string-net models. The liquid we present here is a straight forward generalization of the oriented topological liquid in $1+1$ dimensions from Section 6 to $2+1$ dimensions.

7.1.1 The non-simplified liquid

A 3-manifold can be represented by a simplicial complex (a decomposition of the manifold into tetrahedra) with the following 3-dimensional Pachner moves. The 2-3 Pachner move replaces two tetrahedra glued together at a single face with three tetrahedra glued together such that each pair

---

[3]If we drop the hermiticity move, this is a model also for complex α.

of tetrahedra shares one common face and all three tetrahedra share a common edge

$$\leftrightarrow \qquad . \tag{151}$$
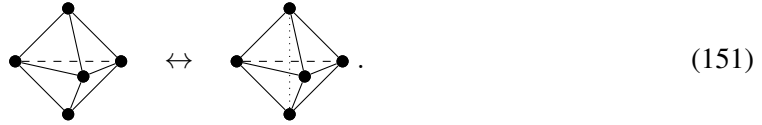
The 1-4 Pachner move replaces a single tetrahedron with 4 tetrahedra, such that every pair shares a common face, every collection of three tetraheda shares a common edge and all tetrahedra share a common vertex

$$\leftrightarrow \qquad . \tag{152}$$
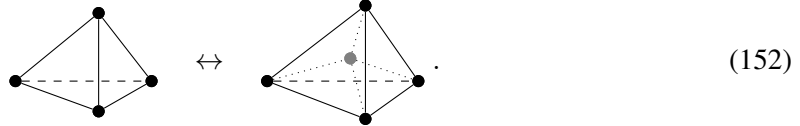
A triangulation is represented by a network with one 4-index atom at every tetrahedron, and one bond between each pair of tetrahedra sharing a face. In order to obtain a liquid with models for a very general class of topological phases, we have to take care of the following details.

To properly represent 3-dimensional manifolds combinatorially, we need to distinguish the different faces of a tetrahedron. On a geometrical level this can be achieved by introducing a branching structure. That is, analogously to the 2-dimensional case, we add an orientation to all edges which is not cyclic around any triangle. The branching structure allows us to uniquely label the vertices of a triangle,

$$\rightarrow \quad T \Big|_{012} , \tag{153}$$
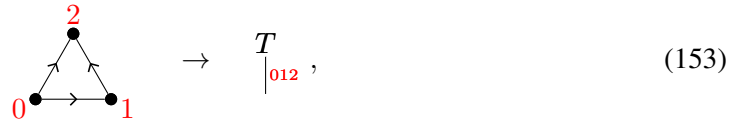
which represents a binding T. This ensures that there is only one way to glue two triangles. It also allows us to uniquely label the vertices of the tetrahedron, yielding an element with distinct indices

$$\rightarrow \quad T \underset{012}{\overset{0123}{\underset{}{\square}}} \!\! \begin{smallmatrix} T \\ 013 \end{smallmatrix} T \,. \tag{154}$$
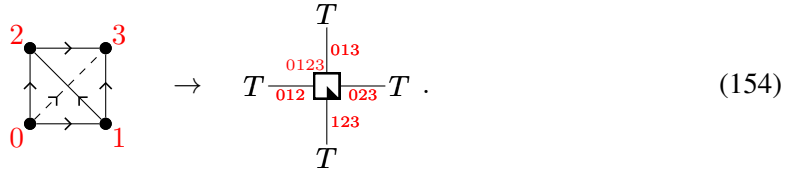
In network notation the 4 indices are distinguished by their location relative to the small black "arrow" inside the square which allows an unambiguous identification despite the fact that we are allowed to rotate and reflect the shape in the diagrams.

We want the models to have a pure-state quantum mechanical interpretation. Thus, we have to work with complex tensors, and we need to introduce an orientation. The orientation allows us to distinguish between the *counter-clockwise* tetrahedron above (whose 01 edge of the 012-triangle is oriented counter-clockwise), and the clockwise tetrahedron which is represented by the different element

$$\rightarrow \quad T \underset{012}{\overset{0123}{\underset{}{\blacksquare}}} \!\! \begin{smallmatrix} T \\ 013 \end{smallmatrix} T \,. \tag{155}$$
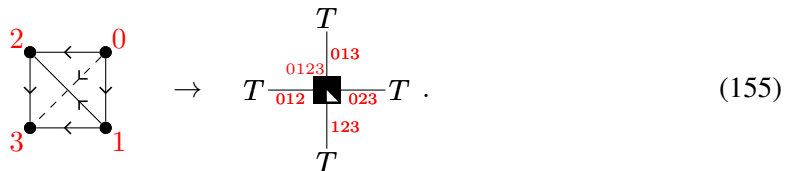
In order to access even more general models, we choose a slightly more complicated network representation of the triangulation. For every edge encircled by tetrahedra we chose one favorite adjacent face shared by one tetrahedron-pair and insert a 2-index atom at the corresponding bond. Those atoms are atoms of one of three different elements (called *edge weights*), depending on

whether the edge is the 01, the 02, or the 12 edge of its favourite face represented by

$$T \xrightarrow[\text{back}]{012} \triangleright \xleftarrow[\text{front}]{} T \, , \tag{156}$$

$$T \xrightarrow[\text{back}]{012} \blacktriangleright \xrightarrow[\text{front}]{} T \, , \tag{157}$$

$$T \xrightarrow[\text{back}]{012} \blacktriangleright \xrightarrow[\text{front}]{} T \, . \tag{158}$$

We can imagine to "inflate" the triangle on the left-hand side of Eq. (156), Eq. (157), and Eq. (158) and into a pillow-like volume with three corners, whose boundary consists of two triangles, one in the back and one in the front. We might think of the edge weight as being contained in the volume. Here and in the following, we will mark edges at the boundary of a volume, which contain an edge weight, with a tick.

It turns out that if we would write down the liquid without edge weights, we would only get models for symmetry breaking order, and none for (actual, irreducible) topological order [4]. However, there are simpler ways to decorate the liquid, which already have non-trivial models, yet not the most general ones. E.g., it suffices to add a 0-index atom [5] associated to every vertex, in order to get models for all discrete (Dijkgraaf-Witten [37]) gauge theories.

After the refinements above, we do not have a single 2-3 and 1-4 Pachner move, but one move for each choice of orientations, branching structure, and possitions of the edge weights. A list of all moves can be obtained in a straight-forward fashion and here we only present one specific example of a 2-3 Pachner move with the special property that all tetrahedra are oriented counter-clockwise. This move will be relevant in the next section, where we present a simplified, yet equivalent liquid. In terms of cell complexes, it looks like

$$\leftrightarrow \tag{159}$$

We observe that the geometric depiction does not reveal where we put the edge weight of the inner 13 edge on the right hand side. However, this information is contained in the corresponding network notation

$$\tag{160}$$

----

[4]The edge weight are closely related to the quantum dimensions in the conventional fusion-category framework of non-chiral topological order. No edge weights would mean that all quantum dimensions and the total quantum dimension are 1.

[5]The corresponding scalar would be the inverse total quantum dimension in the fusion-category formulation.

Apart from the 2-3 and 1-4 Pachner moves, we impose the following *full tetrahedron cancellation move* analogous to the *triangle cancellation move* in Eq. (93). Geometrically, it consists in taking a volume glued from a clockwise and a counter-clockwise tetrahedron at three of their faces, and shrinking it down to a single face

$$\leftrightarrow \qquad . \tag{161}$$

In network notation, this face is represented by a free bond

$$012b \;-\!\Box\!-\!\blacksquare\!-\; 012f \;=\; 012b \;-\!\!-\!\!-\; 012f \;. \tag{162}$$

As in the $1 + 1$-dimensional case, the volume on the left hand side of Eq. (161) would be represented by a projector in a real/complex model, and the move corresponds to the convention of restricting everything to the support of that projector.

7.1.2 The simplified liquid

The liquid presented in the preceding section is quite complicated, as it consists of a large number of slightly different versions of Pachner moves. In the following we present an equivalent "simplified" liquid with only one single Pachner move, together with many simple additional moves. The simplified liquid has a geometric interpretation as well – networks do not correspond to triangulations, but more generally to cellulations with different faces and volumes.

The simplified liquid consists only of the counter-clockwise tetrahedron and several additional elements which can be used to flip the edge orientations, and thus allow us to effectively reconstruct the clockwise tetrahedron from the counter-clockwise one (cf. Eq. (181)). The main new ingredient of the simplified liquid is to allow for 2-gon faces. Thus, first of all, we introduce an additional binding D, corresponding to a 2-gon with cyclic edge orientations

$$0 \overset{\frown}{\underset{\smile}{\bullet\!\!-\!\!\bullet}} 1 \quad \rightarrow \quad \underset{01}{\overset{D}{\big|}} \;. \tag{163}$$

The 2-gon has a rotation symmetry, so there are 2 different ways to identify two glued 2-gons. In order to make the gluing unambiguous, we determine one "favourite edge", marked by the small half circle, such that those favourite edges have to coincide when gluing.

The new elements used to flip edge orientations are called *flip hats*. They correspond to 3-cells whose boundary consists of two triangles and one 2-gon and which appear in four different variants depending on orientation and the choice of the favorite edge. I.e., there is

- the *clockwise* 01 *flip hat*

$$\rightarrow \quad T \overset{012}{\underset{01}{\overset{102}{-\!\Box\!-}}} {}^{012} T \;, \tag{164}$$

- the *counter-clockwise* 01 *flip hat*

$$T \xrightarrow[\ \ 01\ \ ]{102 \ \overset{012}{\blacksquare}\ 012} T \ , \qquad \qquad (165)$$

$$D$$

- the *clockwise* 12 *flip hat*

$$T \xrightarrow[\ \ 12\ \ ]{021 \ \overset{012}{\square}\ 012} T \ , \qquad \qquad (166)$$

$$D$$

- and the *counter-clockwise* 12 *flip hat*

$$T \xrightarrow[\ \ 12\ \ ]{021 \ \overset{012}{\blacksquare}\ 012} T \ . \qquad \qquad (167)$$

$$D$$

In addition, there is the 2-*gon flip* which interchanges favourite edges

$$0 \quad \longrightarrow \quad D \xrightarrow[10]{\quad \overset{01}{\blacklozenge}\ 01\quad} D \ . \qquad \qquad (168)$$

The boundary of this volume consists of two 2-gons. The favourite edge of the 2-gon on the front is the 01 edge, whereas for the 2-gon on the back it is the 10 edge.

At last, we need to introduce the edge weights for the simplified liquid. Of the three edge weights from the previous section, it suffices to take the 01 edge weight in Eq. (156), since the other edge weights can be constructed using the elements above. We additionally introduce the 2-*gon edge weight*

$$0 \quad \longrightarrow \quad D \xrightarrow[\text{back}]{\quad \overset{01}{}\ \text{front}\quad} D \ , \qquad \qquad (169)$$

which is a volume like the 2-gon flip, but the favourite edge of both the back and front 2-gon is the 10 edge. According to the name, one of its edges (the 10 edge) carries an edge weight and is therefore marked by a tick. We show in Eq. (179) that in fact all edge weights can be constructed from the 2-gon edge weight only, such that the 01 edge weight is merely an auxiliary element.

The moves of the simplified liquid contain only one single Pachner move, which we choose to be the one with only counter-clockwise tetrahedra in Eq. (160). Instead of the other Pachner moves, there are a number of simpler moves involving the additional elements, from which the former can be derived. In the following, we give a selection of those moves in terms of cell complexes as well as in network notation. The remaining moves can be found in Appendix B. For the cell complexes we can only easily draw the 1-skeletons which do not in general unambiguously determine the cellulation. The network notation on the other hand is clear and completely unambiguous, but does not make the geometric interpretation apparent.

The moves can be divided into three groups. First, there are moves corresponding to symmetries of the elements from which we can derive all other versions of the 2-3 Pachner moves. E.g., there is the $(01)(23)$ *tetrahedron symmetry move* for the corresponding permutation of the tetrahedron vertices. This permutation changes the edge orientations of the (01) and (23) edge,

which is done by using two pairs of flip hats. In the corresponding re-cellulation,

$$\leftrightarrow \quad \text{same 1-skeleton ,} \tag{170}$$
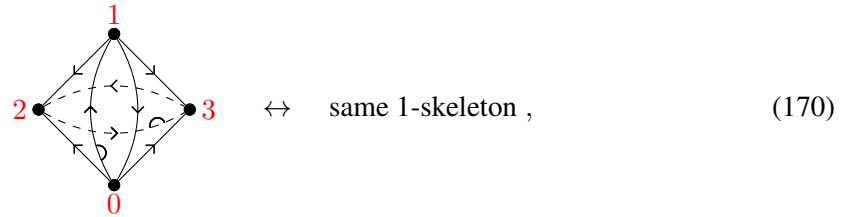
both sides are glued from one tetrahedron and one flip hat from each of the two pairs. On the left, the flip hats are glued to the triangles 013 and 123, whereas on the right, they are glued to the triangles 102 and 032. In network notation, this is

$$\tag{171}$$
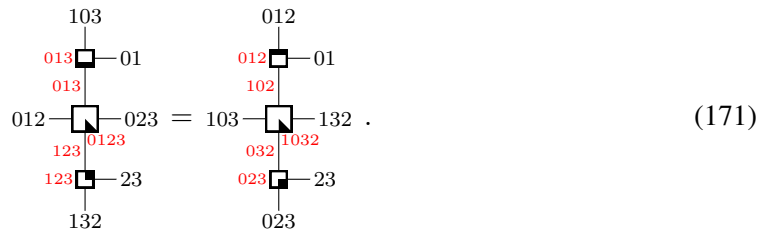
Also the flip hats have a symmetry, namely a π rotation around the axis going through the "tip" of the hat and the centre of the 2-gon. This rotation changes the favourite edge of the 2-gon which can be undone by gluing a 2-gon flip to the 2-gon, as, e.g., in the *clockwise* 01 *flip hat rotation move*

$$\leftrightarrow \quad , \tag{172}$$

in network notation

$$\tag{173}$$
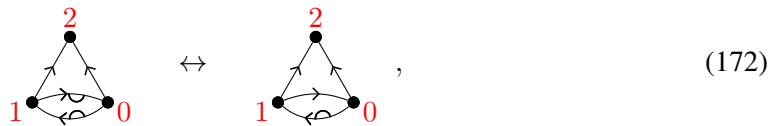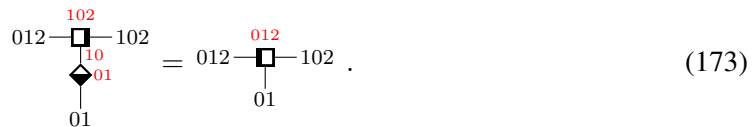
The second group consists of cancellation moves, which allow us to derive the 4-1 Pachner moves from the 2-3 Pachner moves. E.g., gluing two flip hats at one triangle and one 2-gon yields the same pillow-like volume as in Eq. (161), which can be shrinked to a triangle, as in the *oriented* 01 *flip hat cancellation move*

$$\leftrightarrow \quad . \tag{174}$$
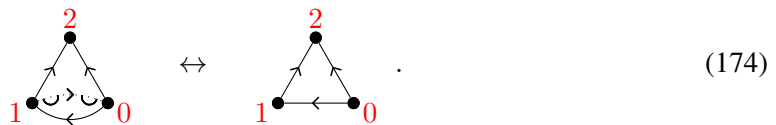
Again, the triangle is interpreted as a free bond in network notation

$$\tag{175}$$
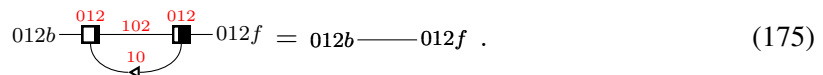
Similarly, the *tetrahedron cancellation move* equates two tetrahedra glued at two triangles on the left hand side with two flip hats glued at the 2-gon on the right hand side,
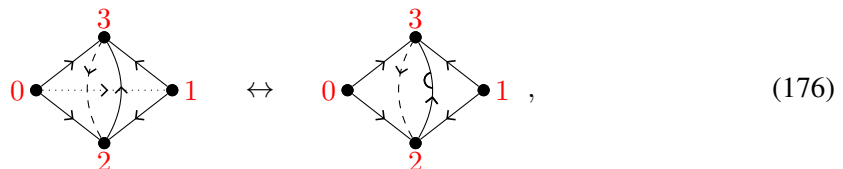
$$\leftrightarrow \quad , \tag{176}$$

$$\tag{177}$$

The third group consists of moves relating the edge weights. In our case there is only one such move, which can be viewed as the definition of the triangle weight from the 2-gon weight

$$\tag{178}$$

In network notation, this is

$$\tag{179}$$

The complete definition contains a few more moves, for which we refer to Appendix B.

Note that there is also a similar variant of the liquid without an orientation. The elements are the same, just that we do not distinguish between clockwise and counter-clockwise versions. The moves are similar, just that there are also tetrahedron symmetry moves corresponding to reflections of the tetrahedron. E.g., there is a (01) tetrahedron symmetry move with only one single flip hat on each side.

7.1.3 Equivalence of the simplified and non-simplified liquid

The equivalence of the simplified liquid and the non-simplified liquids is shown via mappings from one to the other and vice versa. The mappings have to be weak inverses, as introduced in Section 5.4.

We first present the mapping from the non-simplified liquid to the simplified liquid. The triangle binding T, the counter-clockwise tetrahedron, and the 01 edge weight are shared by both liquids and are accordingly mapped onto themselves. The clockwise tetrahedron of the non-simplified liquid can be constructed from the counter-clockwise tetrahedron and two flip hats

$$\tag{180}$$

yielding the mapping

$$\tag{181}$$

Likewise, the 02 and 12 edge weights of the non-simplified liquid can be constructed from the 01 edge weight and two flip hats. E.g., the 02 edge weight is obtained by

$$\tag{182}$$

yielding the mapping

$$012b \xrightarrow{012} 012f \quad := \quad 012b \text{—}\square\xrightarrow[10]{021}\triangleright\xrightarrow{021}\blacksquare\text{—}012f \quad . \tag{183}$$

Let us quickly sketch how the mapped moves of the non-simplified liquid are derived by the moves of the simplified liquid. First note that using flip hat cancellation moves like Eq. (175), we can insert pairs of flip hats at triangles between tetrahedra. Then, using symmetry moves like Eq. (171) individual flip hats can be moved through tetrahedra between different faces adjacent to a fixed edge. Imagine introducing a pair of flip hats at a face adjacent to an inner edge, moving one of the flip hats once around that edge, and then removing the pair of flip hats. This flips the orientation of the inner edge. Via this and similar derivations, we can obtain all different 2-3 Pachner move from only the single move in Eq. (160). Moreover, consider the full tetrahedron cancellation move in Eq. (162) and observe that it can be derived from the tetrahedron cancellation move in Eq. (177) together with a flip hat cancellation move. With the aid of the just derived full tetrahedron cancellation move, we can bring one of the tetrahedra on the left hand side of the 2-3 Pachner move in Eq. (160) over to the right hand side, and obtain a 1-4 Pachner move. Again, we can use the tetrahedron symmetry moves and flip hat cancellation moves to derive all other versions of the 1-4 Pachner move.

Next, we consider the converse mapping from the simplified liquid to the non-simplified liquid. A 2-gon can be triangulated by a pair of triangles, and gluing two 2-gons can be replaced by gluing two triangle pairs instead

$$\tag{184}$$

So we make the following identification between bindings

$$\underset{01}{D} := \underset{012}{T}\,\underset{102}{T} \quad . \tag{185}$$

Next, we consider the mapping of the additional elements. The clockwise 01 flip hat can be triangulated by two tetrahedra

$$\tag{186}$$

In terms of networks, we have

$$102 \text{—}\underset{013,103}{\overset{012}{\square}}\text{—}012 \quad := \quad 102\text{—}\underset{103}{\overset{023}{\boxed{}}}\xrightarrow{123}\underset{012}{\overset{013}{\boxed{}}}\xrightarrow{013}013 \quad . \tag{187}$$

Every time we would glue two 2-gons of the simplified liquid, we now glue two triangle pairs instead. In doing so, the edges 02 and 12 edge in Eq. (184) (the edges 03 and 13 in Eq. (186)) become inner edges, so we have to add the corresponding edge weights. In general, we will include the edge weights of the 02 edge (which is the 03 edge in Eq. (186)) on the side with the clockwise 2-gon and the edge weight of the 12 edge on the side of the counter-clockwise 2-gon.

The mapping of the counter-clockwise 01 flip hat is the similar – we just reverse the orientation and include the 13 edge weight instead of the 03 edge weight

$$
b\!-\!\blacksquare\!-\!a \atop xy := \quad b \longrightarrow x \qquad . \tag{188}
$$

The mapping of the 12 flip hats is defined analogously. At last, the 2-gon flip is mapped to two open bonds

$$
aa' \!-\!\blacklozenge\!-\! bb' := \quad \begin{matrix} a & & b \\ & \times & \\ a' & & b' \end{matrix} \tag{189}
$$

and the 2-gon edge weight can be emulated by an edge weight for one of the two triangles
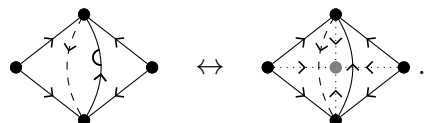
$$
aa' \!-\!\blacktriangleright\!-\! bb' := \quad \begin{matrix} a \longrightarrow a' \\ b \longrightarrow b' \end{matrix} \quad . \tag{190}
$$

All of the simplified moves correspond to re-triangulations, so they must be implied by the Pachner moves. A technical exception to this are moves involving the 2-gon flip and the cancellation moves, for which it is easy to find derivations. E.g., the 2-gon flip cancellation move in Eq. (311) of Appendix B simply becomes

$$
\begin{matrix} b & & b' \\ & \times\!\!\!\asymp & \\ a & & a' \end{matrix} = \begin{matrix} b \longrightarrow b' \\ a \longrightarrow a' \end{matrix} \quad . \tag{191}
$$

Finally, we have to show that the mappings are weak inverses to each other. However, in trying to do so we encounter a formal problem, which we solve by generalizing the notion of weak inverse: So far, we demanded that the network obtained by mapping an element twice is equivalent to the original element under moves. The 2-gon binding of the simplified liquid is twice-mapped to two triangle bindings. Thus, an element with a 2-gon index can not be equivalent to its twice-mapped network, as moves can not change the open indices and their bindings. This issue can be resolved by relaxing the notion of a weakly inverse mapping, in that we only demand that there is circuit move (i.e., a sequence of moves acting on non-overlapping patches), which transforms every doubly-mapped closed network into the original network.

Applied to the case of the twice-mapped 2-gon, we note that every 2-gon in a network is surrounded by a pair of flip hats and two such pairs of flip hats can never overlap in any network. Thus we call the network formed by the pair of flip hats *non-overlapping*. The non-overlapping network consisting of two flip hats has only triangle open indices, and is indeed equivalent to itself after mapping twice. The equivalence corresponds to a recellulation of two flip hats into four tetrahedra

$$
\leftrightarrow \qquad . \tag{192}
$$

So our generalized notion of weakly inverse mappings overcomes the technical difficulties for all closed networks. For networks with open indices, we can end up with additional structures near the boundary formed by the open indices. As a consequence, the double-mapped open network is allowed to have a different number of indices than its original, as we can see for a single tetrahedron.

To justify the generalization of our notion of weakly inverse mappings we invoke the significant similarity to the notion of phases: Both are defined via circuit moves, that is, sequences of

parallel, non-overlapping moves homogenously applied to networks. The definition of a weak inverse from previous sections ensured that if we apply both mappings to a model, we end up with the same model again, and thus, the models of both liquids are in one-to-one correspondence. This property is lost with the new generalized definition. However, this definition is chosen such that the doubly-mapped model is in the same phase, and thus, the phases of both liquids are in one-to-one correspondence.

7.1.4 Hermiticity

If we want to impose Hermiticity, e.g., in order to allow for an interpretation of the liquid models in terms of a imaginary time evolution tensor network, we have to include a move that equates the clockwise tetrahedron and the complex conjugated counter-clockwise tetrahedron. The latter is not an element of our simplified liquid, but can be constructed via Eq. (181) as

$$
\tag{193}
$$

Also the 2-gon edge weight changes its orientation under complex conjugation

$$
\tag{194}
$$

Note that we do not need to impose a Hermiticity move relating the flip hats and their orientation-reversed versions. This is because the flip hats always occur in pairs sharing a 2-gon, and the Hermiticity of each such pair can be derived from the moves above. Also, the Hermiticity move inverting the orientation of the triangle edge weight can be derived from the moves above.

7.1.5 Commuting-projector Hamiltonian

Let us briefly show how models of the present topological liquid yield commuting-projector models, formalized by a liquid mapping from the commuting-projector liquid to the topological liquid. A convenient layout for commuting-projector models are models on a regular triangular grid with one degree of freedom on each triangle. There is one Hamiltonian term on each vertex involving the six degrees of freedom at the surrounding triangles. So, the local ground state projector is a tensor with 12 indices,

$$
\tag{195}
$$

Commutativity of the projectors centered around neighbouring vertices yields three different moves, e.g.,

$$
\tag{196}
$$

Additionally, there is the projector move

$$
\includegraphics{eq197}
\tag{197}
$$

The mapping from this commuting-projector liquid to the topological liquid is as follows. A space-time given by stack of commuting-projector atoms can be transformed into a cellulation of a space-time volume by replacing each projector atom with a "double-pyramide" cell. The latter is a volume whose boundary consists of an identical upper and lower part, both equal to the patch of six triangles above

$$
\includegraphics{eq198}
\tag{198}
$$

As depicted above this volume can be triangulated with six tetrahedra, all sharing the (67)-edge, yielding the liquid mapping

$$
\includegraphics{eq199}
\tag{199}
$$

In the next section we will describe how models of the topological liquid can be considered blocked versions of Turaev-Viro state-sums. With this interpretation, Eq. (199) is nothing but a formal representation of the well-known relation between the latter state-sum, and the (suitably generalized) Levin-Wen string-net models.

7.1.6 Relation to the Turaev-Viro state-sum

Models of the liquid presented here are closely related to the *Turaev-Viro state-sum construction* [34, 35]. Whereas in the state-sum construction one starts with a *fusion category* and proves topological invariance from the properties of the latter, we take the opposite direction, and start from topological invariance to get to an algebraic structure similar to that of a fusion category. Bare fusion categories are *not* exactly the right structure needed for topological models and many versions of fusion categories with some additional structures exist in the literature. In Ref. [34], the input data of the state-sum construction is restricted to a specific class of examples, namely quantized enveloping algebras of sl_2. In Ref. [35], the state-sum construction is formulated for arbitrary *spherical* fusion categories. It is natural to assume that the model also works for multi-fusion categories with an adapted sphericality condition [38]. The string-net models in Ref. [36]

are simplified further in order to be more accessible to the physics community and have additional restrictions such as a very strong notion of tetrahedral symmetry and vanishing Frobenius-Schur indicators. These restrictions render them incompatible with general twisted Dijkgraaf-Witten gauge theories [37, 39], but were partially removed for the Abelian case in Ref. [40].

In contrast, the algebraic structures we obtain in our approach are per construction the right ones to describe fixed-point models of topological phases with gappable boundary. Finding instances of our algebraic structures (i.e., models of liquids) is not fundamentally harder than finding instances of well-known algebraic structures such as fusion categories, as both are solutions to a set of polynomial equations. The only difference is, that for well-known structures there already exist a hand full of examples in the literature.

We now compare the liquids presented here to the Turaev-Viro state-sum models and show that they are equivalent up to technical details. Both constructions associate tensors to tetrahedra of a simplicial complex. The tensor of our liquid model has four indices associated to the faces of the tetrahedron, while the tensor in the Turaev-Viro construction is determined by the so-called *F-symbol* and the *quantum dimension d* of a *fusion category*. It has 10 indices, six of which are associated to the edges of the tetrahedron, and the remaining four to the faces, i.e.,

$$[F^{ab}_{cd}]^{i\alpha\beta}_{j\gamma\delta}(d_j)^{-1} \quad \rightarrow \quad \text{[diagram]} \qquad (200)$$

Just as in our liquid, if two tetrahedra are adjacent to the same face, the corresponding face indices of the tensors are contracted. However, the number x of tetrahedra adjacent to a single edge can be more and less than 2, and we contract all the edge indices coming from those tetrahedra by an x-index delta tensor. Moreover, at each edge there is the vector d containing the quantum dimensions which is connected to the corresponding delta tensor via another index. With these choices, we see that the *pentagon equation* for the F-symbol corresponds to invariance under the 2-3 Pachner move.

The F-symbol is not a tensor in the conventional sense, as one and the same face index can have different dimensions depending on the values i, j, k of the indices at the surrounding edges. Those dimensions are collected into an object $N^{i,j}_k$ known as the *fusion rules*. F can be made into an ordinary tensor by fixing the dimension of the face indices to the maximal possible number in $N^{i,j}_k$, and filling up the new tensor entries with zeros. In the common examples (e.g., the toric code or the double Fibonacci model) all $N^{i,j}_k$ are either 0 or 1, so the face indices can be omitted (i.e., set to dimension 1) and $N^{i,j}_k \neq 0$ is interpreted as a constraint on the edge indices instead.

There are two ways to make the Turaev-Viro state-sum into a model of our liquid. The first is to reshape the tensor F into a proper four-index tensor. To this end, we copy all edge indices using delta tensors, and block each copy with one of the adjacent face indices

$$\text{[diagram]} \qquad (201)$$

Each of the new face indices is a composite of three of the old edge indices and one old face index. The dimension of this composite is fixed and given by

$$\sum_{i,j,k} N^{i,j}_k \;. \qquad (202)$$

The second possibility is to interpret the F-symbol as a tensor of a different type, called *label-dependent tensors* [19]. The data determining such a tensor consists of a set of labels together with one array (of varying dimension) for each value of the labels. When we interpret the moves of the liquid using this tensor type, they turn into the equations of the Turaev-Viro model in their original form.

It is also possible to start from a (conventional) model of the topological liquid and arrive at a state-sum in the Turaev-Viro form in a natural way by using the fact that complex algebras (with a few special properties that we have in this case) can be block-diagonalized. For more details on this procedure we refer to Appendix C.

7.2 Face-edge liquid

In Section 4.2, we have encountered another way to represent 3-dimensional topological manifolds as a liquid, namely by associating atoms to faces and edges instead of volumes. In this section we look at this construction in more detail. Models of the resulting liquid are very similar to the *Kitaev quantum double model* [25] generalized to weak Hopf algebras [41, 42]. They are also similar to the *Kuperberg invariant* of 3-manifolds [43]. As in the sections above, the more general version of the liquid in Section 4.2 has edge orientations, which allow us to distinguish the indices of the face elements. Dually, we add dual orientations to the faces, that is, a favourite adjacent volume.

7.2.1 Elements and moves of the face-edge liquid

Elements. The elements of the face-edge liquid are a collection of decorated face and edge elements from which all other possible decorations can be generated. One possible choice is to use the 2-cells of the simplified $1 + 1$-dimensional liquid in Section 6 with the following orientations

- The clockwise triangle

$$\tag{203}$$

  where the crossed circle in the middle of the triangle represents the dual orientation of the triangle pointing into the plane and we put an ingoing arrow to the indices corresponding to the two edges which are oriented clockwise when looking along the dual orientation.

- The clockwise and counter-clockwise cyclic 2-gon

$$\tag{204}$$

- The clockwise 3-valent edge

$$\tag{205}$$

  where the circle with the dot represents the dual orientation going out of the plane and the index corresponding to the face whose dual orientation is counter-clockwise when looking

along the orientation is marked with an ingoing arrow. With this choice of ingoing/outgoing arrows, every bond in a network representing a piece of 3-manifold will be between one index with ingoing arrow, and one without.

- The 2-valent edge with clockwise and counter-clockwise dual orientations

$$\tag{206}$$

In order to get models for a large class of topological phases (i.e., presumably all topological phase with a gappable boundary), we need to introduce one more additional structure in the network representation of cell complexes – the *corner weight*. A *corner* denotes a volume and an adjacent vertex. At every corner we find an alternating loop of edges and faces connected by bonds. We introduce a 2-index element called the *corner weight*

$$\tag{207}$$

and require that at every corner a corner weight atom is placed between exactly one edge-face pair. For example for the following corner enclosed by three faces and three edges a corner weight is located between the (13)-edge and the (123)-face

$$\tag{208}$$

In fact, there are four different corner weight elements, depending whether the orientation (dual orientation) of the edge (face) points towards or away from the vertex (volume) of the corner. However, the other three corner weights can be constructed from the one specific corner weight given above where both the orientation and dual orientation point towards the vertex and volume. E.g., the corner weight where the face is pointing away from the volume of the corner is obtained by inverting the dual orientation by conjugating with the 2-valent edge

$$a \rightarrow \bullet \leftarrow \boxdot \leftarrow \bullet - b \ . \tag{209}$$

Moves. The moves of the face-edge liquid can partially be obtained from the moves of the oriented $1+1$-dimensional liquid from Section 6. Networks of the face-edge liquid consisting only of face elements separated by 2-valent edges behave like networks representing a cellulation of a 2-manifold. Thus, it makes sense to take all moves of the $1+1$-dimensional liquid of Section 6 as moves for the face elements of the face-edge liquid. More precisely, we have to take the version of the $1+1$-dimensional liquid with vertex weights, and the vertex weight is related to the corner weight of the face edge liquid: Every vertex in the two-dimensional cellulation corresponds to two corners in the three-dimensional cellulation, one with the volume above and one with the volume below. Thus, we identify the vertex weight of the $1+1$-dimensional liquid with two corner weights of the $2+1$-dimensional liquid

$$a \rightarrow \square - b := a \rightarrow \boxdot \bullet \leftarrow \boxdot \bullet - b \ . \tag{210}$$
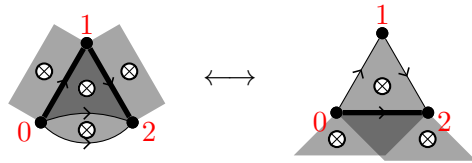
The relation between the face-edge liquid and the $1+1$-dimensional liquid in Section 6 can be formalized as a liquid mapping from the latter to the former, which we refer to as the *2D embedding mapping*.

Dually, consider cellulations consisting only of edges that are all connected to the same 2 vertices separated by non-cyclic 2-gon faces. Also these behave like networks of the $1 + 1$-dimensional liquid alone, and so we also impose the moves of Section 6 for the edge elements of the presented liquid. Analogously to the previous consideration the 2-dimensional vertex weight is now given by

$$a \rightarrow \square - b := a \rightarrow \boxdot \rightarrow \bigcirc \leftarrow \boxdot \rightarrow \bigcirc - b \ . \tag{211}$$
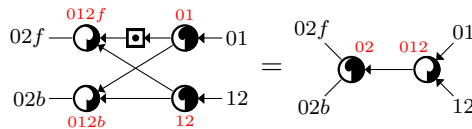
Again, the considerations above can be formalized as a mapping referred to as *dual 2D embedding mapping*.

In addition to the face-liquid moves mapped under the 2D embedding mapping and the dual 2D embedding mapping, we only need a few additional moves which relate face and edge atoms. The most important move is the *corner fusion move*, which we have already seen in Section 4.2 in a simplified form. Including orientations, dual orientations, and corner weights, it is given by
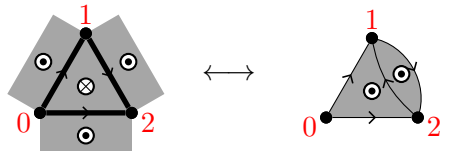
$$\tag{212}$$

which, in network notation, becomes
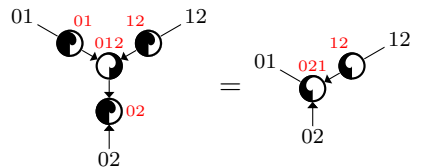
$$\tag{213}$$

Additionally, there are moves which effectively change the orientation of edges and dual edges. For example the dual orientation of a triangle can be changed via cyclic 2-valent edges
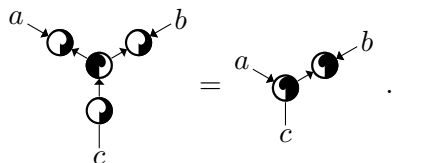
$$\tag{214}$$

As the counter-clockwise triangle is not an element, we have to construct it using a cyclic 2-gon. This yields a move

$$\tag{215}$$

called the *dual orientation flip move*. Dually, we can flip a clockwise edge into a counter-clockwise edge by gluing cyclic 2-gons, yielding the *orientation flip move*

$$\tag{216}$$

At last, the Hermiticity moves are simply the $1 + 1$-dimensional Hermiticity moves from Section 6.4 mapped under the 2D embedding mapping and the dual 2D embedding mapping.

7.2.2 Relation to quantum double models

As mentioned in Section 4.2, the moves above are very similar to the bi-algebra axioms, and even more similar to the axioms of *weak Hopf algebras*. The latter (as any algebraic structure) define a liquid themselves. As such the two liquids are not exactly equivalent, in particular, because the weak Hopf liquid allows for a consistent flow of time, a feature missing in the face-edge liquid. There is only a liquid mapping from the weak Hopf liquid to the present topological liquid [30]. Thus, every model of the face-edge liquid defines a weak Hopf algebra, but not vice versa.

This suggests that models of the face-edge liquids are equivalent to Kitaev quantum doubles for weak Hopf algebras [42]. Indeed, using the commuting-projector mapping shown in the simplified form in Eq. (73), we find that the obtained Hamiltonians are equal. However, weak Hopf algebras are *not* precisely the right algebraic structure needed to obtain topological models. On the contrary the face-edge liquid yields topological models by construction. Comparing our formalism to the axioms of weak Hopf algebras, we see that the weak Hopf algebras in question need to fulfill a few additional properties. E.g., both the algebra and the co-algebra need to be (special) Frobenius (and *-algebras in the Hermitian case), and the antipode must be involutive. The need for technical details of this kind is apparent from our formalism, while it is not straight-forward to see in existing approaches to fixed-point models.

7.3 Equivalence of the face-edge and volume liquid

The volume liquid from Section 7.1 is "topological" due to the known fact that simplicial complexes with Pachner moves are a combinatorial analogue of (piece-wise linear) topological manifolds modulo homeomorphism in the continuum. For the face-edge liquid in Section 7.2, there is no such argument we can rely on. However, we can verify that the latter is topological by showing that it is equivalent to the volume liquid. Note that from our perspective, the connection to continuum topology is merely a guiding intuition and all that matters is that the liquid defines a sensible notion of deformability to which physical models can be extended.

In this section, we present two weakly inverse mappings between the volume and the face-edge liquids, sketch why they are well-defined and why they are indeed weak inverses of each other. The mapping from the face-edge liquid to the volume liquid has a geometric interpretation. It can be seen as refining a cellulation such that each volume of the refined cellulation corresponds to either an edge or a face of the original cellulation. The mapping is given by the following prescription.

- Every face is replaced by a "double pyramid", that is, we add one vertex x "above" and one vertex y "below" the face, and connect all vertices with x and y. For edges with counter-clockwise orientation the corresponding edge of the double pyramid carries an edge weight. E.g., for the clockwise triangle, an edge weight is associated to the 02-edge

$$\tag{217}$$
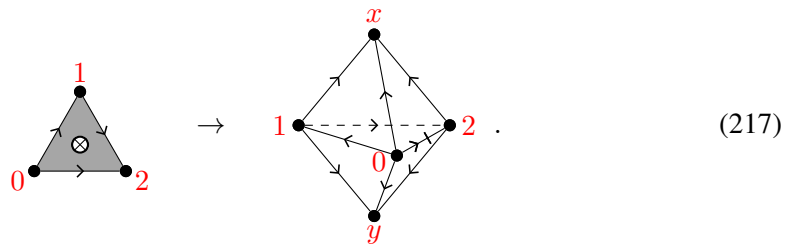
This volume can be triangulated by two tetrahedra. In network notation we have

$$
\begin{array}{c}
aa' \searrow\!\!\nearrow bb' \\
\bigcirc_{012} \\
cc'
\end{array}
\quad :=\quad
\begin{array}{c}
c \\
a \!-\!\square^{012x}\!-\! b \\
\blacktriangledown\, 012 \\
a' \!-\!\blacksquare_{012y}\!-\! b' \\
c'
\end{array}
\quad .
\tag{218}
$$

The clockwise 2-gon is mapped to a volume which can be glued from two flip hats

$$
0\,\bullet\!\!\otimes\!\!\bullet\,1 \quad\rightarrow\quad
\begin{array}{c}
x \\
0\,\bullet\quad\bullet\,1 \\
y
\end{array}
\quad ,
\tag{219}
$$

with the following network notation

$$
aa' \rightarrow\!\!\bigcirc\!\!\leftarrow bb' \;_{01}\; :=\;
\begin{array}{c}
a \!-\!\blacksquare^{01x}\!-\! b \\
a' \!-\!\square_{01y}\!-\! b'
\end{array}
\quad .
\tag{220}
$$

The counter-clockwise 2-gon is defined analogously, just that edge weights are included for both the 01- and the 10-edge.

- Every edge is replaced by a volume constructed as follows. The two vertices adjacent to the edge (x and y in the figure below) are connected by edges that replace the adjacent faces (a, b, c in the figure) and edge weights are associated to all edges for which the corresponding faces have clockwise dual orientation. An additional vertex is added between each pair of edges and connected to the vertices. For the 3-valent edge we obtain

$$
\begin{array}{c}
y \\
b\,\odot\quad\otimes c \\
\quad\uparrow \\
x\,\odot\, a
\end{array}
\quad\rightarrow\quad
\begin{array}{c}
y \\
b\,1\,\bullet2\,\bullet\; c\,\curvearrowright a\; \bullet\,0 \\
x
\end{array}
\quad .
\tag{221}
$$

The volume above has the following triangulation in network notation

$$
\begin{array}{c}
cc'\searrow\!\!\nearrow bb' \\
\bullet \\
aa'
\end{array}
\quad :=\quad
\begin{array}{c}
a\quad b \qquad\qquad c \\
\blacklozenge_{xy02}\;\;\lozenge_{xy12}\;\square_{y012}\;\lozenge_{xy01} \\
a'\; b' \qquad\blacksquare_{x012}\qquad c'
\end{array}
\quad .
\tag{222}
$$

With a bit of geometric imagination one can verify that all volumes from the two points above fit together and form a "refining" without any holes and overlaps. If an edge is adjacent to a face

in the original cellulation, the two corresponding volumes after refining share a pair of triangles. Thus, the face-edge binding is mapped to two triangle bindings, that is, every index in a face-edge network corresponds to a pair of indices in a triangle network,

$$
| := \begin{matrix} T & T \\ | & | \end{matrix} \; .
\tag{223}
$$

At last we check that the edge weights of the refined cellulation are distributed correctly over the elements of the face-edge liquid. The edge weights of edges that separate pairs of triangles constituting composite indices are already included into the triangle and face elements. They contain the weight if the second triangle in the pair has two clockwise edges. The other edges correspond to corners of the original triangulation and thus those edge weights are mapped to corner weights

$$
aa' \!-\!\boxed{\bullet}\!\leftarrow\! bb' := \begin{matrix} a \text{———} b \\ a' \text{—}\!\blacktriangleleft\!\text{—} b' \end{matrix} \; .
\tag{224}
$$

In order to prove that the above recipe defines a liquid mapping, we would have to give derivations for all the mapped moves. This is a straight-forward and purely combinatorial procedure. However, it is quite tedious and lengthy, thus we only give a quick argument why the mapping is well-defined: The mapping is constructed such that all mapped moves are retriangulations. As it is known that any retriangulation corresponds to a sequence of Pachner moves, it is clear that all mapped moves can be derived.

The mapping from the volume liquid to the face-edge liquid also has a geometric intuition in terms of a refining, such that every edge and face of the refined cell complex can be unambiguously associated to a volume of the original cell complex. To this end, we first split each triangle into two triangles separated by a pillow-like volume, such that every n-valent edge becomes $2n$-valent. Then, we replace every such $2n$-valent edge into n 4-valent edges which are cyclically connected by n trivial (non-cyclic) 2-gons. Like this, each original volume turns into one face for each of its faces, and one 4-valent edge for each of its edges.

Applying this to the tetrahedron we get a network consisting of 4 triangles and 6 4-valent edges. As we will see below, this network is equivalent to a simpler one which has one face (the 012 face below) missing and the adjacent edges being only 3-valent. As the counter-clockwise triangle is not explicitly part of our liquid, we have to construct it using the cyclic 2-gon

$$
\tag{225}
$$

In network notation this is

$$
\tag{226}
$$
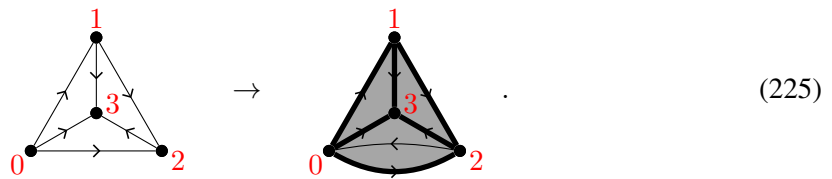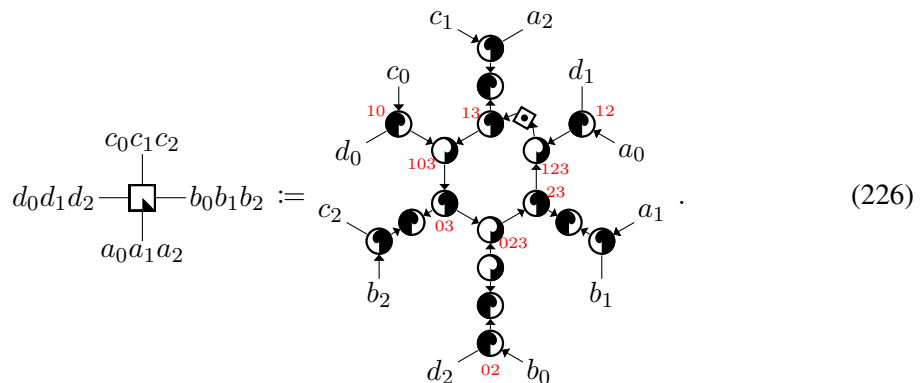
Regarding the bindings, we note that a triangle has three edges and thus the triangle binding is mapped to three times the face-edge binding. Therefore in the above equation one index on the left corresponds to three indices on the right,

$$\overset{T}{\underset{|}{|}} := |\quad|\quad|. \tag{227}$$

Let us sketch how the mapped moves can be derived from the moves of the face-edge liquid. The edge orientations and dual face orientations can be changed arbitrarily by inserting/moving around cyclic 2-gons and 2-valent edges using the 2-gon cancellation move in Eq. (132) and triangle symmetry move in Eq. (129) for either the edge or face elements. So, for simplicity, we will neglect those orientations in the following considerations and focus on the derivation of the 2-3 Pachner move. We work with the geometric intuition that atoms are associated to the triangles and edges of a 3-manifold triangulation. Internally, n-valent edges have to be decomposed into 3-valent edges. However, the different decompositions are all equivalent using the (dually mapped) 2-dimensional moves, and we assume that these moves are applied implicitly. For the remaining considerations it is convenient to introduce some terminology.

- The corner fusion move depicted in Eq. (212) from left to right is denoted by $C(012|02)$,

- the 2-2 Pachner move, as depicted in Eq. (89), from left to right, by $P_2(012|023)$,

- and the following move

$$\tag{228}$$
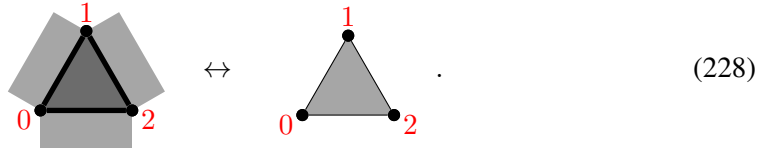
  which replaces a single triangle by two duplicates separated by a pillow-like volume by $T(012)$.

The last move is derived by using the triangle cancellation move to bring one triangle in the corner fusion move in Eq. (212) from the right to the left.

Next, we consider two variants of tetrahedra that are relevant in the 2-3 Pachner move and apply a sequence of the moves above in order to remove several of their faces.

- For a tetrahedron with 3-valent edges where in the mapped network all four triangles and all six edges are represented by atoms

$$\tag{229}$$

  we can remove the face 012, such that only the triangles 013, 123, 023, and the edges 03, 13, 23, are represented by atoms. This can be done by the sequence of moves

$$\overline{T(123)} \to \overline{C(123|12)} \to P_2(012|123)$$
$$\to C(013|03) \to T(023) \,, \tag{230}$$

  where the bars denote the move in the opposite direction.

- Start with a tetrahedron where all faces and edges are represented by triangle atoms and 3-valent edge atoms, except for the edge 12 which is a trivial 2-valent edge and thus not represented by an atom. We can remove both the 012- and the 123-face, such that only the triangles 013, 023, and the edge 03 are represented by 3-index atoms. This can be done by the following sequence of moves

$$P_2(012|123) \rightarrow C(013|03) \rightarrow T(023) \ . \tag{231}$$

Note that it is precisely the move derived in Eq. (230) which allows us to add/remove the 012 face on the right hand side of the tetrahedron mapping in Eq. (226). If we now apply the face-edge mapping to the 2-3 Pachner move, each triangle will be doubled (taking the version of the mapping including the 012 triangle). We can apply the move T in Eq. (228) to reduce each triangle pair to a single triangle. Next, we can apply the moves derived in Eq. (230) and (231) to remove all interior triangles and edges on the left and right, which yields an equation between twice the same network. Applying this procedure in the opposite direction, we have found a derivation of the mapped 2-3 Pachner move from the moves of the face-edge liquid.

We still have to show that the two mappings are weak inverses to each other. The mappings change the bindings, such that applying both mappings maps every open index to six open indices. Thus, we have to use the generalized notion of weak inverse from Section 7.1.3. We won't explicitly show that the two mappings applied in sequence (in both orders) are equivalent to a circuit of moves acting on non-overlapping patches. However, it is easy to see that the composition of the two mappings defines a topology-preserving refinement of the cellulation, which can be undone by moves.

8 Fermions

In this section we will demonstrate how fixed-point models with fermionic degrees of freedom can be formalized as liquid models. In the first part we will introduce fermionic tensors, the tensor type which is the domain of fermionic liquid models. In the second part we will discuss the kind of liquid that fermionic systems typically extend to, namely combinatorial representations of spin manifolds. In the third part, we will illustrate the formalism in $1+1$ dimensions, by giving a liquid which has a model corresponding to the Kitaev chain.

8.1 Fermionic tensors

In Section 2, we have demonstrated how quantum spin systems can be formulated in terms of tensor networks. In many condensed matter models we also have fermionic degrees of freedom. We could just use a Jordan-Wigner transformation to write the fermionic system as a spin system. However, such a transformation is generally non-local, and even in $1 + 1$ dimensions where it is local in principle, it changes the homogeneity of the model. That is, a translation-invariant fermionic system (with periodic boundary conditions) does not translate into a translation-invariant spin system/tensor network.

We can still write fermionic systems as tensor networks. However, the "tensors" cannot be just arrays, as for spin systems, but have to take the canonical anti-commutation relations for fermions into account. A fermionic operator acting on n modes labelled $0, \ldots, n-1$, can be expanded as

$$\sum_{\substack{s_0, \ldots s_{n-1} \\ s'_0 \ldots, s'_{n-1}}} A^{s_0, \ldots, s_{n-1}}_{s'_0, \ldots, s'_{n-1}}$$

$$(c_0^\dagger)^{s_0} \cdots (c_{n-1}^\dagger)^{s_{n-1}} |0\rangle \langle 0| (c_y)^{s'_{n-1}} \cdots (c_0)^{s'_0} \ , \tag{232}$$

where the s_i and s_i' are either 0 or 1 depending on whether the fermionic degree of freedom is occupied or not. We observe the following.

- The operator must preserve fermion parity. That is, A can have non-zero entries only when

$$\sum_i s_i + \sum_i s_i' = 0 \, ,\tag{233}$$

where the summation is understood mod 2.

- In order to specify the operator, we have to both specify A, but also the ordering of creation and annihilation operators, in the case above $0', \ldots, n-1', n-1, \ldots, 0$. The same fermionic operator may also be written down with any other ordering, just that then also the coefficients A change. E.g., if we exchange 0 and 1 at the end of the ordering above, the anti-commutation of c_0 and c_1 tells us that we have to modify A by

$$(A')^{s_0,\ldots,s_{n-1}}_{s_0',\ldots,s_{n-1}'} = A^{s_0,\ldots,s_{n-1}}_{s_0',\ldots,s_{n-1}'} \quad (-1)^{s_0 s_1} \, .\tag{234}$$

More generally, we can consider degrees of freedom with i configurations without a fermionic charge, and j configurations with a fermionic charge, instead of only having only one charge-free (non-occupied) and one charged (occupied) configuration. This motivates the following definitions:

A *fermionic tensor* is an equivalence class of pairs (A, O), where A is an array, and O is an ordering of its indices (compare also Ref. [44]). The $i + j$ configurations of each index of A are divided into i *even* configurations, writing $|x| = 0 \in \mathbb{Z}_2$ for $0 \leq x < i$, and j *odd* configurations, writing $|j| = 1 \in \mathbb{Z}_2$ for $i \leq x < i + j$. A has to have even parity, that is

$$A_{i,j,\ldots} = 0 \quad \text{if} \quad |i| + |j| + \ldots \neq 0 \, .\tag{235}$$

Two pairs (A, O) and (A', O') are equivalent if O' and O are related by a transposition of two consecutive indices x and y, and A and A' are related as

$$O' = \tau_{xy}(O) \, ,$$
$$(A')_{s_0,s_1,\ldots} = A_{s_0,s_1,\ldots}(-1)^{|s_x||s_y|} \, .\tag{236}$$

A conventional fermionic operator acting on n modes can be represented by a fermionic tensor with $2n$ indices, each with only one even and one odd configuration.

The tensor product of two fermionic tensors is the tensor product of arrays, together with the concatenation of orderings:

$$(A_1, O_1) \otimes (A_2, O_2) = (A_1 \otimes A_2, O_1 \cap O_2) \, .\tag{237}$$

The order in which we concatenate O_1 and O_2 does not matter, as the minus signs collected from exchanging all indices of A_1 with all indices of A_2 is trivial due to the even parity constraint in Eq. (235). The contraction of two indices x and y of a fermionic tensor (A, O) consists of the following steps.

- Go to a representative where y comes right after x in O.

- Contract x and y in A.

- Remove x and y from O.

Roughly, the philosophy of this work is that, once we have chosen a particular liquid, we can interpret the same equations in terms of fermionic tensors to obtain fermionic fixed point models. However, fermionic tensors do not obey exactly the same graphical calculus as array tensors. There are two small differences.

The first difference is that contracting indices x and y for a fermionic tensor is different from contracting y and x, as we explicitly specified that y is *after* x in O. If we instead wanted y to be *before* x, we would have to exchange them yielding a factor of $(-1)^{|s_x|}$ in A before the contraction, and hence a different result. The ordering in the contraction can be incorporated into the graphical calculus by associating a *bond direction* to each bond in a network, represented by an arrow, e.g.,

$$\rightarrow \!\!\!\!\! \overset{\longrightarrow}{A} \, \square \qquad . \qquad\qquad (238)$$

Note that also the open indices have a bond direction. An inwards pointing bond direction means we multiply by the fermion parity $(-1)^{|x|}$, where x is the configuration of the open index. An outwards bond direction is assumed by default.

The second difference is that contracting two index pairs a, a' and b, b' one after the other is different from blocking them into a single index pair $ab, a'b'$ that is contracted. In order to perform the former contractions, we would have to order the indices like $aa'bb'$, which differs from $aba'b'$ by a sign of $(-1)^{|b||a'|}$. Note that despite this, the contractions of a, a' and b, b' still commute with each other, which justifies the network calculus. However, liquid mappings for fermionic tensors are not allowed to block multiple indices into one.

The second point can be fixed by dividing the basis configurations in "particle" and "hole" configurations (in addition to the partition into even and odd). Then we can associate elements of $\mathbb{Z}_4$ to the different configurations as

parity	even	odd	even	odd	
$\vert \cdot \vert \in \mathbb{Z}_2$	0	1	0	1	
particle-hole	particle	particle	hole	hole	.
$\langle \cdot \rangle \in \mathbb{Z}_2$	0	0	1	1	
$\langle \vert \cdot \vert \rangle \in \mathbb{Z}_4$	0	1	2	3	

$$(239)$$

When we block indices, we use this $\mathbb{Z}_4$ grading

$$\langle |(a, b)| \rangle = \langle |a| \rangle + \langle |b| \rangle \,, \qquad\qquad (240)$$

where (a, b) denotes a configuration of two indices blocked into a single one. A particle (odd-particle configuration) and a hole (odd-hole configuration) together yield nothing (even-particle), which motivates the terminology (which should otherwise not be taken too seriously). We do *not* demand that the tensors are $\mathbb{Z}_4$-graded, only the global parity has to be even. So the configurations of all indices of a tensor can either block to even-particle or even-hole.

We also have to modify the contraction by introducing a factor of -1 for the hole configurations of the contracted indices:

$$A_{ijk} \rightarrow B_i = \sum_x A_{ixx} (-1)^{\langle x \rangle} \,. \qquad\qquad (241)$$

The factor of -1 cancels the difference from contracting the blocked index pair versus the separate pairs, which cures the incompatibility of contraction and blocking.

We will refer to the latter tensors as *particle-hole fermionic tensors*, and to the former tensors without particle and hole sectors as *plain fermionic tensors*. Note that plain fermionic tensors are a subset of particle-hole fermionic tensors that is closed under tensor product and contraction. So as long as we do not consider any index-blocking mappings, we can restrict to plain fermionic tensors without any inconsistencies.

8.2 Liquids with spin structure

It would be very much in the spirit of the work to take, e.g., the liquid in Section 6, look for models in fermionic tensors, and interpret them as fixed point models for fermionic topological phases in $1 + 1$ dimensions. Unfortunately, things are not quite as simple: First of all, the liquids we defined for spin models do not have bond directions, which we need for considering models in fermionic tensors. This is not a huge problem however, as we can for example fix the bond direction to point "towards the left" relative to the orientation of the according edge in the cellulation.

However, it turns out that "generic" fermionic models (originally defined on square lattices) simply do not extend to bare topological manifolds. Moreover, trying to find fermionic models for a bare topological liquid seems to not yield any interesting results. Instead, fermionic models like to be extended to *spin manifolds*, which are manifolds equipped with some extra structure (the *spin structure*) of the same kind as an orientation. In the context of quantum field theory this is known as the *spin-statistics relation*.

In fact, we had a similar situation earlier when talking about orientations: One could look for complex models of a non-oriented liquid, however, (apart from those models being unphysical) we would not find very interesting models. So complex tensors "harmonize" well with liquids featuring an orientation, just as fermionic tensors harmonize with liquids featuring a spin structure.

In order to get a liquid representing spin manifolds, we need a combinatorial representation of a *spin structure* [45]. A spin structure is a $\mathbb{Z}_2$-valued 1-cochain η, whose boundary is the second *Stiefel-Whitney class*, represented by a 2-cocycle ω_2. In an n-dimensional simplicial complex, η can be represented as a subset (or $\mathbb{Z}_2$ colouring) of $n - 1$-simplices, and ω_2 as a subset (or colouring) of $n - 2$-simplices. The boundary relation is obvious: The $\mathbb{Z}_2$-colour of an $n - 2$-simplex in the boundary of η is the sum of $\mathbb{Z}_2$-colours of adjacent $n - 1$-simplices. A formula for computing ω_2 in terms of the combinatorics of a simplicial complex is given in Ref. [46].

8.3 The liquid in $1 + 1$ dimensions

In this section we will give a topological liquid with spin structure in $1 + 1$ dimensions, and discuss its models in fermionic tensors. For simplicity, and to avoid discussions on what time-reversal symmetry means for fermions, we will also add an orientation, and look for models in fermionic tensors with complex entries.

8.3.1 Spin structures in $1 + 1$ dimensions

In $1 + 1$ dimensions, ω_2 is a $\mathbb{Z}_2$-colouring of vertices, and the formula for the coloring of a vertex v in a simplicial complex is:

$$\omega_2(v) = 1 + \#E_0(v) + \#T_0(v) \pmod 2 , \tag{242}$$

where $\#E_0(v)$ is the number of edges starting in v, and $\#T_0(v)$ is the number of triangles which have v as their 0th vertex (when numbering them according to the branching structure).

η is a collection of edges, which form a pattern of lines whose (modulo 2) endpoints are ω, and which are closed otherwise. Consider, e.g., the following patch of triangulation with a combinatorial spin structure η

$$\tag{243}$$
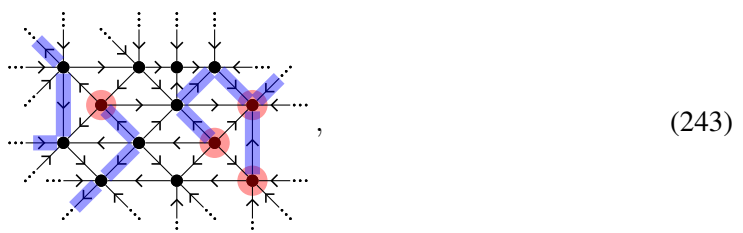
where the ω_2-vertices were marked red, and the η-edges were marked blue.

While ω_2 is fixed, there are many possible choices of η. The precise choice is irrelevant to a large degree, as different choices are considered equivalent if they are related by *homology moves*. A homology move changes η by adding the boundary of a triangle (modulo 2), e.g.,

$$\qquad\qquad \leftrightarrow \qquad\qquad . \tag{244}$$

Equivalence classes of η-triangulations under homology moves (as well as Pachner moves) are in one to one correspondence with spin manifolds. There are as many equivalence classes as there are first homology classes of the manifold (or non if the manifold is not spin), though there is no canonical identification between the two. Of course, the spin structure also has to be incorporated into the Pachner moves. As the latter exchange a disk with a disk, and a disk has trivial 1-homology, all different ways of adding η to a Pachner move are equivalent.

8.3.2 The liquid

A triangulation with orientation and η-chain is represented by a liquid (with bond directions) in the following way: As in the non-spin case, there are atoms for the clockwise and counter-clockwise triangles. The bond direction at an edge which is not part of η is towards the left when looking along the branching-structure orientation of that edge (in order to know what "left" means we need the underlying global orientation). At an edge which is part of η, it is the other way round. With this encoding, the equations corresponding to homology moves are automatically fulfilled by any model, as simultaneously flipping all bond directions around a fixed atom does not change anything due to the parity constraint of the corresponding tensor.

As in previous sections, we are looking for a simplified liquid, whose networks can be interpreted as cellulations with other types of faces. In order to do the same for η-triangulations, we have to think about how to equip arbitrary cellulations with spin structure.

The generalization of chains and boundaries to arbitrary cellulations is obvious. A generalized rule for ω_2 is the following: For every type of face, we have to specify one *special corner*, and we replace $\#T_0(v)$ in Eq. (242) by the number of adjacent faces for which v is in the special corner. We denote the special corner by a small angle, e.g., the special corner of the branching-structure triangle is the 0-vertex

$$\qquad\qquad . \tag{245}$$

Consider the sum of the ω_2 colourings of all vertices of a triangulation of a manifold with boundary. Every vertex, every edge and every triangle contributes exactly 1 to this sum, so we see that we obtain the *Euler characteristic* (modulo 2) of the manifold. If we want to use a different type of face, we have to define it via a η-triangulation. As the Euler characteristic (modulo 2) of a disk is 1, η will always have an odd number of "open ends" at the boundary of the new face. Without loss of generality, we can choose one single open end at the special corner.

The simplified liquid is very similar to the non-spin case in Section 6, just that we have to include bond directions determined by the spin structure. The elements and their interpretations as faces (with special corners) are the following.

- The clockwise triangle

$$\qquad\qquad \rightarrow \qquad\qquad . \tag{246}$$

- The clockwise cyclic 2-gon. Note that this element looses its rotation symmetry due to the spin structure (it gets replaces by a modified symmetry move though, see Eq. (258)),

$$
\begin{array}{cc}
\text{(diagram)} & \rightarrow \quad 01 \longrightarrow\!\!\triangleright\!\!\longrightarrow 10 \quad .
\end{array}
\tag{247}
$$

- The counter-clockwise cyclic 2-gon

$$
\begin{array}{cc}
\text{(diagram)} & \rightarrow \quad 01 \longrightarrow\!\!\blacktriangleright\!\!\longrightarrow 10 \quad .
\end{array}
\tag{248}
$$

The moves are the same as in Section 6, just that we have to add a choice of η on the left and right.

- The *spin 2-2 Pachner move*

$$
\begin{array}{ccc}
\text{(diagram)} & \leftrightarrow & \text{(diagram)} \quad .
\end{array}
\tag{249}
$$

This move does not change ω_2, so we can choose η to be trivial. In network notation, we get

$$
\text{(diagram)} \quad = \quad \text{(diagram)} \quad .
\tag{250}
$$

- The *spin triangle cancellation move*

$$
\text{(diagram)} \quad \leftrightarrow \quad \text{(diagram)} \quad .
\tag{251}
$$

This move adds/removes the interior vertex 0 with odd ω_2-colour, and changes the ω_2-colour of the boundary vertex 0. The minimal choice of η which corrects this, is the 10 edge on the left. In network notation,

$$
02 \longrightarrow\!\!\triangleright \!\!\triangleleft\!\!\longrightarrow 20 \quad = \quad 02 \longrightarrow\!\!\blacktriangleright\!\!\longrightarrow 20 \quad ,
\tag{252}
$$

the bond direction corresponding to that edge is reversed.

- The *spin (012) triangle symmetry move*

$$
\text{(diagram)} \quad \leftrightarrow \quad \text{(diagram)} \quad .
\tag{253}
$$

62

Again, nothing changes with ω_2, so η can be chosen empty. In network notation, again, we find

$$
\text{(figure)} \tag{254}
$$

- The *spin 2-gon cancellation move*

$$
\text{(figure)} \quad \leftrightarrow \quad \text{(figure)} . \tag{255}
$$

Here we chose the position of the special corners such that again ω_2 does not change. In network notation, this is

$$
a \longrightarrow\!\!\!\blacktriangleright\!\rightarrow\!\blacktriangleleft\!\!\!- b = a \longrightarrow\!\!\longleftarrow b \tag{256}
$$

The special corner of the spin 2-gon spoils its index permutation symmetry,

$$
\text{(figure)} \quad \leftrightarrow \quad \text{(figure)} . \tag{257}
$$

As the position of the special corner changes, ω_2 changes for both vertices 0 and 1, so we have to add an η-edge between them on one side. In network notation, we have to add an inwards arrow to one of the open indices

$$
a \longrightarrow\!\!\!\blacktriangleright\!\!\!- b = a \rightarrow\!\blacktriangleleft\!\!\!- b . \tag{258}
$$

Note that, analogous to the non-spin case in Section 6, this symmetry move is derived directly from the spin triangle cancellation move in Eq. (252). From there, the analogous move for the counter-clockwise 2-gon,

$$
a \longrightarrow\!\!\!\blacktriangleright\!\!\!- b = a \rightarrow\!\blacktriangleleft\!\!\!- b , \tag{259}
$$

is derived via the 2-gon cancellation move in Eq. 256.

8.3.3 Hermiticity

The Hermiticity condition is another point where it appears natural to distinguish between particle and hole sectors. If we express a fermionic Hamiltonian as an ordinary operator in Fock space, we would expect this operator to be Hermitian, e.g.,

$$
\text{(figure)} \tag{260}
$$

where H is the array tensor representing a fermionic tensor with the fixed index ordering $abb'a'$. If we interpret the same equation with H being an actual fermionic tensor (plain, or particle-hole with all configurations in the particle sector), we get an additional reordering sign, as we have to invert the ordering according to

$$
(-1)^{|a|(|b|+|b'|+|a'|)+|b|(|a'|+|b'|)+|b'||a'|}
$$

$$
= \begin{cases} 1 & \text{if} \quad |a|+|b|+|a'|+|b'| = 0 \mod 4 \\ -1 & \text{if} \quad |a|+|b|+|a'|+|b'| = 2 \mod 4 \end{cases} = (-1)^{\langle (a,b,a',b') \rangle} , \tag{261}
$$

where (a, b, a', b') denotes a configuration of all 4 indices blocked into a single one. So in total, we leave the global even-particle sector as it is, and multiply the global even-hole sector by a factor of -1. This operation, like complex conjugation, is in fact a tensor mapping, which we denote by

$$\text{\underline{\hspace{1.5cm}} } R \text{ \underline{\hspace{1.5cm}}} \ . \tag{262}$$

Indeed, the mapping R is compatible with tensor products, e.g.,

$$\tag{263}$$

However, it *inverts* bond directions, e.g.,

$$\tag{264}$$

In other words, the mapping makes former particle configurations behave like hole configurations and vice versa. We therefore refer to it as the *particle-hole mapping*.

　　If H is Hermitian as an ordinary operator in Fock space, this means that H as a fermionic tensor is invariant under transposition followed by complex conjugation and the mapping R which reverts the reordering sign we get from the transposition. This behaviour is inherited by the tensors of fermionic liquid models: Being Hermitian means being invariant under orientation reversal together with the combination of the mappings K and R. E.g.,

$$\tag{265}$$

This form of Hermiticity also appears natural without relying on the conventional formulation of fermionic many-body physics: In order to compare a network with its orientation-reversed version, we need to invert the bond directions as those are tied to the orientation. This is precisely the job of the mapping R as we have seen in Eq. (264).

　　Note that this formulation of Hermiticity only works for particle-hole fermionic, not for plain fermionic tensors. Surely, the reordering sign in Eq. (261) is a well-defined operation on plain fermionic tensors as well. However, for plain fermionic tensors, this operation depends on how indices are blocked, as

$$|(a, b)| \mod 4 \neq |a| + |b| \mod 4 \ . \tag{266}$$

Thus, it cannot be incorporated into network notation as a "zig-zag line" such as for complex conjugation, and does not form a tensor mapping.

　　Another viewpoint on the issue is to see that R can be realized (acting on a plain fermionic tensor) by contracting each index with the matrix

$$\begin{pmatrix} \mathbb{1} & 0 \\ 0 & i\mathbb{1} \end{pmatrix} \ , \tag{267}$$

where the first and second block act on the even and odd sector, respectively. This matrix cannot be a representation of (the additive 1-element of) $\mathbb{Z}_2$, but it is a representation of (the additive 1-element of) $\mathbb{Z}_4$, consisting of only 0 and 1 irreducible representations. The even-hole and odd-hole sectors are simply the missing 2 and 3 irreducible representations of $\mathbb{Z}_4$. Note that the square of the matrix is $(-1)^{P_f}$, where P_f is the fermion parity. Thus, KR is an anti-unitary which squares to $(-1)^{P_f}$, and these are exactly the properties that are usually required for a *time-reversal operator* in a fermionic system.

8.3.4   Models

Let us look for models of the liquid in fermionic tensors. Finding models does not involve any blocking of indices, so we can restrict ourselves to plain fermionic tensors. We choose a fixed index ordering for each tensor, and see what the equations mean for the array tensors representing the fermionic tensors with this ordering. Then we look at what minus signs we pick up from reordering the indices on both sides of the equation in order to perform the contractions, and equate the two sides. A choice of orderings that turns out to be particularily convenient is

$$
\begin{array}{cc} & \\ \end{array}
\qquad\qquad 0 \rightarrow\!\!\!\triangleright\!\!-1\,, \qquad 0 \rightarrow\!\!\!\triangleright\!\!-1 \,. \tag{268}
$$

In order to compute the reordering sign appearing in the fermionic liquid moves, we can proceed as follows. We start by concatenating the orderings of the involved tensors (in an arbitrary order). Then, we use index transpositions to move indices that are to be contracted next to each other, and then remove them. We record the minus signs collected when we perform the index transpositions on the way. We do this for both sides of an equation. In the end, we move the indices, such that the orderings on each side of the equation are equal. Of course, we can also cancel reordering signs on both sides.

In the following, we use a short-hand notation for sign calculations in contractions. E.g., $(bc + ab)|x'abdxc|(xx')$ will denote an intermediate step in the computation of the reordering sign, with index ordering $x'abdxc$, where we still need to contract x and x' (in that order), and we already collected a sign of $(-1)^{|b||c|+|a||b|}$. For the spin 2-2 Pachner move we get the following

$$
\begin{aligned}
|x'abdxc|(xx') &= |dayy'bc|(yy'), \\
(dx)|abdc| &= |dabc|, \\
(dx + cd)|abcd| &= (d)|abcd|, \\
|abcd| &= |abcd| \,.
\end{aligned}
\tag{269}
$$

We find that all the reordering signs on the left and right cancel. The other reordering signs are computed in Appendix D. Interestingly, also all other signs cancel. Note that this would not have been the case without the spin structure modification. This is not a general property of fermionic liquid models, though. First of all, we would have gotten non-trivial reordering signs if we had chosen a different index ordering in Eq. (268). Second, the fact that we can find an index ordering for which the reordering signs vanish seems to be specific to the $1 + 1$-dimensional case, and we do not find the same to be true in dimensions $2 + 1$ or higher.

The vanishing of the reordering signs implies that the models of the liquid in fermionic tensors are in one-to-one correspondence to the models in array tensors which have a $\mathbb{Z}_2$-grading. Note that the latter are agnostic of the bond directions, and so the liquid we get is equal to its non-spin analogue in Section 6.3. A fixed array tensor model might allow for different inequivalent $\mathbb{Z}_2$-gradings, corresponding to different fermionic models. Technically, there always exists a grading by considering every configuration as even. Those models are trivial though, in the sense that they do not have any fermionic charges.

We should warn the reader that despite there being a one-to-one correspondence, fermionic spin-topological and $\mathbb{Z}_2$-graded topological models are still different models. In particular, the one-to-one correspondence will break when we add other (non-topological) moves, such as invertibility, or commutativity.

8.3.5   Kitaev chain

In this section we consider the only interesting model of the described liquid, which turns out to be equivalent to the Kitaev chain. The $\mathbb{Z}_2$-graded algebra that it is based on is probably the simplest

one one can think of, namely the group algebra of $\mathbb{Z}_2$ itself. Written as arrays for the fixed index ordering in Eq. 268, the tensors of the model are given by

$$
\underset{c}{\overset{b \quad a}{\triangle}} = \frac{1}{\sqrt{2}} \cdot \delta_{a+b,c} = \frac{1}{\sqrt{2}} \left(\begin{pmatrix} 1 & 0 \\ 0 & 1 \end{pmatrix} \begin{pmatrix} 0 & 1 \\ 1 & 0 \end{pmatrix} \right) \, ,
$$

$$
a \,\blacktriangleright\, b = \delta_{a,b} = \begin{pmatrix} 1 & 0 \\ 0 & 1 \end{pmatrix} \, , \tag{270}
$$

$$
a \,\blacktriangleright\, b = \delta_{a,b} = \begin{pmatrix} 1 & 0 \\ 0 & 1 \end{pmatrix} \, .
$$

Here, a, b and c are understood as elements of $\mathbb{Z}_2$ and in the expressions for the triangle tensor a and b label rows and columns, while $c = 0, 1$ refers to the first and second matrix, respectively. It can be easily seen that the model is also Hermitian: All tensors are real, only supported in the particle sector (by construction, as we used plain fermionic tensors), and invariant under orientation reversal. Thus, the model is invariant under each K, R, and orientation reversal separately, and certainly under all three operations together.

The *Kitaev chain* [47], to which this model is equivalent, is a fermionic chain with a nearest-neighbour Hamiltonian of Majorana fermionic operators

$$
H = - \sum_i (c_i + c_i^\dagger)(c_{i+1} - c_{i+1}^\dagger) \, . \tag{271}
$$

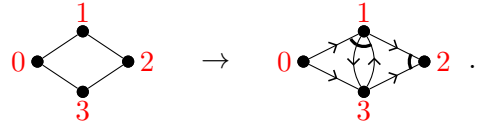It is a commuting-projector model, with the projector given by

$$
\begin{aligned}
P &= \frac{1}{2}(\mathbb{1} + (c_0 + c_0^\dagger)(c_1 - c_1^\dagger)) \\
&= \frac{1}{2} \left(|0\rangle \langle 0| + c_0^\dagger |0\rangle \langle 0| c_0 + c_1^\dagger |0\rangle \langle 0| c_1 + c_0^\dagger c_1^\dagger c_1 c_0 - c_1 c_0 + c_1^\dagger c_0 + c_0^\dagger c_1 - c_0^\dagger c_1^\dagger \right) \, .
\end{aligned} \tag{272}
$$

Applying the expansion in Eq. (232) yields

$$
A^{s_0 s_1}_{s_0' s_1'} = \frac{1}{2} \delta_{s_0 + s_1, s_0' + s_1'} (-1)^{s_0 s_1 + s_0' s_1'}. \tag{273}
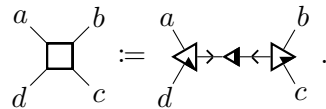$$

A becomes a fermionic tensor with index ordering $s_0' s_1' s_1 s_0$.

In order to compare this commuting-projector model with our liquid model, we use a liquid mapping identifying a projector with a rhombus-like cell of space-time, similar to how we did in Section 5.5.3,

$$
\underset{3}{\overset{1}{\underset{0 \quad \quad \quad 2}{\diamond}}} \quad \rightarrow \quad \underset{3}{\overset{1}{\underset{0 \quad \quad \quad 2}{\diamond}}} \quad . \tag{274}
$$

The shown cellulation of the rhombus yields the mapping

$$
\underset{d \quad \quad c}{\overset{a \quad \quad b}{\square}} := \underset{d \quad \quad c}{\overset{a \quad \quad b}{\triangleleft \blacktriangleright \, \blacktriangleleft \, \triangleright}} \, . \tag{275}
$$

In order to evaluate the network on the right hand side, we first compute the reordering sign we get when bringing the indices in the ordering $dcba$, starting from the orderings in Eq. (268), to find

$$
\begin{aligned}
|daxy'x'cyb|(xx')(yy') &= x|day'cyb|(yy') = x + yb|dacb| \\
&= x + yb + a(c+b)|dacb| = dc + ab|abcd| \, .
\end{aligned} \tag{276}
$$

So for the chosen index ordering, the array representing the fermionic tensor is given by

$$
\sum_x (\frac{1}{\sqrt{2}} \delta_{d+x,a})(\frac{1}{\sqrt{2}} \delta_{c+x,b})(-1)^{dc+ab} = \frac{1}{2} \delta_{a+b,c+d}(-1)^{dc+ab} \, , \tag{277}
$$

which exactly equals the array in Eq. (273).

9 Topological order in $3 + 1$ dimensions

In this section, we will sketch two liquids for topological order in $3 + 1$ dimensions. One is a very straight-forward liquid based on *simplicial complexes*, and the other one is analogous to the face-edge liquid in $2 + 1$ dimensions, with volumes and faces being represented by atoms.

9.1 The 4-cell liquid

In this section, we will sketch what is probably the most straight-forward generalization of the volume liquid in $2 + 1$ dimensions to $3 + 1$ dimensions: There is one 5-index atom for every 4-simplex of a (branching structure) triangulation of a 4-manifold, and if two 4-simplices share a 3-simplex, the corresponding atoms are connected by a bond.

The liquid we will sketch describes topological manifolds *without* an orientation, for reasons of variety and because the resulting liquid is a little more simple. The main element of the liquid is the 4-simplex

$$\tag{278}$$
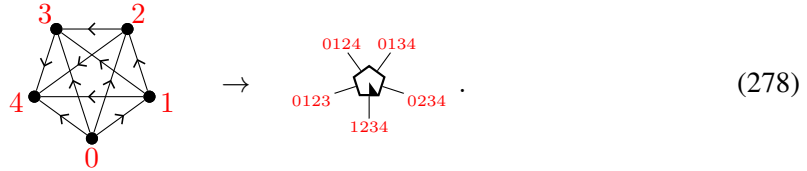
In 4 dimensions, there are 3-3, 2-4, and 1-5 Pachner moves for this element, and there are many different versions of those moves due to the edge orientations. One particular 3-3 Pachner move is given by

$$\leftrightarrow \quad \text{same 1-skeleton .} \tag{279}$$

In network notation, this is

$$\tag{280}$$
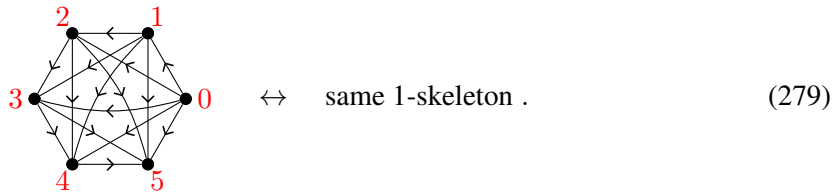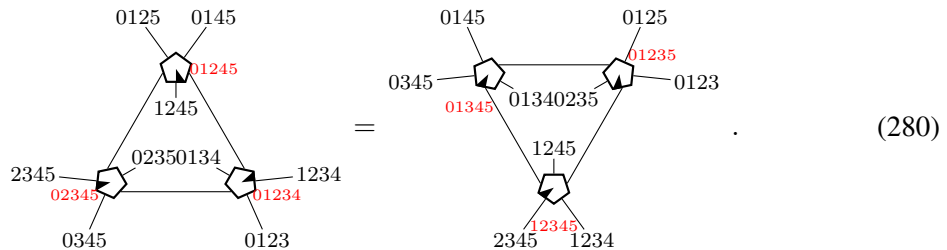
As in the lower-dimensional cases, we can restrict to only this single 3-3 Pachner move if we introduce additional bindings, elements, and moves, which have geometric interpretations in terms of more general cellulations. The 3-cells for the additional bindings are just the 3-cells for the additional elements of the $2 + 1$-dimensional volume liquid, e.g., there are two flip hat bindings, and a 2-gon binding. As in $2 + 1$ dimensions, we need cancellation moves which allow us to derive 2-4 and 1-5 Pachner moves from the 3-3 Pachner moves, and symmetry moves which allow us to derive Pachner moves with different edge orientations. Permuting the vertices of the 4-simplex changes the edge orientations though, so we have to glue elements called *4-flip hats* in order to flip them back. A 4-flip hat is given by 4-cells consisting of two flip hats and two tetrahedra, e.g.,

$$\tag{281}$$
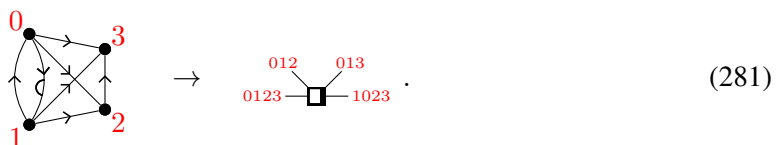
We can flip an edge of a 4-dimplex by gluing three 4-flip hats to three boundary tetrahedra sharing that edge. E.g., the (01) 4-*simplex symmetry move* equates a 4-simplex mirrored at the 01 edge with one whose 01 edge was flipped. More precisely, we use a more powerful version of this move where one of the three 4-flip hats was brought to the other side:

$$
\text{[diagram]} \qquad \leftrightarrow \qquad \text{same 1-skeleton .} \tag{282}
$$

In network notation, this gives

$$
\text{[diagram]} \qquad = \qquad \text{[diagram]} . \tag{283}
$$

We get 3 different versions of the element in Eq. (281), depending on how we choose the orientations of the edges adjacent to the vertices 2 and 3. Using those, we also get a (12)-, (23)- and (34)- tetrahedron permutation move, which generate the whole 4-simplex symmetry group. Moreover, the 4-flip hats have symmetries which however change the favourite edge of the involved 2-gon, and we need additional elements for changing the latter.

The most important example of a cancellation move is the *4-simplex cancellation move*

$$
\text{[diagram]} \qquad \leftrightarrow \qquad \text{[diagram]} . \tag{284}
$$

The left hand side consists of two 4-simplices, glued at two of their tetrahedra, whereas the right hand side consists of 3 4-flip hats glued at their tetrahedra in a cyclic fashion. In terms of networks, we find

$$
\text{[diagram]} \qquad = \qquad \text{[diagram]} . \tag{285}
$$

There are also cancellation moves for the 4-flip hat, and so on.

In order to get the most general physical phases with gappable (i.e. topological) boundary, we would also have to introduce face weights analogous to the edge weights in $2+1$ dimension. Any face in (the interior of) a 4-dimensional cellulation corresponds to a cycle of 4-cells adjacent at 3-cells. E.g., the loop on the left side of Eq. (280) corresponds to the 024 face, and the one on the right side to the 135 face. Into each such loop we have to insert exactly one face weight.

We do not guess the bindings, elements, and moves from scratch, but follow some systematics, which we will outline briefly. The different bindings correspond to different 3-cells, and the elements to different 4-cells of those cellulations. The moves are equations between two different cellulations of the 4-ball, and if we glue both sides of a move together, we get a cellulation of a 4-sphere, which can be seen as the boundary of a 5-cell.

In order to find those 3-cells, 4-cells and 5-cells, we need an operation called the *stellar cone*, which transforms a n-cell into a $n+1$-cell by the following procedure. First, add an additional

vertex called *central vertex*. Then, for every boundary x-cell, add an $x + 1$-cell which is spanned by this x-cell and the central vertex (the original n-cell together with the central vertex span the $n + 1$-cell itself). If there is a branching structure, there are two different choices of orientation for the new edges. Either they are all pointing towards the central vertex, or away from it.

In general, in the n-dimensional n-cell liquid, we can take as x-cells the stellar cones of the $x - 1$-cells, which are the same as the $x - 1$-cells of the $n - 1$-dimensional $n - 1$-cell liquid. E.g., the 3-3 Pachner moves yield a 5-simplex, which is the stellar cone of the 4-simplex representing an element. The 4-flip hat element is the stellar cone of the flip hat, which is a binding of the present liquid, as well as an element of the 3-dimensional volume liquid (Eq. (164)), as well as the (01) triangle symmetry move of the unoriented 2-dimensional face liquid (Eq. (99)). At the same time, the 4-flip hat is the (01) tetrahedron symmetry move of the unoriented version of the 3-dimensional volume liquid. As another example, both the (01) 4-simplex symmetry move as well as the 4-simplex cancellation move yield the same 5-cell which the stellar cone of the 4-flip hat.

As the last example shows, the 5-cells can be decomposed into two 4-ball triangulations in different ways. We certainly do not want to choose all those decompositions, as, e.g., different decompositions of the 5-simplex yield all different variants of the 4-dimensional Pachner moves already. However, it always suffices to take a single Pachner move (one of the ones with the most open indices), together with symmetry cancellation moves from which we can derive all others.

The idea that fixed-point models for topological order in general dimensions can be described by "Pachner-move invariant simplex tensors" is rather straight-forward, and has been explicitly spelled out, e.g., in Ref. [48]. Our contribution here is to give a framework which allows us to arrive at a refined set of moves, containing only a single Pachner move together with a collection of simpler "auxiliary moves". An example for a model is the so-called *Kashaev invariant*, for which the 4-simplex tensor has explicitly been spelled out in Ref. [49].

9.2   The volume-face liquid

In this section, we sketch a less straight-forward topological liquid in $3 + 1$ dimensions. It is similar to the face-edge liquid in $2 + 1$ dimensions, in that we associate elements to $d - 1$-cells and $d - 2$-cells in a d-dimensional cellulation. There is one atom at every volume and one atom at every face. If a volume and a face are adjacent, the corresponding atoms share a bond. Note that in a 4-dimensional cell complex, a face can be adjacent to more or less than two volumes. Faces adjacent to exactly 2 volumes are not represented by atoms; instead, the two volumes are directly connected by a bond. When restricting to networks with such trivial faces, we get a mapping from 3-dimensional cell complexes to 4-dimensional cell complexes, which we will call the *volume mapping*. It makes sense to use the volumes of the simplified volume liquid in $2 + 1$ dimensions (Section. 7.1) as volume elements, and make all of the $2 + 1$-dimensional moves into volume-only moves of the $3 + 1$-dimensional liquid.

9.2.1   The liquid

A face in a 4-dimensional cell complex is Poincaré dual to another face. The adjacent volumes, and thus indices, correspond to the edges of that dual face. The full shape of the face is specified by both the shape of the face itself and the shape of the dual face. E.g., when we have a triangle face, whose dual face is a 4-gon, we will call this a 4-valent triangle. Similar to 2-valent faces, pillow-like volumes whose boundary consists of two equal faces are just represented by a direct bond between those faces. Restricting to cell complexes with triangle faces (with different dual faces), separated by such trivial pillow-like volumes, yields a mapping from $1 + 1$ to $3 + 1$-dimensional cell complexes, which we will call the *triangle face mapping*. So it makes sense to take the triangle and cyclic 2-gon as dual shapes for the triangle faces, together with all the

mapped $1 + 1$-dimensional moves. Analogously, we get a *2-gon face mapping* by restricting to cyclic 2-gon faces with different dual faces. We will draw the 2-dimensional liquid formed by the 2-gon faces as filled circles.

Each edge is equipped with an orientation, and each volume is equipped with a dual orientation, i.e., a favourite adjacent 4-cell. Those orientations allow us to pick a 01 edge and a 01 volume of a non-cyclic and dually non-cyclic 3-valent triangle. Considering the face itself and its 01 edge inside its 01 volume, we can decide whether the face is clockwise or counter-clockwise relative to the global orientation.

Analogous to the face-edge liquid in $2 + 1$ dimensions, we need to introduce a 2-index *corner weight* element in order to get models for a very general class of phases

$$\longrightarrow\!\!\boxdot\!\!\longrightarrow \ . \tag{286}$$

At every pair of edge and adjacent 4-cell, there is an alternating cycle of face and volume elements. We demand that, in a network representing a 4-manifold, there is one weight atom inserted at every such cycle. More precisely, the weight atoms are of different elements depending on the edge-4-cell pair and the face and volume between which they are inserted. The element depends on whether the face is a 2-gon or a triangle, whether the edge is the 01, 02, or 12 edge of the triangle or the favourite or non-favourite edge of the 2-gon, and whether the dual orientation of the volume points towards or away from the 4-cell. The corner weight depicted above is for the favourite edge of a 2-gon, with the volume pointing towards the 4-cell. All other corner weights can be constructed from this single one. E.g., the favourite edge 2-gon corner weight for the volume pointing away from the 2-gon is obtained by

$$a\rightarrow\!\!\bullet\!\!\leftarrow\!\!\boxdot\!\!\bullet\!\!-b \ . \tag{287}$$

Or, following Eq. (179), the corner weight for the 01 edge of the triangle is obtained by

$$b\rightarrow\!\!\boxtimes\!\!-f \ := \ {}^{b}\!\!\underset{\boxdot\rightarrow\diamondsuit\leftarrow\boxdot}{\overset{\blacksquare\quad\quad\square}{\rule{0pt}{1pt}}}\!\!{}^{f} \ . \tag{288}$$

Similarly, the corner weights for the 02 edge and the 12 edge

$$\longrightarrow\!\!\boxtimes\!\!-\ , \qquad \longrightarrow\!\!\boxtimes\!\!\longrightarrow \tag{289}$$

can be constructed, e.g., following Eq. (183) for the case of the 02 edge.

Edges of $2 + 1$-dimensional cell complexes stay edges under the volume mapping, and then have two adjacent 4-cells. Thus, the edge weights of the $2 + 1$-dimensional volume liquid can be constructed from two corner weights of the present $3 + 1$-dimensional liquid. For the 2-gon edge weight, we get

$$a\longrightarrow\!\!-b \ := \ a\rightarrow\!\!\boxdot\!\!\bullet\!\!\leftarrow\!\!\boxdot\!\!\bullet\!\!-b \ . \tag{290}$$

Or, for the 01 edge weight

$$a\longrightarrow\!\!-b \ := \ a\rightarrow\!\!\boxtimes\!\!\bullet\!\!\leftarrow\!\!\boxtimes\!\!\circ\!\!-b \ . \tag{291}$$

Vertices in $1 + 1$-dimensional cell complexes become 4-cells under the triangle face mapping, and are then adjacent to three edges. Thus, the vertex weight of the $1 + 1$-dimensional triangle face liquid can be constructed from three corner weights

$$a\rightarrow\!\!\square\!\!-b \ := \ a\rightarrow\!\!\boxtimes\!\!\rightarrow\!\!\boxtimes\!\!\rightarrow\!\!\boxtimes\!\!-b \ . \tag{292}$$

Similarly, the vertex weight of the $1 + 1$-dimensional 2-gon face liquid consists of two corner weights

$$a\rightarrow\!\!\blacksquare\!\!-b \ := \ a\rightarrow\!\!\boxtimes\!\!-\diamondsuit\!\!-\boxtimes\!\!-\diamondsuit\!\!-b \ . \tag{293}$$

So far, we got one copy of the 3-dimensional volume liquid, and two copies of the 2-dimensional face-liquid. We now need moves which connect the elements of those liquids, by "pulling faces through volumes". Roughly, every such move can be constructed from a quadrupel consisting of a volume V, a dual face F_D, a special face of the volume, and a special edge of the dual face. The move involves one V volume atom for each edge of F_D, and one F_D-valent F_V face atom for each face F_V of V. The volume and face atom corresponding to the special edge and face are on one side of the move, and all the others on the other side.

As an example, pick for V the 01 flip hat (with one of the triangles as special face), and for F_D the triangle (with the 02 edge as special edge). The corresponding pull-through move is given by

$$\tag{294}$$

Here, the empty circles represent the triangle face atoms, and the full circles represent the 2-gon face atoms (both 3-valent in this case). Note that the two $1 + 1$-dimensional liquids formed by the triangle and 2-gon tensors do *not* form a $2 + 1$-dimensional face-edge liquid together, as in Section 7.2.

As another example, pick for V the 12 flip hat, and for F_D the cyclic 2-gon. We get a move that pulls the 2-valent face-atoms through the flip hat and thereby changes its orientation,

$$\tag{295}$$

As a further example, pick for V the tetrahedron, and for F_D the triangle. We get

$$\tag{296}$$

Unfortunately, the pull-through moves as described above are not quite enough to have a fully topological liquid (such that there is an invertible mapping to the 4-simplex liquid sketched in the section above). We also need to allow moves where V has two special faces, such that the left hand side consists of a volume atom with *two* face atoms. However, this move would not be topological (that is, it would prevent a mapping back from the 4-simplex liquid to the present liquid). In order to make it topological, we need to add a "projector onto two neighbouring triangles", which we can build from 4 flip hats

$$\tag{297}$$

9.2.2   Models

A well-known class of fixed-point models for topological phases in $3 + 1$ dimensions are *second order gauge theories*. Analogously to ordinary gauge theories being based on a gauge group, a

second order gauge theory is based on a *2-group*. A 2-group is concretely defined by what is called a *crossed module*. The latter consists of two groups G and H, with a homomorphism

$$h : H \to G \tag{298}$$

from H to G, and an action

$$\alpha : G \times H \to H \tag{299}$$

of G on H.

Following Ref. [50], a more condensed representation of (equivalence classes of) 2-groups is given by a group Π_1, a commutative group Π_2 (arising from G and H as the kernel and co-kernel of h), an action α, and a Π_2-valued group 3-cocycle of Π_1 with action α, that is, a map

$$\beta : \Pi_1 \times \Pi_1 \times \Pi_1 \to \Pi_2 \ , \tag{300}$$

such that

$$\begin{aligned}
\beta(ab, c, d) &+ \beta(a, b, cd) \\
&= \alpha(a, \beta(b, c, d)) + \beta(a, bc, d) + \beta(a, b, c) \ ,
\end{aligned} \tag{301}$$
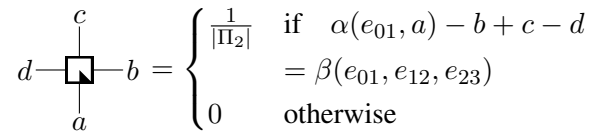
where we denoted group multiplication in Π_2 additively.

Like the fusion category models of the $2 + 1$-dimensional volume liquid, 2-group models of the present liquid are most conveniently formulated using label-dependent tensors. The labels are the elements of Π_1, and might be thought of as being located at the edges of the complex. The dimension of the indices at a face is either $|\Pi_2|$ if the edge labels around the face multiply up to 1, and 0 otherwise. All face tensors are given by delta functions (in every valid edge label configuration), e.g.,

$$\begin{array}{c} a \qquad b \\ \bigcirc \\ c \end{array} = \begin{array}{c} a \qquad b \\ \bullet \\ c \end{array} \ . \tag{302}$$

where a, b and c are elements of Π_2. If we denote the label of, e.g., the 03 edge of the tetrahedron by e_{03}, then tetrahedron is given by

$$d - \boxed{} - b \ \begin{array}{c} c \\ \\ a \end{array} = \begin{cases} \frac{1}{|\Pi_2|} & \text{if} \quad \alpha(e_{01}, a) - b + c - d \\ & \quad = \beta(e_{01}, e_{12}, e_{23}) \\ 0 & \text{otherwise} \end{cases} \ . \tag{303}$$

The edge weights are all identity matrices. The flip hats can be obtained from the tetrahedron by the mapping in Eq. (187). The resulting dimension of the 2-gon index is $|\Pi_1||\Pi_2|^2$. Of course, we can also interpret the edge labels as indices, copy them and block them into the face indices to obtain ordinary tensors.

10　Summary and conclusion

In this work we introduced a systematic graphical language which allows us to think about fixed-point models for (topological) phases for various scenarios in a unified way, and stimulates and facilitates the search for new families of fixed-point models corresponding to combinatorial representations of space-time.

There are four main goals we attempt to achieve with the formalism introduced. The first goal is to sort the vast body of existing literature on fixed-point models by introducing a simple and unified mathematical language. All of those models are based on algebraic or categorical structures defined by a set of equations. All those equations are manifestations of one central property, namely topological invariance in Euclidean space-time. All other properties, such as

commuting-projector Hamiltonians, or PEPS representations with virtual symmetries, are direct consequences of the topolgical invariance, but not the other way round. That's why we believe that topological invariance should be the point to start with. Instead of "guessing" an algebraic or categorical structure used as an input to fixed-point construction, we derive algebraic structures from the topological invariance. Tensor networks with their familiar Penrose notation appear as the natural mathematical language, as they represent at the same time combinatorial representations of the space-time topology (and their moves) as well as the path integral itself (and its equations). We would also like to mention that unlike "string diagrams" in conventional algebra or category theory, tensor networks are not formulated with an inherent flow of (real-)time, and thus more natural to represent path integrals in Euclidean space-time.

The second goal is to obtain a deeper understanding of existing families of models, and formulate them in their most general form. In the literature, clear explanations of why known state-sum constructions or fixed-point models take the form they have are lacking. We deliver many of those explanations: We explain the role of an orientation, and show the necessity to add a branching structure to state-sums based on triangulations. It is easy to see that every topologically invariant path integral with topological boundary can be coarse grained into a Pachner-move invariant simplicial tensor network. We show how to get from many Pachner-move equations (due to different branching structures) to a single one by extending the construction to more general cellulations. In Appendix C, we show how to arrive at the usual Turaev-Viro form of the state-sum. Furthermore, we introduce a new path integral picture for weak Hopf algebra based quantum doubles. Quantum double models have been mostly studied from the perspective of commuting-projector Hamiltonians [41, 42]. The commutativity follows from the weak Hopf axioms, however, a direct motivation for why weak Hopf algebra related structures are the correct input for those models was still lacking. We demonstrate that those structures directly emerge from a combinatorial version of topological invariance. In particular, the central bi-algebra axiom corresponds to a topological move which "pulls an edge through a face" as in Eq. (213).

The first two goals have been addressed to a large extent in the present paper by working out concrete examples. The other two goals will be worked out in future publications. The third goal is that we can systematically construct new combinatorial representations of topolgical manifolds, yielding new classes of models. Using our formalism, this can be achieved very quickly with a bit of geometric intuition and creativity. To sketch one example in 2+1D, think of cellulations where all vertices are colored red, blue, or green, and all faces are triangles with one red, one blue, and one green vertex. Now, associate tensors to the volumes and contract between volumes sharing a face. The simplest volume compatible with the coloring is the octahedron. The topological moves are, among others, given by commuting two tetrahedron tensors past each other in different ways. Octahedron tensors obeying the moves form a new family of models, one of which turns out to be the well-known color code. If we add appropriate edge weights, the "tricolored" liquid will be equivalent to a standard triangular liquid, so the two families of models describe the same phases. In particular, the color code is known to be phase-equivalent to two copies of the toric code. It is, however, a different microscopic model and has advantages (and disadvantages) over the latter for error-correction purposes. Having different microscopic realizations of the same phases is important for engeneering those phases (e.g., for building a quantum computer), and our framework yields a method of systematically constructing such new realizations.

As a fourth goal, we would like to mention that, apart from obtaining new models for the same phases, our formalism has the potential to go beyond known constructions and obtain fixed-point models for new phases. There are liquids that are not equivalent to the standard ones, which means that the corresponding path-integral tensor networks cannot be coarse-grained into a standard simplicial form [33]. This does not directly imply that the more general liquids have models for more general phases, but it does indicate that this is indeed possible. An exciting candidate for more general phases are chiral phases in 2+1D which are lacking any fixed-point description so far. The

generalized liquid models are compatible with the absence of both a topological (i.e. gapped) boundary and commuting-projector Hamiltonians, features characteristic for chiral phases.

One of the central tools that we have introduced are liquid mappings. The most important use of liquid mappings in this paper was to define a notion of equivalence of liquids. Liquid mappings formalize various operations and relations in a unified way, such as the following.

- The equivalence between ad hoc topological liquids and their more sophisticated simplified forms.

- The equivalence between different liquids representing the same deformability class, as we have, e.g., seen in Section 7.3.

- The relation between topological liquids and known algebraic structures, as described, e.g., in Section 4.1.2.

- Topological deformations, such as reshaping a boundary into a bulk as in Section 4.3.3, or compactifications or suspensions like the 2D embedding mapping in Section 7.2.

- The relation of liquids to commuting-projector Hamiltonians, as seen, e.g., in Section 4.1.4.

- The relation of fixed-point liquid models to square lattice models, as introduced in Section 4.1.1.

In this work, we have focused on liquids for topological order as such. Boundaries, anyons, and other sorts of defects are described by liquids as well, as we have sketched in Section 4.3. E.g., there is a liquid describing anyons within the 3-dimensional face-edge liquid, whose models are similar to representations of quantum doubles of weak Hopf algebras. Or, there is a liquid describing boundaries of the 3-dimensional volume liquid, whose models are similar to modules of fusion categories. We have already seen the possibility to add extra structures like orientations in Section 6 or spin structures in Section 8, and the possibility to add beyond-topological moves, such as the ones that guarantee invertibility of the model in Section 6.6. A much more novel pursuit would be the formalization of conformal, not topological, field theories in terms of liquid models. To this end, one would need a combinatorial representation of conformal manifolds (more precisely, a combinatorial representation for a dense set in the conformal moduli space), together with moves preserving the conformal structure.

All of our liquid models are microscopic physical models defined by a concrete local partition function. This is in contrast to the description of phases via more abstract and indirect invariants, such as (non-fully extended) axiomatic TQFT, giving rise to structures like (non-special) commutative Frobenius algebras in $1 + 1$ dimensions, or modular tensor categories in $2 + 1$ dimensions. All these structures can be formulated as liquids as well, as long as they have a finite set of generators and relations (which roughly appears to be the case for TQFTs extended down to at least the circle). The relation between those more abstract invariant liquids and the concrete microscopic liquids is formalized by a liquid mapping from the former to the latter. The most famous example for this is the quantum double, or Drinfeld centre of fusion categories, or Hopf algebras.

The systematics and simplicity of our language also makes it more accessible to automatization. The standard task on the combinatorial/graphical level of liquids is to find derivations of moves from a given set of moves. This is needed in order to prove that substrate mappings are actually liquid mappings, which is important for showing that certain liquids are equivalent. We think that it is possible to automatize the process of finding derivations numerically. Of course, in the general case, finding derivations is an undecidable and certainly hard problem, as tasks like theorem proving can be relatively easily encoded in finding derivations. However, the networks we deal with do not represent arbitrary logical statements, but patches of low-dimensional manifolds. Surely, proving the equivalence of manifolds based on triangulations is a hard and undecidable

problem as well in general, but this is only if we scale the complexity of the topology. In our case, the manifold patches have a simple and constant topology (two balls if we're dealing with topological liquids), and we merely scale the size of the triangulation and not the complexity of the topology itself.

The standard task on the level of models is, of course, finding models. For conventional array tensors, but also for fermionic tensors or tensors with symmetry, the moves turn into polynomial equations for the tensor entries. In principle, even though with a possibly high computational effort, we can find roots to those equations by iterative numerical optimization methods, such non-linear conjugate-gradient, or Gauss-Newton methods. Surely, finding roots of general liquids has a bad scaling in the bond dimension: The cost of per iteration scales with rather high polynomials (depending on the algorithm and on how complicated the liquid is) in the bond dimension, and the volume of initial conditions for which the iteration actually converges to a global minimum might be small. We should keep in mind though, that only the simplest phases, i.e., the ones realizable with a low bond dimension, are physically relevant. Roughly speaking, the higher the bond dimension needed to realize the phase, the more unlikely it will be to encounter it in nature, and the harder it will be to experimentally realize it. So for practical purposes, we can restrict to small bond dimensions where numerical methods might still be feasible. Note that also for known families of fixed-point models, their equations boil down to polynomials. However, due to the systematics of our language we don't have to write a separate algorithm for every different family of fixed-point model, but can take the latter as an input to a single algorithm.

One point that was not the focus of this work is the role of tensor types. We saw that models with symmetries, fermions, or models which are deformable only up to pre-factors, can be seen as different tensor types. We also saw that certain tensor types seem to "get along" well with certain kinds of extra structures added to liquids, such as complex tensors and orientation, or fermionic tensors and spin structures. What we did not mention so far is that certain restrictions to "exactly solvable" classes of models can also be formulated as tensor types, such as non-interacting (i.e., Gaussian, quadratic, free) fermionic models, or models that can be formulated within the stabilizer formalism. It is the hope that this work stimulates such further endeavours.

11   Acknowledgements

A   Overview over the complete vocabulary

In this section, we give an overview over the complete vocabulary introduced in the main text. A *substrate* consists of a finite set of *elements*. Each of these elements has a finite set of *indices*. Additionally, there is a finite set of *bindings*, and each index is associated to a binding.

A *network* (of a given substrate) consists a finite set of *atoms*. Each atom has a specific element. There is a finite set of *bonds* connecting pairs of indices of the individual atoms. A bond might also have one or two *open indices* which are not connected to any other atom.

A *move* is a pair of networks, together with a bijection between their open indices. A *liquid* is a substrate together with a set of *moves*. Moves can be composed to yield other moves, and such a composition is called a *derivation* of the resulting move.

A *liquid mapping* between two liquids A and B associates 1) to every binding of A a collection of bindings of B and 2) to every element of A a network of B, such that every index of the A-

element corresponds to an according collection of open indices of the B-network. Applying this replacement to all elements in a move of A, we obtain another move, called the *mapped move*. The mapped moves have to be derived moves of B.

A *model* of a substrate consists of 1) one bond dimension for each binding, and 2) one tensor for each element. The indices of the tensor and their bases correspond to the indices of the element and their bindings,

$$\begin{aligned} \text{Binding} &\rightarrow \text{Dimension} \\ \text{Element} &\rightarrow \text{Tensor} \end{aligned} \tag{304}$$

A *model* of a liquid is a model of the corresponding substrate. Every move defines an equation between two tensors via the evaluations of the two corresponding networks. All these equations have to hold,

$$\begin{array}{ccc} \text{network 1} & \xrightarrow{\quad\text{move}\quad} & \text{network 2} \\ \text{evaluate}\Big\downarrow & & \Big\downarrow\text{evaluate} \cdot \\ \text{tensor 1} & \xrightarrow[\quad=\quad]{} & \text{tensor 2} \end{array} \tag{305}$$

B   Remaining moves for the volume liquid in 3 dimensions

In this appendix, we complete the moves of the simplified $2 + 1$-dimensional liquid from Section 7.1.2. In order to generate the full orientation-preserving symmetry group of the tetrahedron, we have to add the (012) *tetrahedron symmetry move*

$$\tag{306}$$

We also need the remaining symmetry moves of the flip hats, i.e., for ones for the counter-clockwise 01, the clockwise 12 and the counter-clockwise 12 flip hats

$$\tag{307}$$

$$\tag{308}$$

$$\tag{309}$$

Regarding the cancellation moves, we need to add the cancellation move for the 12 flip hats

$$\tag{310}$$

and the 2-*gon flip cancellation move*

$$\tag{311}$$

C From the face-edge liquid to Turaev-Viro models

In this section, we describe how to reshape complex models of the 3-dimensional face-edge liquid into state-sums of Turaev-Viro form. First of all, we further extend the liquid by introducing the non-cyclic 2-gon as a further binding. The latter can be triangulated with two triangles

$$0 \, \text{⌢} \, 1 \quad \rightarrow \quad 0 \, \text{⬯} \, 1 \, , \tag{312}$$

so, the new binding is defined by

$$C \Big|_{01} := T \Big|_{012} T \Big|_{102} . \tag{313}$$

Note that the favourite edge is needed to determine the ordering of the two triangles. We also need it to define when a 2-gon is clockwise or counter-clockwise. With the new 2-cell binding, we can construct banana-like volumes whose boundaries consist of non-cyclic 2-gons glued at edges, e.g.,

$$\left(\quad , \quad \right) . \tag{314}$$

The boundary of the volume on the right consists of 3 2-gons, two in the front and one in the back. If we want to construct this new element, we have to replace every 2-gon by two triangles as in Eq. (312), and triangulate the resulting volume. Precisely the same volume was triangulated in Eq. (221), and thus the corresponding element is the same as the edge element of the equivalent face-edge liquid, defined in Eq. (222). So bananas define a (mapping from a) $1 + 1$-dimensional face liquid.

The *01 hat* can be triangulated by two tetrahedra

$$\rightarrow \tag{315}$$

In network notation, we have

$$x - \boxed{}^{ab} - y := x - \boxed{}_{0123f} \blacktriangleright \blacksquare^{b}_{0123b} - y . \tag{316}$$

This element defines a topological boundary for the banana liquid. Consider the following re-cellulation from two flip hats glued at a triangle on the left to one flip hat and a banana glued at a 2-gon on the right

$$\rightarrow \quad \text{same 1-skeleton} . \tag{317}$$

This corresponds to the move whose simplified version is depicted in Eq. (76)

$$x - \boxed{}^{a} - \boxed{}^{b} - y = \,\,^{a}\!\!\seardown\!\!\bullet\!\!\swarrow^{b}_{x - \boxed{} - y} . \tag{318}$$

Note that there is also a counter-clockwise version of the 01 hat, for which the 13 instead of the 03 edge carries an edge weight. Also, there are the 02 and the 12 hats (together with their counter-clockwise counterparts), which are the same apart from different edge orientations of the 02 and 12 edges in Eq. (315). The topological moves further imply that those representations commute, thus they form a single representation of the product of the three algebras.

Consider an arbitrary 3-volume with boundary, the network P representing it, and an arbitrary edge on the boundary of the volume together with the two adjacent triangles, e.g.,

$$\begin{array}{c} \text{(diagram)} \end{array} \quad \rightarrow \quad \begin{array}{c} \text{(diagram)} \end{array} . \tag{319}$$

We can glue two hats at their 2-gons, and then glue the resulting "double-hat" to the two adjacent faces above. This corresponds to a topological move

$$\begin{array}{c} \text{(diagram)} \end{array} \quad \leftrightarrow \quad \begin{array}{c} \text{(diagram)} \end{array} \tag{320}$$

Which hats we take depends on the edge orientations. In our case, we get a move

$$\begin{array}{c} \text{(diagram)} \end{array} = \begin{array}{c} \text{(diagram)} \end{array} . \tag{321}$$

This is as far as we get on the combinatorial liquid level, and now we have to make use of the fact that we're looking for models of the liquid in complex tensors. All the algebras and representations in question have extra properties due to the topological moves which make them block-diagonalizable. That is, we can go to a basis where the algebra is given by

$$\beta cd - \!\!\!\bullet\!\!\!- \gamma ef \quad = \quad \begin{array}{c} \text{(diagram)} \end{array} , \tag{322}$$

and the representation is given by

$$\beta cx - \square - \gamma dy \quad = \quad \begin{array}{c} \text{(diagram)} \end{array} . \tag{323}$$

Here, $\alpha, \beta, \ldots$ are called *irreducible representation indices*, $a, b, \ldots$ are called *block indices*, and x, y *multiplicity indices*. Note that this is a fake tensor network notation, as the dimension of both block and multiplicity index are allowed to dependent on the value of the irreducible representation indices.

As we saw above, the vector space of the triangle is equipped with a representation of three times the banana algebra. Going to the block-diagonal basis, we can decompose the vector space into three indices corresponding to irreducible representations of the banana algebra, three block

indices, and one joint multiplicity index. The irreducible representation and block indices can be associated to the three edges of the triangle each. Note that the dimension of each block index depends on the dimension of the corresponding irreducible representation index, and the multiplicity index depends on the values of all three irreducible representation indices (this dimension becomes the N_c^{ab}).

All we need to show is that 1) we can get rid of the block indices and 2) the two irreducible representation indices at an edge coming from the two adjacent triangles can be unified into one. To this end, we look at Eq. (321) with the representations in their block-diagonal form

$$ \tag{324} $$

Applying these procedure to all edges, we get a tensor $\widetilde{P}$ with irreducible representation indices at all edges and multiplicity indices at all faces. Now, we plug the above equation into the network representing a cellulation. For each edge of the cellulation, we get 1) a completely disconnected loop of block indices, and 2) a loop of delta tensors connected to the tensors at the adjacent volumes. The loop 1) can be contracted to a scalar which can be incorporated into the edge weight, and the loop 2) can be contracted to a single delta tensor, e.g., for an edge with 3 adjacent volumes we get

$$ \tag{325} $$

where m consists of the multiplicities of the different irreducible representations.

D   Reordering signs for the remaining fermionic moves

In this appendix, we compute the reordering signs for the remaining moves of the 1+1-dimensional fermionic liquid, and find that they all cancel out.

- For the spin triangle cancellation move Eq. (252)

$$\begin{aligned}
|y'x'axyb|(xx')(yy') &= |ab|, \\
(a+x+y)|ba| &= |ab|, \\
|ab| &= |ab| \ .
\end{aligned} \tag{326}$$

- For the spin (012) triangle symmetry move Eq. (254)

$$\begin{aligned}
|y'cxax'by|(xx')(yy') &= |abc| \\
(ax)|bcxx'a| &= |abc|, \\
(a)|bca| &= |abc|, \\
|abc| &= |abc| \ .
\end{aligned} \tag{327}$$

- For the spin 2-gon cancellation move Eq. (256)

$$\begin{aligned}
|axbx'|(xx') &= |ba|, \\
|ab| &= |ab| \ .
\end{aligned} \tag{328}$$

References

[1] B. Zeng, X. Chen, D. Zhou and X.-G. Wen, *Quantum information meets quantum matter – from quantum entanglement to topological phase in many-body systems*, Springer, Berlin (2015).

[2] M. Levin and X.-G. Wen, *Detecting topological order in a ground state wave function*, Phys. Rev. Lett. **96**, 110405 (2006).

[3] J. I. Cirac, D. Perez-Garcia, N. Schuch and F. Verstraete, *Matrix product states and projected entangled pair states: Concepts, symmetries, and theorems* ArXiv:2011.12127.

[4] R. Orus, *A practical introduction to tensor networks: Matrix product states and projected entangled pair states*, Ann. Phys. **349**, 117 (2014).

[5] J. C. Bridgeman and C. T. Chubb, *Hand-waving and interpretive dance: An introductory course on tensor networks*, J. Phys. A **50**, 223001 (2017).

[6] J. Eisert, M. Cramer and M. B. Plenio, *Area laws for the entanglement entropy*, Rev. Mod. Phys. **82**, 277 (2010).

[7] M. B. A. Sahinoglu, D. Williamson, N. Bultinck, M. Marian, J. Haegeman, N. Schuch and F. Verstraete, *Characterizing topological order with matrix product operators* ArXiv:1409.2150.

[8] N. Schuch, I. Cirac and D. Perez-Garcia, *PEPS as ground states: degeneracy and topology*, Ann. Phys. **325**, 2153 (2010).

[9] N. Schuch, D. Perez-Garcia and I. Cirac, *Classifying quantum phases using matrix product states and projected entangled pair states*, Phys. Rev. B **84**, 165139 (2011).

[10] N. Bultinck, J. Williamson, J. Haegeman and F. Verstraete, *Fermionic projected entangled-pair states and topological phases*, J. Phys. A **51**, 025202 (2017).

[11] C. Wille, O. Buerschaper and J. Eisert, *Fermionic topological quantum states as tensor networks*, Phys. Rev. B **95**, 245127 (2017).

[12] M. Fannes, B. Nachtergaele and R. F. Werner, *Finitely correlated states on quantum spin chains*, Comm. Math. Phys. **144**, 443 (1992).

[13] S. R. White, *Density matrix formulation for quantum renormalization groups*, Phys. Rev. Lett. **69**, 2863 (1992).

[14] D. Perez-Garcia, F. Verstraete, M. M. Wolf and J. I. Cirac, *Matrix product state representations*, Quantum Inf. Comput. **7**, 401 (2007).

[15] N. Schuch, Perez-Garcia and I. Cirac, *Classifying quantum phases using matrix product states and peps*, Phys. Rev. B **84**, 165139 (2011).

[16] X. Chen, Z.-C. Gu and X.-G. Wen, *Classification of gapped symmetric phases in one-dimensional spin systems*, Phys. Rev. B **83**, 035107 (2011).

[17] F. Pollmann, A. M. Turner, E. Berg and M. Oshikawa, *Entanglement spectrum of a topological phase in one dimension*, Phys. Rev. B **81**, 064439 (2010).

[18] A. Bauer, *Quantum mechanics is *-algebras and tensor networks* (2020), ArXiv:2003.07976.

[19] A. Bauer and A. Nietner, *Tensor types and their usage in physics*, In preparation (2020).

[20] T. Cubitt, Perez-Garcia and M. M. Wolf, *Undecidability of the spectral gap*, Nature **528**, 207 (2015).

[21] X. Chen, Z.-C. Gu and X.-G. Wen, *Local unitary transformation, long-range quantum entanglement, wave function renormalization, and topological order*, Phys. Rev. B **82**, 155138 (2010).

[22] M. B. Hastings and X.-G. Wen, *Quasi-adiabatic continuation of quantum states: The stability of topological ground state degeneracy and emergent gauge invariance* (2005), ArXiv:cond-mat/0503554.

[23] S. Bravyi and M. B. Hastings, *A short proof of stability of topological order under local perturbations* (2010), ArXiv:1001.4363.

[24] U. Pachner, *P. l. homeomorphic manifolds are equivalent by elementary shellings*, Europ. J. Comb. **12**(2), 129 (1991).

[25] A. Y. Kitaev, *Fault-tolerant quantum computation by anyons*, Ann. Phys. **303**, 2 (2003).

[26] R. Verresen, R. Moessner and F. Pollmann, *One-dimensional symmetry protected topological phases and their transitions*, Phys. Rev. B **96**, 165124 (2017).

[27] R. Raussendorf and H. J. Briegel, *A one-way quantum computer*, Phys. Rev. Lett. **86**, 5188 (2001).

[28] X. Chen, Z.-C. Gu, Z.-X. Liu and X.-G. Wen, *Symmetry protected topological orders and the group cohomology of their symmetry group*, Phys. Rev. B **87**, 155114 (2013).

[29] M. Fukuma, S. Hosono and H. Kawai, *Lattice topological field theory in two dimensions*, Commun. Math. Phys. **161**, 157 (1994), doi:10.1007/BF02099416, `hep-th/9212154`.

[30] A. Bauer, J. Eisert and C. Wille, *Towards a mathematical formalism for classifying phases of matter* (2019), ArXiv:1903.05413.

[31] N. Schuch, D. Perez-Garcia and I. Cirac, *Classifying quantum phases using matrix product states and projected entangled pair states*, Phys. Rev. B **84**(16) (2011).

[32] A. Kapustin and L. Fidkowski, *Local commuting projector Hamiltonians and the quantum Hall effect*, Commun. Math. Phys. **373**, 763 (2019).

[33] A. Bauer, *Generalized topological state-sum constructions and their universality* (2019), ArXiv:1909.03031.

[34] V. G. Turaev and O. Y. Viro, *State sum invariants of 3-manifolds and quantum 6j-symbols*, Topology **31**, 865 (1992).

[35] J. W. Barrett and B. W. Westbury, *Invariants of piecewise-linear 3-manifolds*, Trans. Amer. Math. Soc. **348**, 3997 (1996).

[36] M. A. Levin and X.-G. Wen, *String-net condensation: A physical mechanism for topological phases*, Phys. Rev. B **71**, 045110 (2005).

[37] R. Dijkgraaf and E. Witten, *Topological gauge theories and group cohomology*, Commun. Math. Phys. **129**, 393 (1990).

[38] S. X. Cui and Z. Wang, *State sum invariants of three manifolds from spherical multi-fusion categories* (2017), ArXiv:1702.07113.

[39] Y. Hu, Y. Wan and Y.-S. Wu, *Twisted quantum double model of topological phases in two dimensions*, Phys. Rev. B **87**, 125114 (2013).

[40] C.-H. Lin and M. Levin, *Generalizations and limitations of string-net models*, Phys. Rev. B **89**, 195130 (2014).

[41] O. Buerschaper, J. M. Mombelli, M. Christandl and M. Aguado, *A hierarchy of topological tensor network states*, J. Math. Phys. **54**, 012201 (2013).

[42] L. Chang, *Kitaev models based on unitary quantum groupoids*, J. Math. Phys. **55**, 041703 (2014).

[43] G. Kuperberg, *Involutory Hopf algebras and 3-manifold invariants*, Internat. J. Math. **2**(1), 41 (1990).

[44] T. Barthel, C. Pineda and J. Eisert, *Unitary circuits for strongly correlated fermions*, Phys. Rev. A **80**, 042333 (2009).

[45] D. Gaiotto and A. Kapustin, *Spin tqfts and fermionic phases of matter*, Int. J. Mod. Phys. A **31**, 1645044 (2016).

[46] R. Z. Goldstein and E. C. Turner, *A formula for Stiefel-Whitney homology classes*, Proc. Amer. Math. Soc. **58**, 339 (1976).

[47] A. Kitaev, *Unpaired Majorana fermions in quantum wires* (2000), ArXiv:cond-mat/0010440.

[48] M. B. Sahinoglu, *A tensor network study of topological quantum phases of matter*, Ph.D. thesis, Universität Wien (2016).

[49] D. J. Williamson and Z. Wang, *Hamiltonian models for topological phases of matter in three spatial dimensions*, Ann. Phys. **377**, 311 (2017).

[50] A. Kapustin and R. Thorngren, *Higher symmetry and gapped phases of gauge theories* (2013), ArXiv:1309.4721.